University of Washington
Department of Civil and Environmental Engineering

RIGID BODY MOTION OF A FLOATING BREAKWATER: SEAKEEPING PREDICTIONS AND FIELD MEASUREMENTS

Robert W. Miller
Derald R. Christensen
Ronald E. Nece
Billy J. Hartz

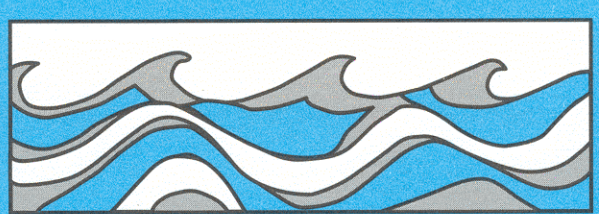

Water Resources Series
Technical Report No. 84
February 1984

Seattle, Washington
98195

Department of Civil Engineering
University of Washington
Seattle, Washington 98195

RIGID BODY MOTION OF A FLOATING BREAKWATER: SEAKEEPING PREDICTIONS AND FIELD MEASUREMENTS

Robert W. Miller
Derald R. Christensen
Ronald E. Nece
Billy J. Hartz

Water Resources Series
Technical Report No. 84

February 1984

University of Washington
Department of Civil Engineering
Environmental Engineering and Science Program
Seattle, Washington 98195

RIGID BODY MOTION OF A FLOATING BREAKWATER: SEAKEEPING PREDICTIONS AND FIELD MEASUREMENTS

by

Robert W. Miller
Derald R. Christensen
Ronald E. Nece
Billy J. Hartz

Water Resources Series
Technical Report No. 84
February 1984

Project Title: Floating Breakwater Prototype Test-Monitoring Program, West Point, WA

Contract No.: DACW67-81-C-0196

Principal Investigators: Derald Christensen,
Senior Research Associate
Ronald E. Nece,
Professor
Eugene P. Richey,
Professor
Department of Civil Engineering
Universty of Washington

TABLE OF CONTENTS

TABLE OF CONTENTS (Continued)

TABLE OF CONTENTS (Continued)

LIST OF FIGURES

LIST OF FIGURES (Continued)

LIST OF FIGURES (Continued)

LIST OF TABLES

LIST OF SYMBOLS

$A_{i,j}$	hydrodynamic mass matrix
A_{wp}	area of breakwater at water plane
$\{A\}$	translational frequency response operator vector
b	breakwater beam; also body coordinates when used as subscript
B^*_{44}	linearized viscous roll damping coefficient
B_E	linearized square law (viscous roll) damping coefficient due to eddy-making
B_H	linearized viscous roll damping coefficient due to hull friction
B_{ij}	hydrodynamic damping matrix
BM	distance from center of buoyancy to metacenter
C	drag coefficient due to hull shape used in viscous damping calculation
C_{Df}	drag coefficient due to skin friction used in viscous damping calculation
C_{ij}	hydrostatic restoring constants matrix
D	breakwater draft
E_n^2	normalized squared error
f	frequency in cycles per second (hertz)
F_i	excitation force (or moment) in i^{th} mode
g	acceleration due to gravity
GM_l	longitudinal metacenter above center of gravity
GM_t	transverse metacenter above center of gravity
H_j	complex frequency response operator (FRO) for degree of freedom j
$H_{\eta,j}$	displacement frequency response operator
$H_{\ddot{\eta},i}$	acceleration frequency response operator
$H_{\ddot{\eta},b,j}$	body-coordinate acceleration frequency response operator
$/H_j/$	modulus or magnitude of complex frequency response operator

I_{ij}	inertia coefficients matrix
I_{wp}	area moment of inertia of section at water plane
K_{ij}	mooring force restoring coefficients matrix
KG	distance from breakwater keel to center of gravity
L	length of breakwater
M	mass of breakwater
n	exponent of cosine spreading function
Q	wetted surface area of immersed hull
{R}	rotational frequency response operator vector
R_e	bilge radius
r	position vector
S_ζ	incident wave autospectral estimate
$S_{\eta,j}$	displacement autospectral estimate for degree of freedom j
$S_{\ddot{\eta},j}$	acceleration autospectral estimate for degree of freedom j
T	torque, also wave period
[T]	transformation matrix
t	time
uwd	unidirectional wind duration: number of hours (to nearest two hours) in which wind was blowing within 25 degrees of the timeseries mean
$\forall$	immersed volume of breakwater
VR	variance ratio
WD	sectional wetted perimeter
WS	wave steepness = wave length / wave amplitude
w	angular frequency
X,Y,Z	global coordinates
x,y,z	equilibrium coordinates

x_b, y_b, z_b	body coordinates
Z_{cg}	location of center of gravity with respect to coordinate origin
Δt	sampling interval
η	displacement
$\dot{\eta}$	velocity
$\ddot{\eta}$	acceleration
θ	angle of wave attack
θ_o	principal angle of wave attack
λ	wavelength
ν	kinematic viscosity of seawater
ζ	incident wave height
ρ	mass density of seawater
σ^2	variance
$\psi(\theta)$	spreading function
$\hat{}$	(as superscript) designates predicted (as opposed to measured) quantities

ACKNOWLEDGMENTS

The experimental results presented in this report were obtained during a monitoring program conducted by the Department of Civil Engineering, University of Washington, performed under sponsor's Contract Number DACW-67-81-C-0196, "Floating Breakwater Prototype Test-Monitoring Program," for the Seattle District, U.S. Army Corps of Engineers.

Close liaison with the Seattle District throughout the duration of the project was maintained with A. David Schuldt, Eric E. Nelson, and Norman K. Skjelbreia, all of the Navigation and Coastal Planning Section. Laurie L. Broderick and D. Donald Davidson provided liaison with the Coastal Engineering Research Center and the Waterways Experiment Station, U.S. Army Corps of Engineers.

Derald R. Christensen, Senior Research Associate, served as Principal Investigator for the University of Washington, Professors Eugene P. Richey and Ronald E. Nece were Co-Investigators; Professor Billy J. Hartz participated in the project. This report is essentially the MSCE thesis of Robert W. Miller, Research Assistant, who wrote the thesis under the supervision of the co-authors.

CHAPTER I

INTRODUCTION

A) Background

Since the 1940's, floating breakwaters have been recognized as an economical alternative to fixed structures as a means of providing wave attenuation in certain sites and wave climates. While generally ineffective in attenuating long-period waves, floating breakwaters are commonly employed in limited fetch environments where wave periods of four seconds or less tend to predominate. In deep water, where rubble-mound type breakwaters may become prohibitively expensive, a higher percentage of the kinetic energy is contained in the upper portions of the water column and therefore subject to interaction with a floating breakwater.

The West Point Prototype Floating Breakwater Project, initiated by the U.S. Army Corps of Engineers, involved testing a full-scale two-pontoon rectangular concrete breakwater in Puget Sound, near Seattle, Washington. Many important environmental and response parameters were measured (see Chapter III, Section A). A valuable opportunity exists for many of the assumptions and procedures used by practicing engineers to be evaluated through comparison with full-scale field data. Since data gathered by The West Point Prototype Floating Breakwater Project figure prominently in this report, future discussion of floating breakwaters will tacitly assume this type of design.

Of primary interest to the floating breakwater designer is performance, as usually measured by wave transmission characteristics, and cost. Important questions arise during the design of a breakwater regarding the intensity and duration of the forces to be resisted by the various structural components of the system, not only in the walls of the pontoons themselves but in the connectors and the mooring system. Some reasonable idea of these quantities is necessary to produce a cost-effective design. Very little full-scale data is available to help the designer answer these questions, and always, any lack of information or uncertainty at the outset must be compensated for with extra factors of safety, material, and ultimately, money.

B) Scope and Objective

Several methods are currently used for predicting the responses of floating bridges and breakwaters to short-crested seas. A basic distinction is to be made between those methods which calculate the response of the body to a specific sequence of time-varying forces and moments (time domain methods) and those which sum the separate steady-state responses at each discrete frequency of interest (frequency domain methods). While time-domain approaches may give more satisfactory accounting of the higher order (non-linear) terms in the equations of motion, in practice frequency-domain models tend to predominate. Often, the precision with which higher order terms are known does not justify the tremendous increase in computational time required for a thorough time-domain simulation. Proper treatment of frequency-dependent hydrodynamic quantities is also less

straightforward in the time domain. For these reasons, a frequency domain approach was used for breakwater response prediction in this report.

The frequency-domain analysis techniques commonly in use treat the structure either as an ensemble of rigid bodies with prescribed stiffnesses between modules (Hutchison, 1982) or as a large beam on an elastic foundation (Langen, 1981; Georgiadis, 1981). The first method does not directly account for any structural deformations in the modules while the second might be more properly described as a finite element approach. The use of a finite element method might not be extremely informative for a breakwater of the dimensions under consideration (150 feet long, 16 feet wide and 5 feet deep). Calculations in Appendix A indicate that rigid-body modes of motion could be expected to predominate. It is questionable whether such a structure would provide the most favorable test conditions for important aspects of a finite element model. On the other hand, if the behavior of a large structure consisting of many modules is to be adequately modeled in the frequency domain as an assemblage of rigid bodies, then the behavior of a single module must be well understood. The West Point prototype floating breakwater is of suitable dimensions to provide this test. If reasonable response estimates can be obtained for a module of this length, then the successful application of the rigid body assumption to more complex cases could be viewed optimistically.

The objective of this report is to compare estimates of the rigid body accelerations of the West Point prototype floating

breakwater to full-scale measurements. As wide a range of data as feasible will be examined in an effort to see how parameters such as significant wave height or wind duration and direction seem to affect the accuracy of the predictions. It is also hoped that some practical information might be gained regarding appropriate values for damping parameters important in accurate response prediction. If accurate estimates of the time-varying accelerations can be made, it is then possible to estimate the time-varying forces and moments. It should also be feasible to estimate the higher-frequency variations in mooring forces from this information.

C) Method of Approach

The techniques for estimating the six degree-of-freedom response of a rigid body due to harmonic loadings are well known. The equations of motion are formulated as a system of second-order linear coupled ordinary differential equations. Due to the frequency dependence of many of the terms, a system of equations exists for each discrete frequency under consideration, and the total response is the summation of these solutions. A major difficulty of this method of analysis is in obtaining accurate estimates of the hydrodynamic coefficients for a real three-dimensional object. Hydrodynamic coefficients and forces used in motion predictions for this report were obtained from a commercially available ship motion program with demonstrated success for certain ship hull shapes (Salveson et al., 1970).

Once an estimate of displacement response is obtained, it is differentiated twice with respect to time and transformed to a

location and coordinate system consistent with the measured accelerations. Accelerations, rather than displacements were chosen as the final output of the model for the following reasons:

- The data to be used in validating the model were in the form of accelerations
- While the solution to the equations of motion yields displacement information directly, the results must be converted to body coordinate accelerations before estimates of internal forces and moments in the body can be made. This conversion shifts the spectrum by weighting high frequency components more and low frequency components less. By displaying the information as accelerations, a clearer understanding is gained as to which parameters have more influence on generating internal forces and moments in the body.
- Estimation of mooring forces and total body displacement admittedly depends on spectral displacement output. But ultimately the overall magnitude of these displacements may depend as much on the extreme low frequency response of the body as well, and this topic is more adequately addressed through a different type of analysis, for example that described by Oppenheim (1980).

As an aid in evaluating results, statistical measurements of the level of agreement between predicted and measured autospectral estimates are formulated. Finally, the results are

#analyzed with respect to parameters of interest and discussed. Suggestions are made for improvement of the current analysis as well as possible directions for future work.

D) Coordinates and Definitions

All coordinate axes used in this report are orthogonal right-handed systems. The three frames of reference used at various stages in the analysis are depicted in Figures 1.1 through 1.3. Global coordinates (X,Y,Z) are used by program NSRDC, being convenient for use with the wave pressure field because they are aligned with the direction of wave propogation. The equilibrium coordinate system, (x,y,z), has its origin at the mean still water level in the vertical direction and the mean position of the center of mass in the horizontal plane. The distinction between global and equilibrium frames becomes more important in seakeeping theory when uniform velocities or rotations occur between the global and equilibrium frames. In the current analysis, they differ only by the wave angle of attack, θ, which is defined with respect to beam seas.

The body coordinate system, (x_b,y_b,z_b), remains fixed in the breakwater and participates in all translations and rotations with respect to the (x,y,z) system. This system is useful when considering internal forces and moments because inertia quantities remain invariant. The body coordinate system is also the frame of reference implicitly held by any instruments attached to the breakwater such as accelerometers.

When the equations of motion are assembled and solved, the output consists of translations and rotations of the body coord-

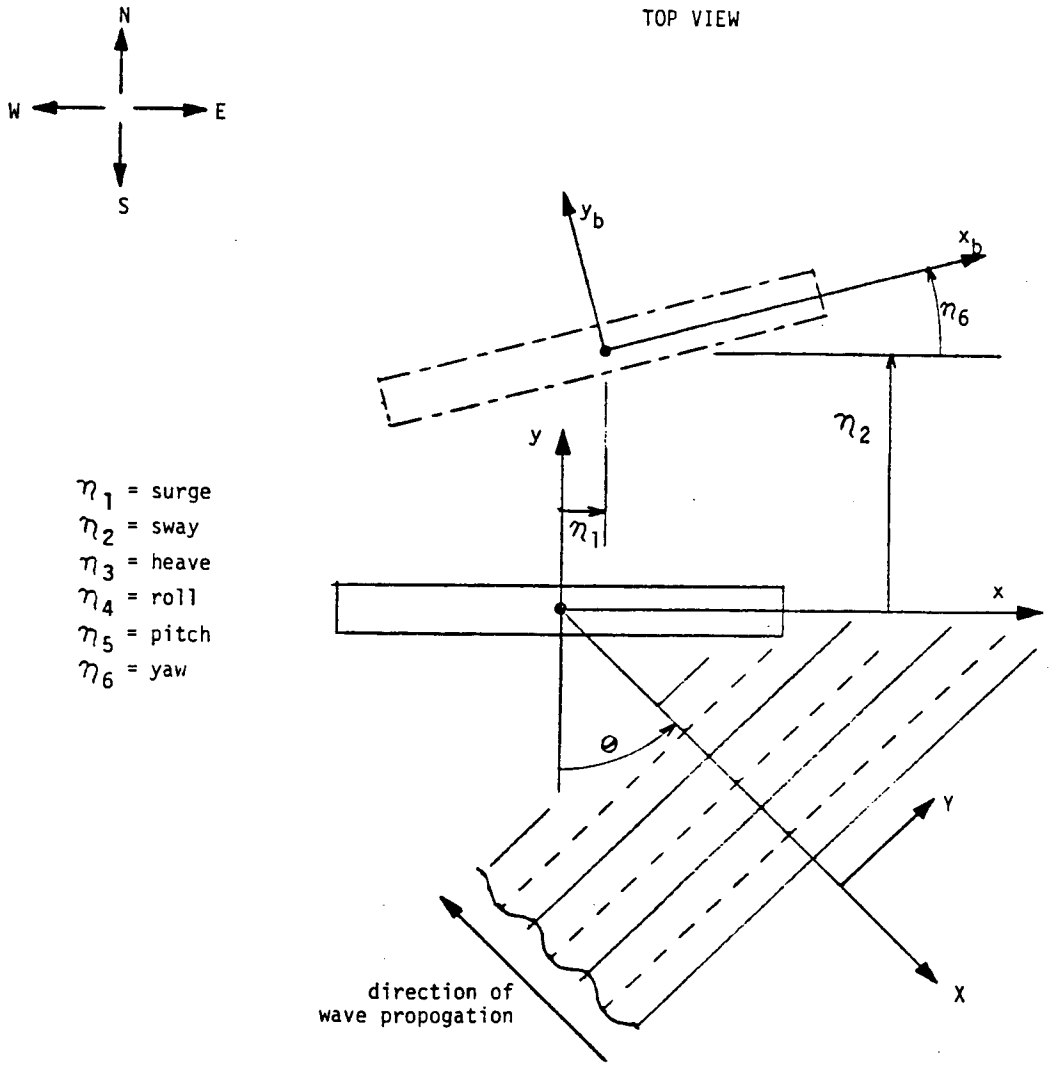

Figure 1.1 Coordinate Definitions: Top View Showing Global (X, Y, Z), Equilibrium (x, y, z) and Body (x_b, y_b, z_b) Frames.

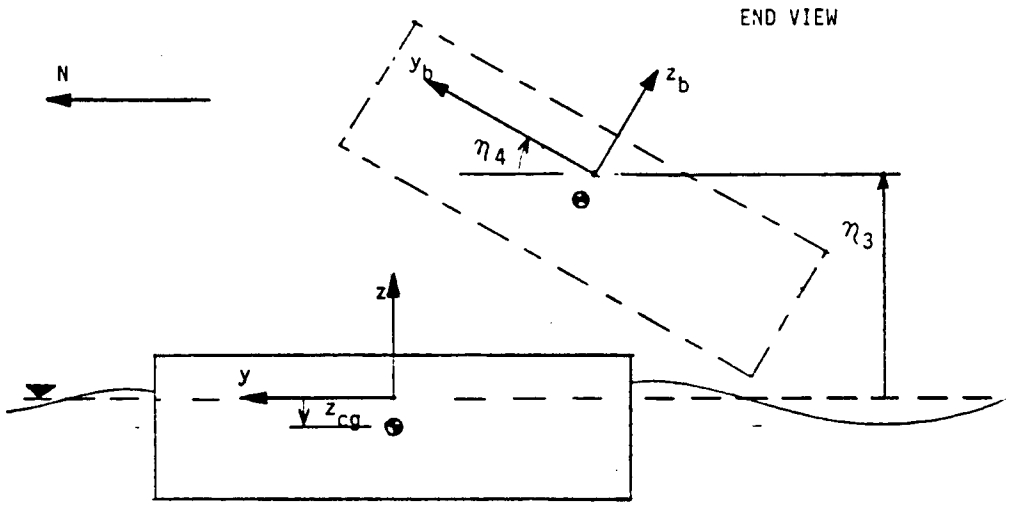

Figure 1.2 Coordinate Definitions: End View

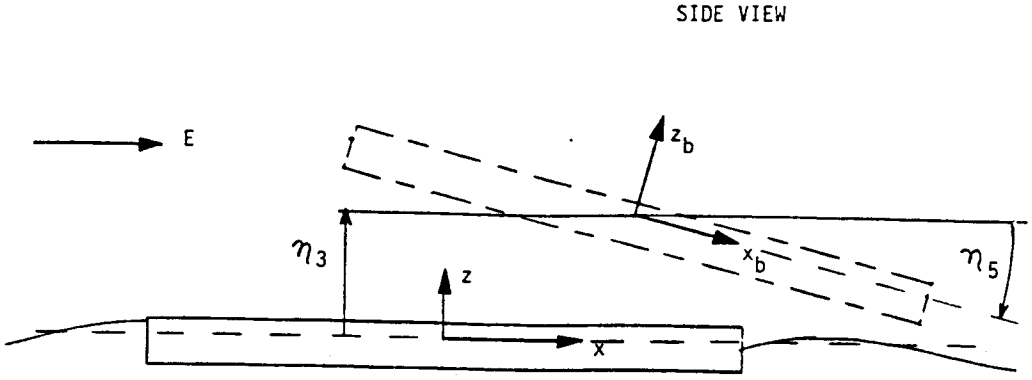

Figure 1.3 Coordinate Definitions: Side View

inate system with respect to the equilibrium frame. These motions are referred to as η_j where j ranges from one to six. The three translations are commonly referred to as surge, sway, and heave for j=1-3, and the rotations roll, pitch and yaw for j=4-6.

A great deal of the discussion in this report refers to breakwater accelerations as expressed in the body coordinate system. The translational accelerations in this frame of reference would properly be referred to as "longitudinal", "transverse", and "normal to the deck," while rolling about the long axis would be "longitudinal rotation." Constant use of these phrases, however, was found to be clumsy. In place, the terms sway, heave, and roll accelerations are often used, despite the fact that the equilibrium frame, rather than the body frame is often implied by their use. Sometimes the word "accelerations" is left off. While incorrect in a strict sense, such free usage is confined to contexts in which confusion will not arise.

Although the analytical model to be presented predicts pitch and yaw displacements and accelerations as well as those of sway, heave, and roll, these degrees of freedom are not discussed directly although they are used in coordinate transformations. If the sway, heave, and roll motions and accelerations can be accurately predicted on both pontoons, then pitch and yaw estimates are also accurate for a body behaving rigidly.

Frequent reference is made throughout this work to frequency response operators. Frequency response operators are complex

quantities defining a transformation between the input and output of a linear system. The magnitudes of such quantities are properly referred to as the modulus of the frequency response operators or modulus of the FRO. Consistent with the notation defined in the Table of Symbols, the quantity $/H_{\ddot{\eta},b,2}/$ would properly be referred to as "the modulus of the body-coordinate acceleration transverse frequency response operator" where the subscript "$\ddot{\eta}$" denotes acceleration, "b" makes reference to the body coordinate system, and "2" refers to the degree of freedom. It is not difficult to see why the term "sway operator" is sometimes employed instead. Again, the context should make it clear precisely which quantity is being mentioned.

Finally, the phrases "measured autospectrum" and "measured operator" are used when what is really meant is "the spectral density estimate based upon the measured timeseries" or "the body-coordinate acceleration FRO modulus derived from measurement -based spectral density estimates." It is not to be implied by use of the adjective "measured" that such quantities are not estimates. The qualifier is intended to distinguish those quantities derived from field measurements from those predicted by the analytical model under evaluation.

CHAPTER II

REVIEW OF THE LITERATURE

A) Seakeeping Theory

The modern theory of ship motion response prediction began with the publication of "On the Motion of Ships in Confused Seas" by Manley St. Denis and Willard J. Pierson (1953). This seminal work, produced by the collaboration of a naval architect and an oceanographer, first postulated that the response of a moving ship to an irregular wave train could be treated as the superposition of responses to regular waves of all frequencies. Since an irregular sea profile can be represented as a summation of regular sinusoidal waves of different frequencies and directions, this idea provided the means to model the response to any sea surface, provided the appropriate responses to regular sinusoidal waves were known. A rational procedure was therefore available for estimating dynamic loads due to stochastic excitations rather than resorting to the ship's maximum static bending moment in a design wave as the major consideration.

Much of the subsequent 30 years of research has been devoted to developing the ability to predict with acceptable engineering accuracy the motions, shear forces, and moments of a ship advancing at constant speed at arbitrary heading in regular sinusoidal waves. The most significant work as it applies to this paper will be briefly mentioned. The reader requiring a more thorough treatment should refer to St. Denis (1953), Salveson(1970), Bhattacharyya (1978), or Ochi (1974).

An important theory was expounded in "Pitching and Heaving Motions of a Ship in Regular Waves" by B.V. Korvin-Kroukovsky and W.R. Jacobs in 1957. They proposed that the three-dimensional added mass and damping coefficients as well as the forcing functions could be calculated for sufficiently thin two-dimensional sections and the results superposed into the three-dimensional body to be analyzed. This "strip theory" as it is commonly called has been shown to give good results provided the two-dimensional slices are taken close enough together and the hull form is sufficiently "slender." Two-dimensional hydrodynamic quantities are commonly obtained either by using the "Lewis form" as outlined in Bhattacharyya (1978), or the method of Frank (1967) which utilizes a close-fit source distribution technique to solve the potential-flow Cauchy problem. The "Frank Close-Fit" method appears to give reasonable results over a wider range of conditions than does the Lewis form. It is appropriate to mention that important experimental and theoretical work by Vugts (1968 and 1970) is very often the standard against which methods for obtaining hydrodynamic coefficients are evaluated.

Significant refinements and extensions to ship motion theory were made by Nils Salveson et al. (1970). This paper is important in that it extends the theory to other modes of motion (particularly coupled roll and sway), oblique waves, and horizontal shear and torsion. The theory presented in this work is the basis for the NSRDC Ship-Motion and Sea-Load Computer Program which calculates motions, forces, and moments for all 6 rigid

body degrees of freedom in regular waves. Since the present work uses program NSRDC to calculate all hydrodynamic terms in the equations of motion, the theory and equations set forth in "Ship Motion and Sea Loads" are directly employed in this report to predict breakwater acceleration response.

Much of the more recent work in ship motion theory has concentrated on corrections for ship forward speed, the effect of bilge keels and other topics which are not directly applicable to breakwater analysis.

B) Barges and Breakwaters

There is some question as to how far rigid-body ship motion theory can be extended. More precisely, does the theory give useful engineering results for objects of breakwater shape and dimensions? Which degrees of freedom are heavily influenced by the presence of mooring restraints and how severe is this influence? Can this influence be adequately modeled by the addition of linear spring constants to the equations of motion? The availability of such information is limited.

Orr (1975) compared the response operators derived from scale model tests of a barge with the results of the Frank close-fit computer program. The analysis only looked at heave and pitch degrees of freedom. Roll, sway, surge and yaw were neglected since Frank's program did not consider these motions and program NSRDC was not yet available. The wave field was assumed to be unidirectional, a questionable assumption for the Puget Sound region. Nevertheless, reasonable results were obtained both for magnitude and shape of the pitch transfer function. The shape of

the heave transfer function also showed good agreement between the scale model and the full-scale predictions, but its magnitude was significantly larger for the predicted barge motions than those obtained from the scale model data. A possible problem in the scaling of the heave data was suspected.

Hutchison (1975) also attempted to correlate computer model predictions of barge motions with the results of two different scale model studies (University of Michigan, 1972 and 1973 and Offshore Technology Corporation in 1975) in uni directional seas. Program SCORES of the Ship Structures Committee was used to calculate hydrodynamic coefficients and solve the equations of motion. Hutchison found reasonable levels of agreement between predicted and measured responses despite some problems with unsuitability in the model test data. Among the more significant discoveries, from the point of view of this work were:

- apparant suitability of barge shapes to strip theory analysis
- better level of agreement for roll displacements in beam seas than in quartering seas
- highly non-linear phenomena (particularly water shipping on deck) appeared to shift the measured roll response to somewhat lower frequencies than predicted
- evidence that non-linear damping played a crucial role in barge roll response
- reasonable heave and pitch responses in magnitude and frequency of peak response, but poorer agreement for lower

frequencies where mooring forces tend to have more effect on the equations of motion.

Hutchison did not compare sway motions as sway data were not available to him.

A model for breakwater motion, mooring force, and transmission characteristic prediction is presented by Adee et al. (1976). The model presented was two-dimensional, predicting sway, heave, and roll in a unidirectional beam sea for an infinitely long breakwater. Considering these assumptions, it is not surprising that all three motions were seriously overpredicted with respect to field measurements obtained in Tenakee, Alaska since a unidirectional beam sea would presumably be a rare event. Nevertheless, reasonable wave transmission characteristics were predicted based on linear theory and some interesting points were made regarding the modeling of mooring forces. In particular, measurements made at Tenakee, Alaska seem to indicate that long-period oscillations (30-60 seconds) have a larger effect on the magnitude of the mooring forces than oscillations occurring at the frequency of the main incident wave energy. A linear theoretical model permits system response to occur only at the frequency of the excitation force. Forces which occur at zero frequency are not accounted for, yet they do exist if higher order terms are carried in the wave potential equations. A more detailed discussion of this phenomenon and its possible effect on this work occurs in Chapter V.

CHAPTER III

FIELD MONITORING PROGRAM

A) West Point Prototype Floating Breakwater Project

The West Point Prototype Floating Breakwater Test Program was initiated in February, 1981 by the United States Army Corps of Engineers to obtain experience and information regarding performance and environmental response of a full-scale floating breakwater.[8] The project took place in Puget Sound near Seattle, Washington (see Figure 3.1). Figure 3.2 shows the project site location including the position of the accelerometer used in this study under discussion. The breakwater itself was composed of two rectangular concrete pontoons each 75 feet in length, with a beam of 16 feet, a draft of approximately 3.5 feet and 1.5 feet of freeboard. Each pontoon is subdivided into eight compartments by intersecting walls running the length and width of the module interiors. The interior walls are 3 inches thick, and the sidewalls, top, and bottom are 4.75 inches thick.

The clump weights depicted in Figure 3.2 weighed 2,000 pounds and were attached to each of ten mooring cables during the entire period under consideration in the report. The pontoons were rigidly bolted together during this period as well.

A major feature of the project was a sophisticated field monitoring system. Among the quantities measured were incident and transmitted wave heights, wind speed and direction, dynamic mooring forces, strains in the concrete pontoons and connectors, relative float motion (during the period when a flexible connecter was in place), linear and rotational accelera-

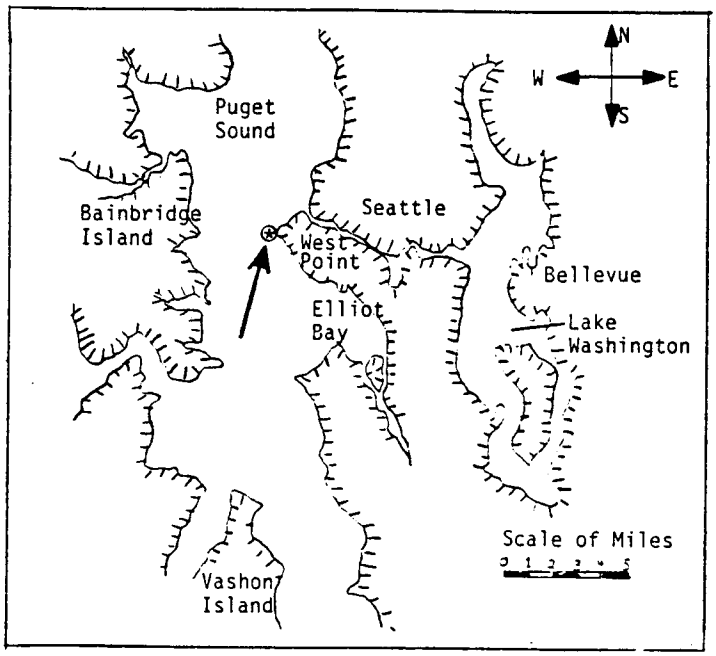

Figure 3.1 West Point Prototype Floating Breakwater Project Site Location

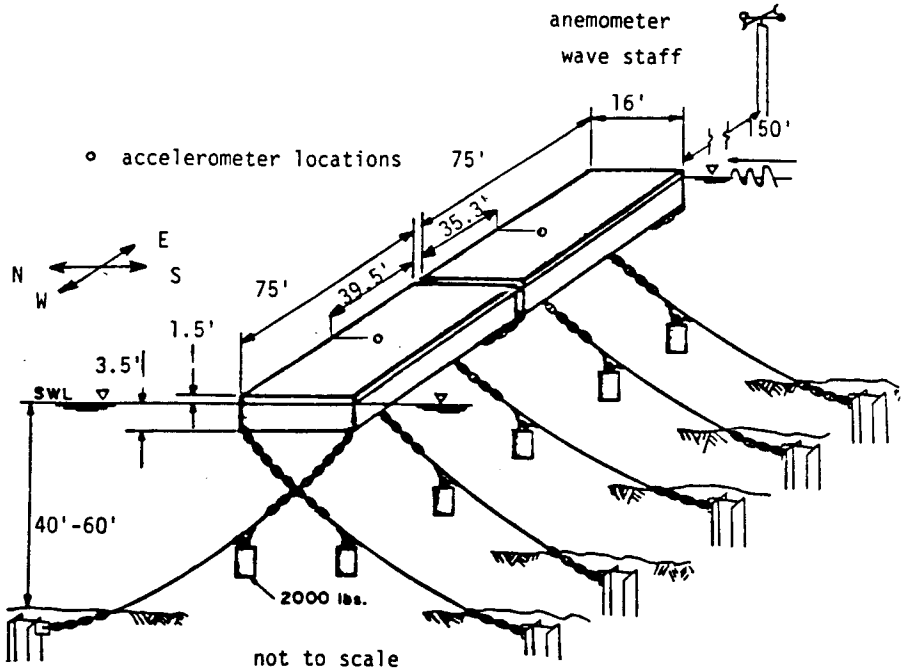

Figure 3.2 West Point Prototype Floating Breakwater: Project Site Instrument Layout

tions, pressure distribution along the breakwater side, water and air temperature, and water current data.

B) Data Acquisition

An RCA microprocessor based data acquisition system capable of sampling 96 channels of data at a sampling rate of up to 4 hertz was used for field monitoring. The system was set to automatically sample certain key parameters such as wind speed and wave height at a preset interval. If certain trigger levels were exceeded during the brief sampling interval, the full system was switched on and a timeseries of 2048 points per channel for 80 input channels was generated with a sampling rate of 4 hertz. The field monitoring took place from December 1982 through January of 1984.

The measurements that are of the most interest from the point of view of investigating the applicability of seakeeping theory to floating breakwaters are incident wave heights, breakwater accelerations, and wind direction. While directional wave data were gathered starting September 1983, results were not available in time for use in this study.

A brief description will be given of the measurements that are relevant to this report.

i) Wave Staffs

The incident wave heights were measured by a resistance type wave gage attached to a piling which was directly exposed to incident waves from both northerly and southerly directions. The data obtained have been in agreement with visual observations and

strip-chart recordings of boat wakes. Figure 3.3 shows an example of a recorded input wave height timeseries for a southerly wind.

ii) Accelerometers

Linear accelerometers measuring normal (to the deck, or heave) and transverse (or sway) acceleration and an angular accelerometer measuring rotation about the longitudinal axis (or roll) were employed on each float. Although some change of equipment and repair took place during the life of the project, all accelerometers employed were of the highly accurate servo type. The design incorporates a feedback mechanism whereby motion of the displacement pickoff produces a countering force (or moment in the case of rotational accelerometers) which accelerates the seismic mass so that it undergoes only a minute displacement from the applied input motion. This feature combined with a flexural suspension system provided for accurate acceleration measurement with minimal nonlinearities and negligible hysteresis. Internal filtering mechanisms provided very clean data, so no additional filtering or detrending was required. Figure 3.4 shows a portion of a recorded acceleration timeseries, in this case the vertical acceleration of the west float. Note that the timeseries clearly resembles a narrow-banded process with few crests appearing in troughs and a well-defined envelope.

iii) Wind Speed and Direction

Wind speed and direction were measured by means of a cup-type anemometer. While the present study does not make use of this

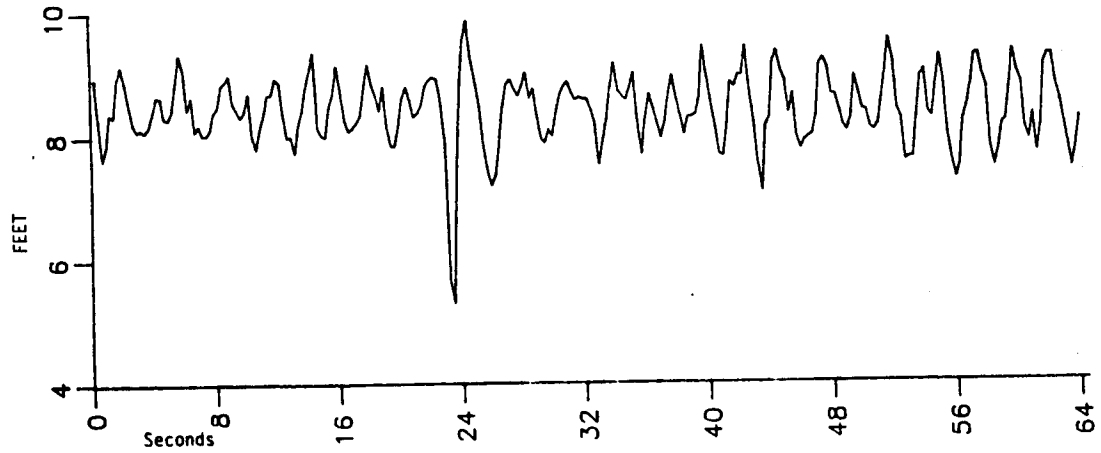

Figure 3.3 Typical Wave Height Record: 64 Seconds of an 8 Minute Timeseries

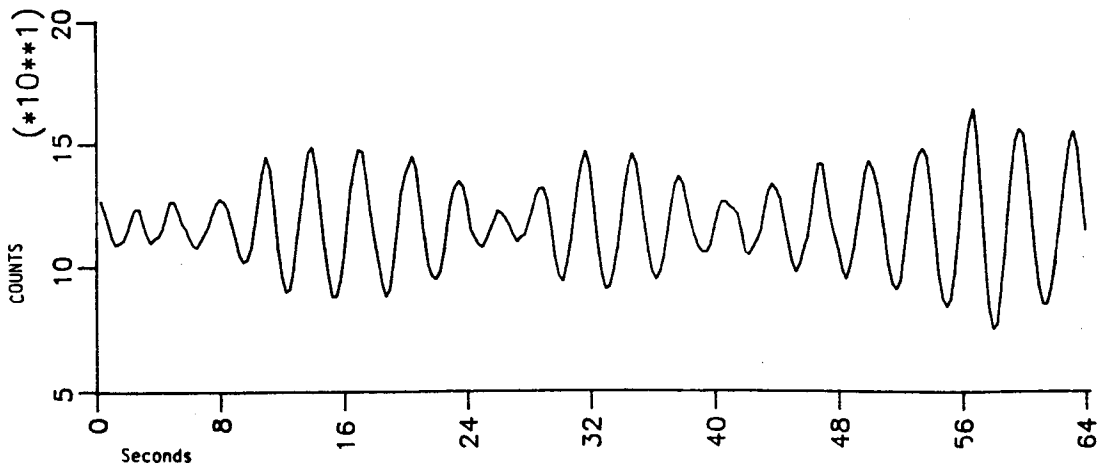

Figure 3.4 Typical Vertical Acceleration Record from West Pontoon (same time sequence as Figure 3.3)

data quantitatively, wind directions and their duration over time are employed as a means in estimating principal angle of wave attack and to a lesser extent, directional distribution of wave energy for input into the model. Actual wind loadings were not considered.

C) Data Reduction Technique

Nearly all applications of the measured data in this report involved obtaining estimates of the power spectral density curves of the timeseries. While several methods exist for accomplishing this, the most common are referred to as the direct and indirect methods (see Geshkinli,(1983)). The indirect method consists of taking the discrete Fourier transform of the autocorrelation estimate of the process, yielding the power spectral density estimate. The second method consists of taking a discrete Fourier Transform of the timeseries directly, squaring the amplitude of the Fourier Coefficients and normalizing the result so that the integral of the resulting function over the frequency domain is equal to the variance of the timeseries. Jenkins (1969) shows that both methods are equivalent for a stationary and ergodic process.

Primarily out of convenience, the direct method was applied in this study, utilizing Fast Fourier Transform techniques. The estimated power spectral density function is then

$$S_{\zeta,est}(f_i) = 2\Delta t n G(f_i) G^*(f_i)$$

where Δt is the sampling interval

$S_{\zeta,est}$ is the power spectral density estimate (henceforth the est will be dropped)

n is the number of samples

f_i is the i^{th} frequency in hertz where i ranges from $1/n\Delta t$ to $1/2\Delta t$

G is the complex Fourier Coefficient at the given frequency

and the superscript * denotes the complex conjugate

The constant $2\Delta tn$ scales the curve so that its area is equal to the variance of the timeseries about the mean.

Incident wave height spectral density estimates are used as an input into the linear model while spectral density estimates of the acceleration timeseries are used for comparison with the output of the model for validation purposes.

CHAPTER IV

ANALYTICAL MODEL

A) Rigid Body Assumption

The application of ship motion theory to the West Point Breakwater is valid only to the extent that the breakwater behaves as a rigid body. Since a rigid body is a mathematical abstraction which is assumed as a matter of convenience, it is worth the time to make some rudimentary checks to see if such an assumption can be justified.

While a rigid body assumption might be out of place for a long, flexible continuous structure such as a floating bridge, the dimensions of the breakwater under consideration are more along the lines of a beam with a length to depth ratio of 30 for vertical bending. If, under some set of reasonable support conditions, it can be shown that bending deformations due to the weight of the breakwater are small compared to the measured motions, then it would seem reasonable to neglect structural deformation of the body as a first approximation in predicting its response. Calculations included in Appendix B indicate a deflection of about 0.25 inches for the breakwater simply supported on the crests of 75 foot waves propagating in the direction of the breakwater long axis. Such conditions would virtually never be reached in the test site. This deflection is on the order of 1/240 of the depth of the breakwater and only a small fraction of the typical measured significant heave displacement which is about 1.25 feet for an incident significant wave height of around 2 feet. Furthermore, rough calcula-

tions (see Appendix B) indicate that the natural frequency of vibration of the breakwater in vertical bending is in the neighborhood of 1.9 hertz. This frequency is out of the region of any significant excitation energy due to waves, so vibrational motions are unlikely to contribute deformations of a large enough magnitude to disturb the rigid body hypothesis in the frequency range of interest. The cutoff frequency for the measured data is 2.0 hertz and it is not unlikely that the true frequency of vibration is higher than calculated due to stiffnesses that have not been taken into account.

Wave and/or wind drift forces could put a non-harmonic load on the structure which might cause additional deformation when resisted by the mooring lines. Such loadings clearly would not cause deformations of the order of magnitude of the measured motions.

The rigid body assumption appears to be a reasonable one for this situation.

B) Floating Breakwater as a Linear System

If the breakwater is considered to be a linear system, it may be represented by means of a system of second order linear coupled ordinary differential equations which may be solved at discrete frequencies and the solutions summed to obtain the total response. Similarly, for the problem to retain a linear character, a water wave based on a linear velocity potential must be assumed in the fluid domain. If this were not the case, hydrodynamic terms would have to be evaluated separately for each input wave height, requiring a prohibitive amount of computation

(assuming a practical technique for solution existed). The usual assumptions implied in a linear velocity potential (incompressible, inviscid fluid, irrotational flow etc.), therefore, apply. In particular, water motion amplitudes and velocities are considered "small" so all but the linear terms of the free surface condition, kinematic boundary condition on the cylinder, and the Bernoulli equation may be neglected. These assumptions are consistent with "small amplitude" or linear wave theory.

Figure 4.1 depicts the breakwater model as a linear system. The system input is the directional incident wave field with phases expressed with reference to a fixed point in inertial space. Solution of the equations of motion for a unit wave amplitude yield complex frequency response operators $H_\eta(w)$ defining a direct linear transformation between the system input, $\zeta(x,y,w,\theta)$, and the system output, the breakwater motions $\eta_j(x,y,w)$.

Components within the system may be viewed as lineartransformations as well. The forcing function $F_i(x,y,w,\theta)$ is obtained by integrating the pressure field derived from the velocity potential of the appropriate linear wave over the body contour. The body is assumed to be rigidly fixed in the incident wave field. Similarly, added mass and damping are obtained by complex integration involving pressure fields derived from an appropriate linear velocity potential (for a complete description of what criteria such a potential must have, see Frank (1967). In this case the body is subjected to unit amplitude oscillations in calm water. The details of the determination of the hydrodynamic

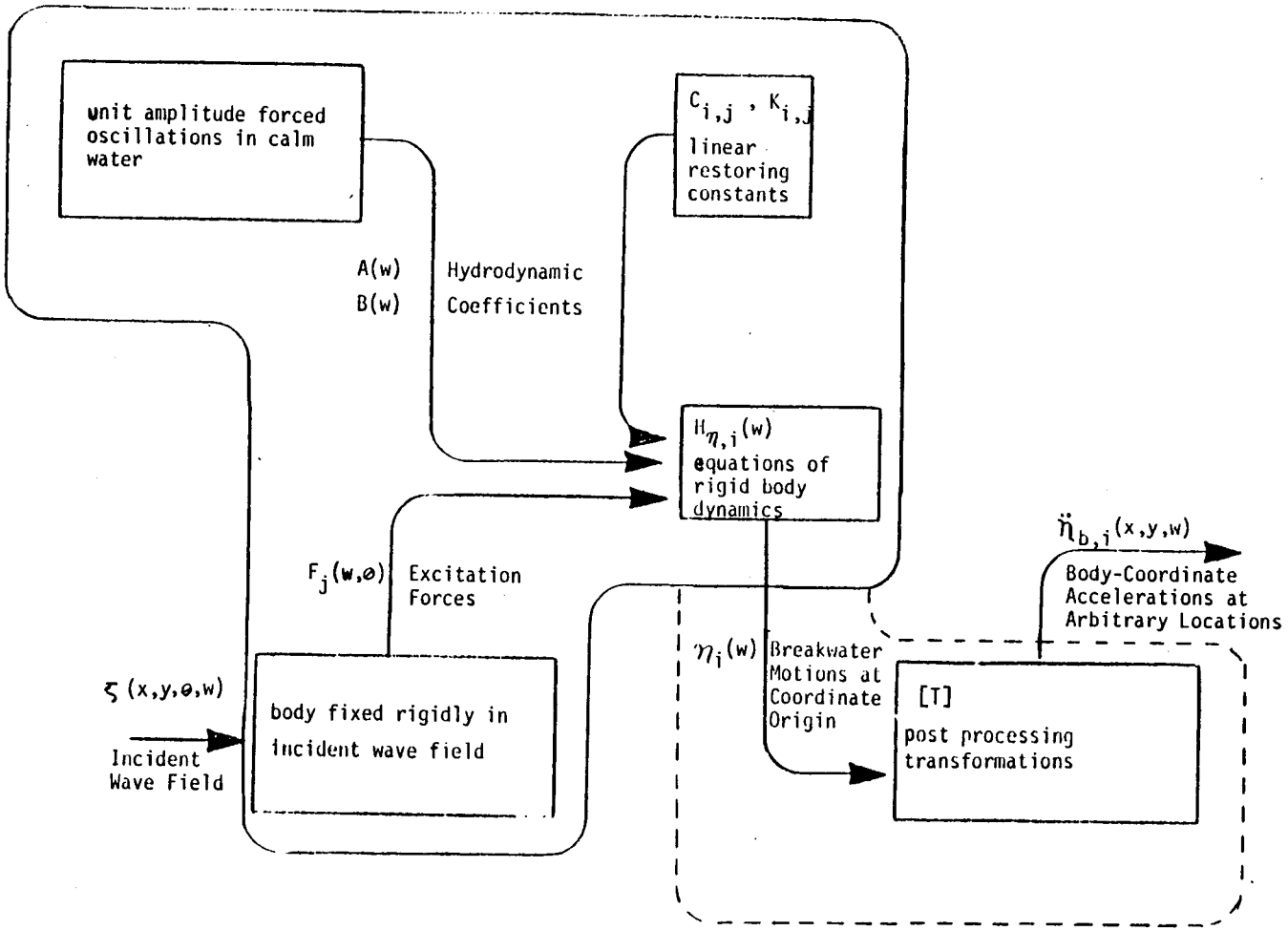

Figure 4.1 Floating Breakwater as a Linear System

quantities required for solution of the equations of motion are beyond the scope of this work but the reader who is interested in the theoretical and numerical aspects of this important procedure is referred to Frank (1967) and Vugts (1970).

C) Governing Equations of Frequency Domain Analysis

Only a brief treatment will be made of the equations governing frequency domain analysis, since detailed treatment is available from a variety of sources. The reader seeking more information is referred to Salveson (1970) for a fairly up-to-date treatment of the topic and full listing of the relevant equations for all the hydrodynamic terms included in the equations of motion. An excellent survey of the field including a full explanation of the response statistics may be found in Ochi (1974). Since the above references are written primarily with ships in mind, they include no treatment of mooring forces.

The basic equation of motion for six degree-of-freedom rigid body response written about the origin shown in Figure 1.1 is:

$$\Sigma_{j=1}^{6} (I_{ij} + A_{ij}(w)\ddot{\eta}_j + B_{ij}(w)\dot{\eta}_j + (C_{ij} + K_{ij})\eta_j \qquad 4.1$$

$$= F_i e^{iwt}; \text{ for } i=1,6;$$

where I is the inertia coefficients matrix,

A is the added mass coefficients matrix,

B is the hydrodynamic damping coefficients matrix,

C is the hydrostatic restoration coefficients matrix,

K is the linearized mooring force restoration matrix,

F is a complex amplitude vector consisting of 6 wave excitation forces,

w is the angular frequency of the incident wave,

η_j is a complex vector describing the amplitude and phase of the motion in the jth direction in the equilibrium frame,

e^{iwt} is a unit vector rotating with angular frequency w and the dots indicate differentiation with respect to time.

The term "coefficients" is used in a mathematical sense and is not intended to imply non-dimensionality.

Some comments about each of the terms is appropriate.

i) Inertia

I_{11}, I_{22}, and I_{33} are simply the mass of the body. The diagonal terms corresponding to j = 4-6 are the mass moments of inertia written about the origin shown in Figures 1.1 through 1.3. The offset of the coordinate origin from the center of mass in the vertical direction gives rise to a $I_{42} = -MZ_{cg}$ term. No other cross-terms exist for a rectangular breakwater.

ii) Hydrodynamic Mass

The hydrodynamic or added mass is the coefficient in the equations of motion which accounts for that portion of the force on the body proportional to the complex acceleration. Complete equations for these terms may be found in Salveson (1970). Hydrodynamic mass is defined as such primarily as a convenience in setting up the equations of motion and should not be interpreted as a definite volume of water which is somehow being

accelerated with the body. It is sometimes described as the difference in inertia between the body oscillating in calm water and the body oscillating in air at angular frequency w.

iii) Hydrodynamic Damping

The coefficient accounting for that portion of the force on the body which is proportional to the complex velocity is commonly referred to as hydrodynamic damping. Hydrodynamic damping accounts for energy radiated from the body as gravity waves produced by its oscillations. It should not be confused with square law or any other higher power damping which would result in non-linear equations of motion. Inclusion of linear (hydrodynamic) damping is sufficient to produce satisfactory results for all degrees of freedom except roll, where viscous damping may play an important role (Ochi, 1974; Schmitke, 1978). Both hydrodynamic damping and mass are functions of the body geometry, frequency, and the linearized velocity potential only. The frequency dependent portion of both hydrodynamic mass and damping arises as a result of oscillations at the fluid surface. The only significant off-diagonal terms in either hydrodynamic coefficient matrix for a rectangular pontoon breakwater are A_{42} and B_{42}; roll coupled into sway.

iv) Hydrostatic Restoring Constants

The only non-zero hydrostatic restoring terms for a rectangular breakwater are C_{33}, C_{44}, and C_{55}. The expressions for these are

$$C_{33} = \rho g A_{wp} \qquad 4.2$$

$$C_{44} = \rho g \nabla GM_t \qquad 4.3$$

$$C_{55} = \rho g \nabla GM_L \qquad 4.4$$

where ρ is the density of seawater

g is the acceleration of gravity

∇ is the immersed volume of the body

A_{wp} is the area of the body at the waterplane

GM_t is the transverse metacentric heightabove the center of gravity.

GM_l is the longitudinal metacentric height abovethe center of gravity.

Also

$$GM = KB + BM - KG \qquad 4.5$$

where

KB = distance from keel to center of buoyancy

BM = distance from center of buoyancy to metacenter

KG = distance from keel to center of gravity

and $$BM = I_{wp}/\nabla \qquad 4.6$$

I_{wp} is the area moment of inertia of the body at the waterplane about the appropriate axis

These terms may be derived from statics. For further explanation of the derivation of these terms, the reader may consult any textbook on naval architecture or marine dynamics such as Bhattacharyya (1978).

v) Mooring Force Restoring Constants

A linear spring stiffness was used to model the mooring restraints. No account was made in the model of any hydrodynamic terms arising from the mooring system itself. A "quasi-linear" or iterative approach may be used as mentioned by Vassiliopoulos

(1971), and Ochi (1974) to account for weak non-linearities in the restoration forces. The potential for such a technique is limited, however, since drift forces are still not considered. Furthermore, a quasi-linear approach was found necessary to account for viscous roll damping and it was felt that successive solutions while varying two coefficients would lengthen the computational procedures considerably.

vi) Exciting Forces

Exciting forces are functions of frequency, angle of attack, and breakwater geometry. They are obtained by integrating the pressure field arising from the velocity potential of a linear water wave over the submerged surface of the body, the assumption being made that the input wave is not altered by the breakwater motion itself. The phase of the exciting force is referred to the same global origin as the incident wave which may be construed as that in Figures 1.1 to 1.3. It should be noted that since the term e^{iwt} is in phase with the incident wave at the origin, the phase information relative to this datum is contained in the complex amplitude F.

vii) Reduction of Equations of Motion to an Algebraic System

If equation 4.1 is rewritten in more compact form, dropping the subscripts and allowing [ ] to denote matrices and { } vectors the following equation is obtained:

$$[I + A]\{\ddot{\eta}\} + [B]\{\dot{\eta}\} + [C + K]\{\eta\} = \{Fe^{iwt}\} \qquad 4.6a$$

Based on the assumption that η is harmonic, the following substitution is made:

$$\{\eta\} \quad \{\tilde{\eta} e^{iwt}\} \tag{4.7}$$

$$\{\dot{\eta}\} = iw\{\tilde{\eta} e^{iwt}\} \tag{4.8}$$

$$\{\ddot{\eta}\} = -w^2\{\tilde{\eta} e^{iwt}\} \tag{4.9}$$

where $\tilde{\eta}$ is a complex vector which is rotating with angular frequency w; giving

$$[C + K - w^2(I + A) + iwB]\{\tilde{\eta}\} = \{F\} \tag{4.10}$$

where the e^{iwt} term has been cancelled. A system of second ordinary differential equations has been reduced to an algebraic system. If

$$\{\tilde{\eta}\} = \{u + iv\} \tag{4.11}$$

is substituted and real and imaginary parts are collected the following two sets of six equations are obtained:

$$[(C + K) - w^2(I + A)]\{u\} - w[B]\{v\} = \text{Real}(\{F\}) \tag{4.12}$$

$$w[B]\{u\} + [(C + K) - w^2(I + A)]\{v\} = \text{Imag}(\{F\}) \tag{4.13}$$

where u and v are the real and imaginary parts of $\tilde{\eta}$ respectively.

It is worthy of mention that the $[C + K] - w^2[I + A]$ expression in equations 4.12 and 4.13 weights the influence of the linear-spring terms to the lower frequencies while inertia terms predominate at higher frequencies.

viii) Displacement Frequency Response Operators

Equations 4.12 and 4.13 for a six-degree-of-freedom system represent a system of twelve coupled algebraic equations. If these equations are solved using excitation forces derived from

unit-amplitude waves at attack angle θ, the solution results in the complex frequency response operator $H_{\eta,j}(w, \theta)$ describing the magnitude and phase of the displacement response η_j relative to the input wave. Some authors refer to this quantity as the transfer function or the frequency response function.

D) Modeling of Square Law Roll Damping

It was mentioned previously that higher order damping terms have been found necessary to obtain reasonable results in roll. An approximation to square law roll damping may be obtained by equating the energy dissipated by the nonlinear viscous effect during one roll cycle to that dissipated by a linear damping term. Since terms involving the roll amplitude appear in the linearized roll damping coefficient, B^*_{44}, the solution must be pursued iteratively until the roll amplitude assumed is sufficiently close to that calculated.

The following development is based on Schmitke (1978). For a breakwater with zero forward speed, the equivalent linear viscous roll damping coefficient is expressed as the sum of the contribution from the eddy-making resistance of the hull, B_E, and that due to hull friction, B_H; that is:

$$B^*_{44} = B_E + B_H \qquad 4.14$$

Each of these contributions will now be briefly developed.

i) Eddy-making

An expression for the roll-resistance force due to eddy-making is

$$F = (1/2)\rho(r\dot{\eta}_4)^2 QC \qquad 4.15$$

where r is the distance from the origin to the point of eddy generation, assumed to be the bottom corners of the breakwater, ρ is the density of seawater, Q is the wetted surface area of the hull section and C is a drag coefficient depending upon hull shape. Assuming that

$$\eta_4 = /\eta_4/\sin wt \qquad 4.16$$

the torque about the origin is

$$T = Fr = (1/2)\ \rho r^3 QC/\eta_4/^2 w^2 \cos^2 wt \qquad 4.17$$

and the energy dissipated during one rolling cycle is

$$E = 4\int_0^{/\eta 4/} T d\eta_4 = (4/3)\ \rho r^3 /\eta_4/^3 w^2 QC \qquad 4.18$$

Similarly, B_E is a torque about the origin against which

$$4\int_0^{/\eta 4/} B_E \eta_4 d\eta_4 = 4w^2 B_E \int_0^{\pi/2w} \cos^2 wt\ dt = \pi w B_E /\eta_4/^2 \qquad 4.19$$

work is done. Combining equations 4.18 and 4.19 gives

$$B_E = (4/3\pi)\rho w /\eta_4/ r^3 QC \qquad 4.20$$

Empirical equations are presented in Appendix 3 of Schmitke (1978) who is citing N. Tanaka in "A Study on the Bilge Keels." For the breakwater under consideration these reduce to

$$C = .25\exp\{-(1.41-46.7/\eta_4/ + 61.7/\eta_4/^2)R_e/D\} \qquad 4.21$$

where R_e is the effective bilge radius and D is the draft. The bilge radius is the radius of curvature at the point of eddy generation.

ii) Hull Friction

Using similar arguments to those just stated, the equivalent linear hull frictional coefficient is given by

$$B_H = (4/3\pi)\rho w/\eta_4/C_{Df}\int_L\int_{WP} r(yn_2 + zn_3)^2 ds\, dx \qquad 4.22$$

where C_{Df} is a skin friction drag coefficient, n_2 and n_3 are unit outward normals in the indicated directions, the integration in the x direction is over the length of the body and the contour WP refers to the sectional wetted perimeter where s is used as the variable of integration along WP, and

$$r = (y^2 + z^2)1/2 \qquad 4.23$$

The drag coefficient, C_{Df}, for a breakwater may be expressed as

$$C_{Df} = 1.328\, R_n^{-0.5} + 0.014 R_n^{-0.114}, \qquad 4.24$$

$$R_n = (3.22/D\nu)\,(\bar{r}^*/\eta_4/)^2 \qquad 4.25$$

where r is the average distance from the origin, D is the draft, ν is the kinematic viscosity of seawater, and R_n is a Reynolds number based on average rolling velocity and r.

E) Post Processing

The term post processing is used in reference to all operations which occur after the equations of motion are solved. This is a convenient distinction to make in the analysis because often the same equilibrium-frame motion frequency response operators may be used to model several different choices of input spectra, directional spreads of the same input point spectrum, or

heading angles. Similarly, once obtained the operators may or may not be differentiated with respect to time, transformed into body coordinates or to other spatial locations.

i) Successive Differentiation to Obtain Acceleraton FROs

It may be seen from the following expressions

$$H_{\dot{\eta}}(w, \theta) = d/dt \{/H_{\eta}(w, \theta)/e^{iwt}\} = iw/H_{\eta}(w, \theta)/e^{iwt} \quad 4.26$$

and $$H_{\ddot{\eta}}(w, \theta) = d^2/dt^2\{/H_{\dot{\eta}}(w, \theta)/\} = -w^2/H_{\eta}(w, \theta)/e^{iwt} \quad 4.27$$

that integrating in the frequency domain is simply a matter of scaling the FRO's by a factor of iw.

ii) Transformation of FRO's

The solution of the equations of motion results in frequency response operators which are referred to the origin of the (x,y,z) coordinate system. In general, two transformations are necessary in order to bring the predicted accelerations into the frame of reference of the measured accelerations. The operators must first be transferred to the spatial locations on the breakwater that are of interest. Secondly, they must be transformed into body coordinates.

a) transfer of FRO's to other locations

In general, if A is the vector of translational frequency response operators and R is the rotational frequency response operator vector then

$$\{A(x,y,z)\} = \{A_0(x_0,y_0,z_0)\} + \{R_0\} x \{r\} \quad 4.28$$

$$\{R\} = \{R_0\} \quad 4.29$$

where the subscript o denotes the original position (in this case the origin about which the equations of motion are solved), $\{r\}$ is the position vector from (x_o, y_o, z_o) to (x,y,z), and x denotes the vectorcross product. The relations expressed in equations 4.28 and 4.29 are valid for $\{A\}$ and $\{R\}$ expressing motions, velocities, or accelerations in global coordinates. Equation 4.29 expresses the fact that the frequency response operators relating to angular quantities are not functions of position on the body and remain invariant to a spatial transformation.

b) Conversion to body coordinates

Accelerations in the body coordinate system are defined by the following relation

$$\{\ddot{A}_b\} = [T]\{\ddot{A}\} \qquad 4.30$$

The small-angle coordinate transformation matrix T for a sequence of rotation of the Euler angles η_6, η_5, η_4 is

$$[T] = \begin{bmatrix} 1 & \eta_6 & -\eta_5 \\ -\eta_6 & 1 & \eta_4 \\ \eta_5 & -\eta_4 & 1 \end{bmatrix} \qquad 4.31$$

If surge is neglected as in this analysis, then only the lower right 2 x 2 submatrix need be considered. A development of

the coordinate transformation matrix may be obtained from any textbook on rigid body dynamics. A graphical depiction of this transformation in two dimensions (neglecting surge) is shown in Figure 4.2.

In attempting to compare analytical results to measured quantities, it must be determined what account is to be made, if any, of the gravity vector. The servo-accelerometers do not measure a constant gravitational pull. For the small roll and pitch angles which are normally encountered, the component of the gravity vector normal to the breakwater deck would remain nearly constant, and would have a negligibly small harmonic component. This would not be the case, however, for transverse accelerations. As the breakwater undergoes a roll angle, a component of the earth gravity vector acts transverse to the breakwater. This component is "felt" by the transverse or "sway" accelerometers as an acceleration with an opposite sense as the gravity vector. Figure 4.3 depicts the following transformation:

$$\ddot{\eta}_b',2 = \ddot{\eta}_b,2 + g\sin(\eta_4) \qquad 4.32$$

which for small angles become

$$\ddot{\eta}_b',2 = \ddot{\eta}_b,2 + \eta_4 g \qquad 4.33$$

The final form of the transformation into body coordinates for the two translational degrees of freedom under consideration (dropping the ') is then

$$\ddot{\eta}_b,2 = \ddot{\eta}_2 + \ddot{\eta}_3 \ \eta_4 + g\eta_4 \qquad 4.34$$

$$\ddot{\eta}_b,3 = \ddot{\eta}_3 + \ddot{\eta}_2 \ \eta_4 \qquad 4.35$$

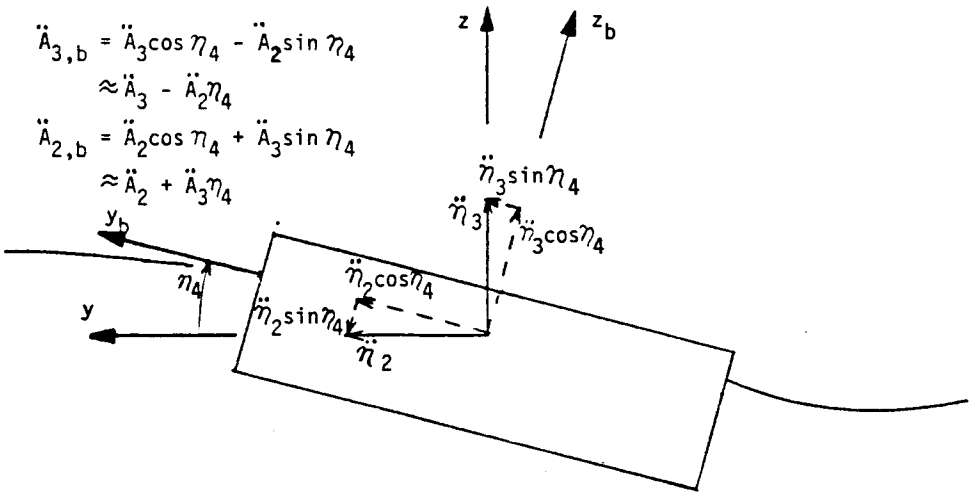

Figure 4.2 Transformation of Acceleration Vector into Body Coordinates

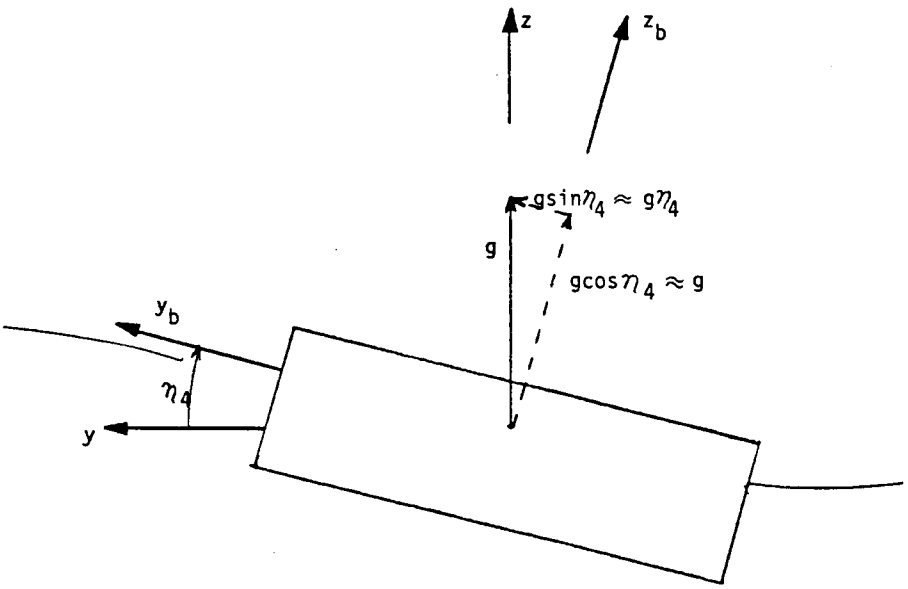

Figure 4.3 Resolution of Gravity Vector into Body Coordinates

iii) Directional Sea Input

The analytical model presented thus far has developed acceleration frequency response operators in body coordinates at the desired locations on the breakwater. In order to formulate a response spectrum the equation

$$S_{resp}(w) = H_{resp}(w, \theta)S_{input}(w, \theta)H^*_{resp}(w, \theta) \qquad 4.36$$

is used. Here, "resp" and "input" are used to signify general input and response categories while H is the FRO defining the transformation between them. It has been shown that the frequency response operators obtain their dependency on attack angle, θ, from the wave excitation force. Little has been said, however, about the dependency of the input or incident wave height spectrum on θ. While a unidirectional wave spectrum is conceivable (ocean swells and boat wakes might approach such a case), a more general wave spectrum would also be a function of direction S_ζ (w, θ). Such a sea spectrum is often said in the literature to represent a short-crested seaway. A common method of treating the directional sea spectrum is to consider it as the product of the point spectrum and a spreading function $\psi(\theta)$ so that

$$S_\zeta(w, \theta) = S_\zeta(w)\psi(\theta) \qquad 4.37$$

To ensure that the directional spectrum contains the same energy as the point spectrum, $\psi(\theta)$ must satisfy the relationship

$$\int_{-\Pi}^{\Pi} \psi(\theta)d\theta = 1.0 \qquad 4.38$$

A commonly used spreading function (Hutchison, 1982; Bhattacharyya,1978) which is employed in this analysis is

$$\psi(\theta) = K\cos^{n}(\theta - \theta_{o}), \quad -90° < \theta - \theta_{o} < 90° \qquad 4.39$$
$$\psi(\theta) = o \text{ otherwise}$$

where K is a normalizing constant chosen to satisfy equation 4.38, θ_o is considered to be the direction of peak wave energy or the principal attack angle and n is an exponent which depends upon the sea state under consideration. As n approaches infinity, the sea state approaches a unidirectional sea.

iv) Response Spectra

The discrete formulation for the body-coordinate acceleration power spectral density function becomes

$$S_{\ddot{\eta},j}(w) = \Sigma_{\theta} S_{\zeta}(w, \theta) H_{\ddot{\eta},b,j}(w, \theta) H^{*}_{\ddot{\eta},b,j}(w, \theta) \qquad 4.40$$

The subscript "b" for body coordinates will henceforth be dropped as all further discussion will occur in body coordinates unless otherwise indicated. The term $H_{\ddot{\eta}}(w,\theta)H^{*}_{\ddot{\eta}}(w,\theta)$ is often referred to as the response amplitude operator in the literature and sometimes as the transfer function. The RAO serves as a linear transformation between the input and the output spectra. From the response spectrum $S_{\ddot{\eta}}(w)$, the response variance may be obtained merely by summing the area under the response power spectral density curve. If the response process is a steady-state

Gaussian process and narrow-banded, then various other statistical quantities may also be inferred by simple application of the appropriate Rayleigh factor. An excellent discussion of the input and response processes and their relationship to one another in the time, frequency, and probability domains may be obtained from Ochi (1974).

The analytical procedure outlined above was carried out on 13 different data sets by means of a digital computer. The reader who wishes to read a description of the computer software used to implement the above model should turn to Appendix A.

CHAPTER V

ANALYSIS AND DISCUSSION

A) Methodology

i) General Approach

Inputs into analytical models such as the one described above generally fall into two categories: those whose values are known with a reasonable degree of accuracy and those whose exact values must be guessed or inferred. Since one of the purposes of this work is to determine which of certain key input values result in accurate response predictions, it was desirable to formulate a systematic procedure for varying input quantities whose values are not certain. Given the not inconsiderable time required for processing field data on the facilities that were available, however, it was also necessary to retain flexibility and room for judgment in order to ensure that a reasonable number of records were examined. The following is a general description of the approach adopted. Basic inputs into the analytical model included the geometrical and inertial properties of the breakwater and linearized force-displacement relationships of the mooring system. Based upon these values, predicted acceleration frequency response operators in the body coordinate system are calculated at the spatial location of the accelerometers using the methods described in the preceding chapter. These operators describe the response of the breakwater to a wave of unit amplitude and specified attack angle. Predicted acceleration autospectral estimates are developed by means of equation 4.40 using the incident wave height autospectral density estimate, $S_{\zeta}(w)$,

based upon measured timeseries, and a suitable spreading function, $\psi(\theta)$.

The predicted autospectra are then directly compared to similar estimates developed directly from digital recordings of field accelerometers as described in Chapter III. The two sets of curves are then compared in various ways and are often distinguished from one another with the adjectives "predicted" and "measured". It should be kept in mind, however, that the "predicted" acceleration autospectra are derived in part by means of "measured" incident wave spectra and that "measured" spectra are estimates as well.

Initially some assumptions about the character of the wave field were necessary. Since measured information regarding the wave field consisted of point spectra only, it was necessary to assume that the principal direction of wave attack, θ_o, coincided with the measured mean wind direction. Clearly this assumption will be valid at some times and not at others.

The remaining quantities to be ascertained or assumed were the value of the exponent n in the cosine power spreading function, the values of any mooring coefficients included in the analysis, the effective bilge radius of the breakwater cross-section, and the reciprocal of the wave steepness, 1/WS, used in roll damping calculations.

It is shown in Section C part v that mooring coefficients noticeably affect the sway accelerations only, while the effective bilge radius and wave slope are parameters used in estimating square law roll damping (see Chapter IV). The value of n is

the only unknown parameter which significantly affects the heave acceleration response. Previous studies (Hutchison, 1977; Orr, 1975) indicate that reasonable results for barge-like shapes may be obtained for heave using strip theory. Since the heave response is largely uncoupled from sway and roll in this analysis, it seemed reasonable to use the heave acceleration response as an initial aid in determining a suitable cosine power for calibration purposes.

Calibration of R_e, the bilge radius, was performed by selecting an input wave spectrum based upon measurements taken during a strong steady wind which blew for several hours directly to beam. A value of n was found which appeared to give good results for heave acceleration response. The values of R_e and the wave slope for roll damping were then varied until good results in roll were obtained. While the wave slope could be expected to change with variations in the wave climate, the bilge radius is a property of the breakwater cross-section and should not change, although its proper value for a cross-section with flat sides and sharp corners is not obvious. Therefore, after initial calibration, its value was not altered in subsequent runs.

Subsequent runs proceeded by varying the value of n and 1/WS to yield the best results possible for the three degrees of freedom of interest. While it would undoubtedly be possible to develop an algorithm which would iteratively converge upon the best possible fit in a least squares sense, the processing time involved would be prohibitive for a microcomputer. Furthermore,

uncertainty in spectral estimates made the value of such a procedure questionable. It appeared to be more practical to rely on graphical output and judgment to determine when results were close enough to optimum for the range of reasonable input values available. In practice this appeared to work quite adequately.

ii) Acceleration Frequency Response Operator Modulus Plots

Although the final output of the analytical model described above was in the form of acceleration autospectral estimates, it was not always convenient to use this form of presentation when investigating the effect of individual parameters. Utilizing equation 4.36 with the measured point spectrum, the following quantity is defined which no longer explicity depends upon θ.

$$/H_{\ddot{\eta},j}(w)/ = \sqrt{\{S_{\ddot{\eta},j}(w)/S_{\zeta,j}(w)\}} \qquad 5.1$$

where the term $/H_{\ddot{\eta},j}(w)/$ is referred to as the modulus or magnitude of the complex frequency response operator. Since both terms on the right hand side of equation 5.1 are available as spectral estimates based upon measured timeseries, the values of $/H_{\ddot{\eta},j}(w)/$ based upon both analytical predictions and measurements may be directly compared. By calculating values for $/H_{\ddot{\eta},j}(w)/$ based on measured acceleration and wave energy autospectral estimates, it is possible to see more readily how the breakwater accelerations respond to wave energy at each frequency. Such a comparison of operator moduli often gives a clearer indication of where problems may be occurring in the analytical solution because the weighting due to variations in the input wave energy is removed. If the breakwater truly behaves as a

linear system, then its operator plots would be identical if the incident wave amplitude only is varied.

As an example, Figures 5.1 and 5.2 show measured and predicted acceleration autospectra while Figures 5.3 and 5.4 show operator moduli for the same data. These two sets of plots are related by the input wave energy spectrum shown in Figure 5.5 through equation 5.1. In this case it can be seen that the fairly reasonable agreement of the two autospectra in general shape and peak values are due to the close coincidence of points on the predicted and measured operator plots in the 0.3 to 0.4 hertz range, but that poorer results would be expected for other input wave spectra. The apparent disparity in peak response between the operator functions, if seen consistently over several timeseries, would be an indication of something wrong with some of the coefficients in the equations of motion or of more general problems with the model.

To avoid confusion, $/H_{\eta,j}(w)/$ based upon seakeeping predictions will henceforth be written $/\hat{H}_{\eta,j}(w)/$ to distinguish it from the corresponding quantity derived from the measured timeseries. The symbol $\hat{}$ will also be used with corresponding sense for other quantities.

iii) Statistical Measures of Predictive Accuracy

It is appropriate to mention that the spectral density functions derived from measurements are estimates. The 95% confidence band for each of the 32 points plotted between 0 and one hertz ranges between 0.65 and 1.75 of the plotted ordinate. In most cases, differences between analytical model outputs and

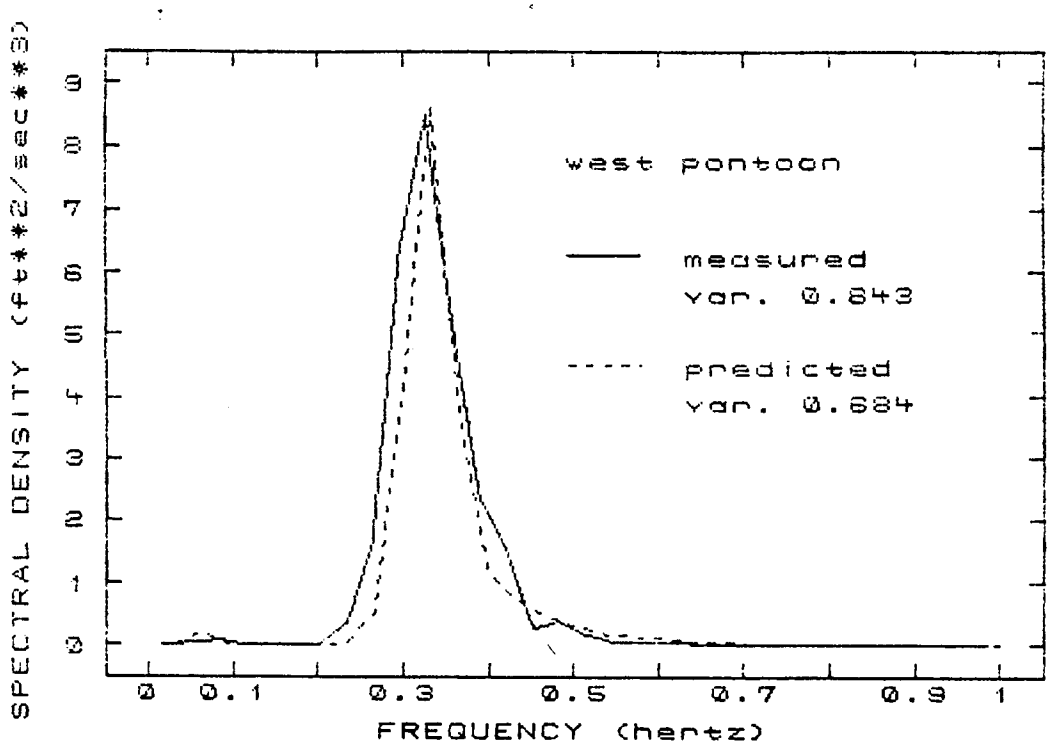

Figure 5.1 Measured and Predicted Sway Acceleration Auto-spectral Estimates for West Pontoon: Run 4

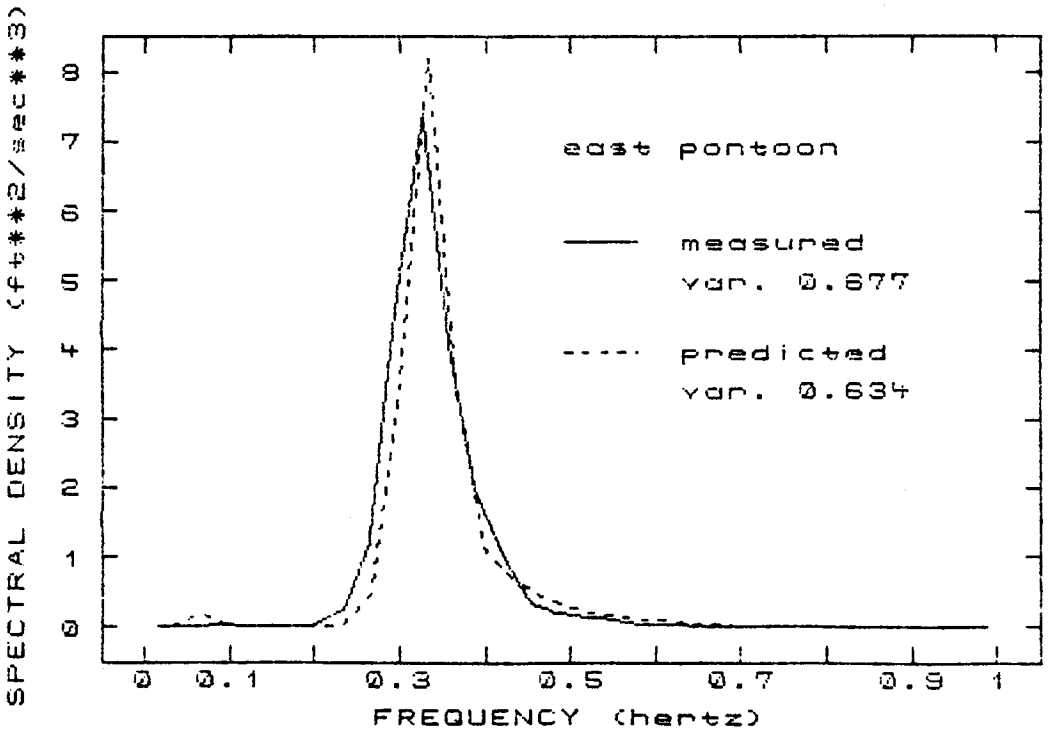

Figure 5.2 Measured and Predicted Sway Acceleration Auto-spectral Estimates for East Pontoon: Run 4

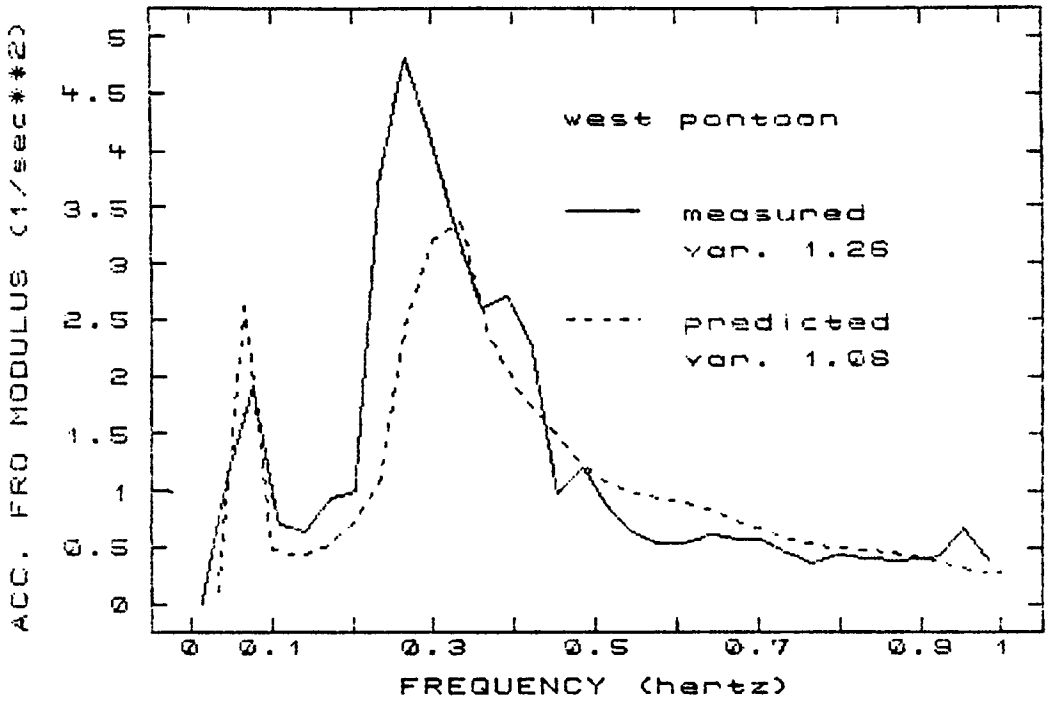

Figure 5.3 Measured and Predicted Sway Acceleration FRO Moduli for West Pontoon: Run 4

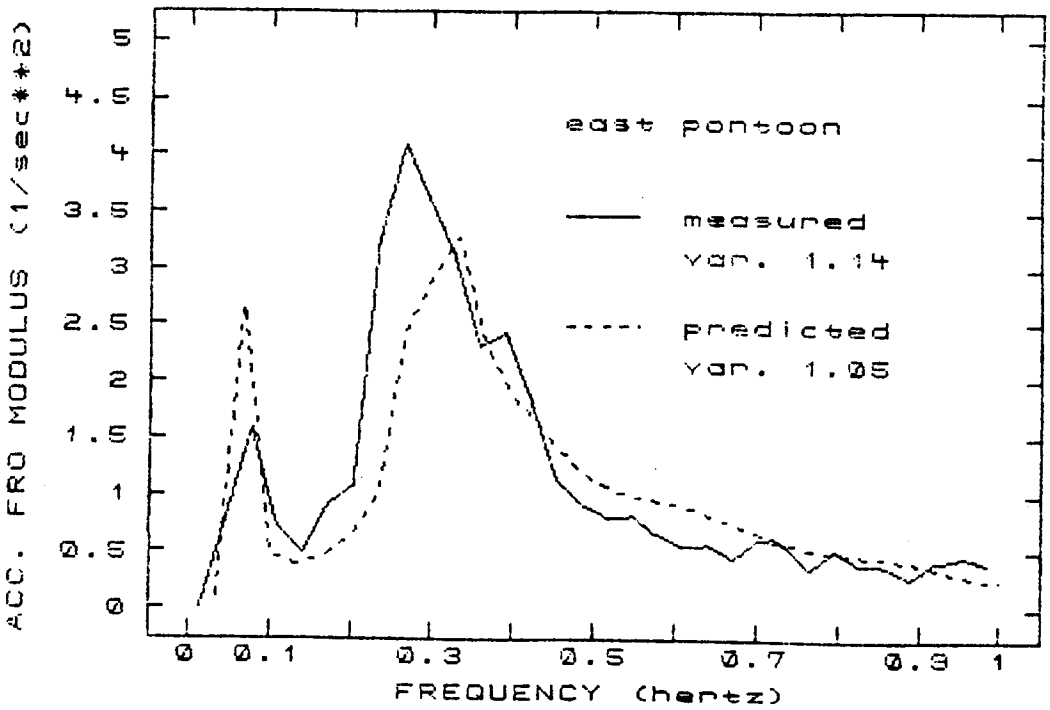

Figure 5.4 Measured and Predicted Sway Acceleration FRO Moduli for East Pontoon: Run 4

spectral estimates based on measurements will fall well within the 95% confidence band. Accordingly, Figure 5.5 is labeled as an estimate but all autospectral and operator plots shown are estimates as well. For this reason, conclusions should be drawn based upon trends in the analysis which appear over several runs rather than upon one record only.

In order to present and discuss the results meaningfully for large numbers of runs, it was desirable to develop some quantitative measure of closeness of the predicted and measured autospectral estimates. Two quantities were used for this purpose: the predicted variance normalized by the measured variance henceforth referred to as the variance ratio, VR;

$$VR = \hat{\sigma}^2 \; / \; \sigma^2 \qquad 5.2$$

and the normalized squared error, E_n^2 as defined by the following equation:

$$E_n^2 = \Sigma_w[\{(\hat{S}_{\ddot{\eta}}(w)/\hat{\sigma}^2) - (S_{\ddot{\eta}}(w)/\sigma^2\}^2] \qquad 5.3$$

where the summation is over each of the discrete frequencies analyzed.

The variance ratio is intended as an indication of the closeness of the predicted to the measured response magnitudes with 1.0 expressing perfect agreement, numbers greater than 1.0 indicating overprediction, and numbers less than 1.0 indicating underprediction of the acceleration response magnitude. This statistic, however, does not consider the closeness of the shapes of the curves under comparison, which may differ appreciably

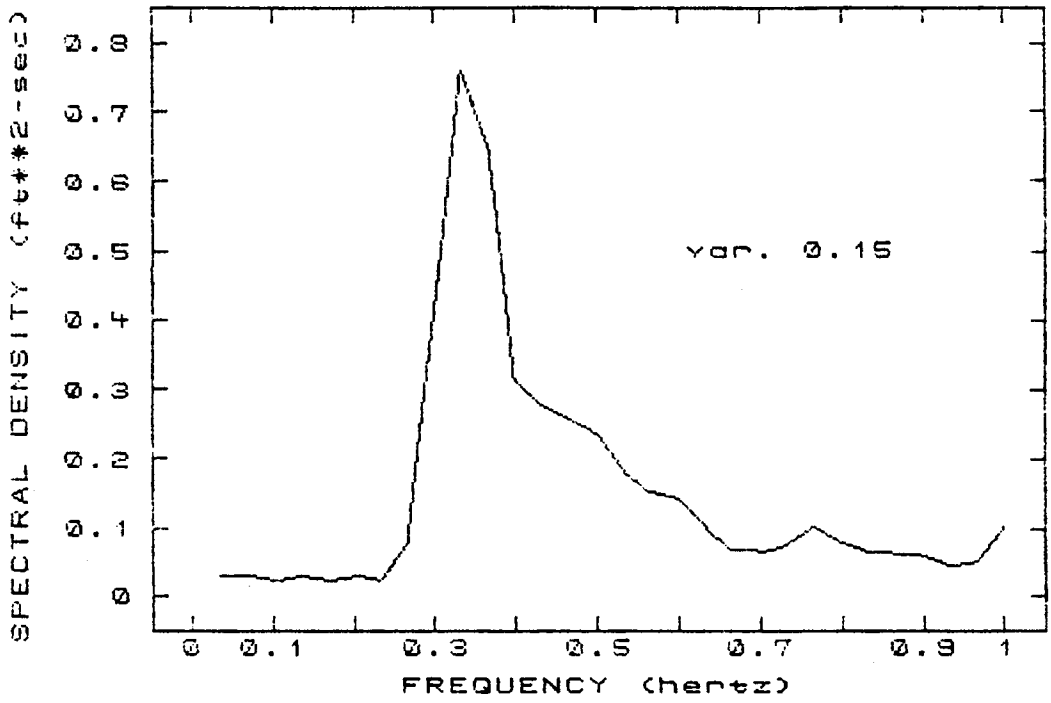

Figure 5.5 Input Wave Height Spectral Estimate: Run 4

while enclosing the same area. When both spectra to be compared are normalized so that each encloses a unit area, the extent to which E_n^2 differs from zero is strictly a result of differences in general shape between the two curves. Identical curves, translated with respect to one another along the frequency axis, however, would have different values of E_n^2.

B) Evaluation of Results

Table 5.1 and Figures 5.6 and 5.7 summarize the results obtained for all model runs made. Overall agreement is generally good except where the wind direction was not steady for several hours or when the significant wave height was low. Wind direction data from routine system sampling was only available every two hours so unidirectional wind duration entries on Table 5.1 marked four hours should be interpreted as greater than four but less than six etc. No obvious overall trends were evident, except perhaps for the sway and roll variance ratios to be low rather than high, while in heave they tended to be slightly high rather than low. It is encouraging that no degree of freedom experienced inordinately poorer results than the others, suggesting proper balance of terms in the equations of motion.

Figures 5.8 through 5.11 show typical graphical results obtained for the heave and roll degrees of freedom while Figures 5.1 through 5.4 depict typical results in sway. The familiar nulls seen on many plots of frequency response operators do not occur here because the excitation sea state is usually not unidirectional and because the spatial position for which the

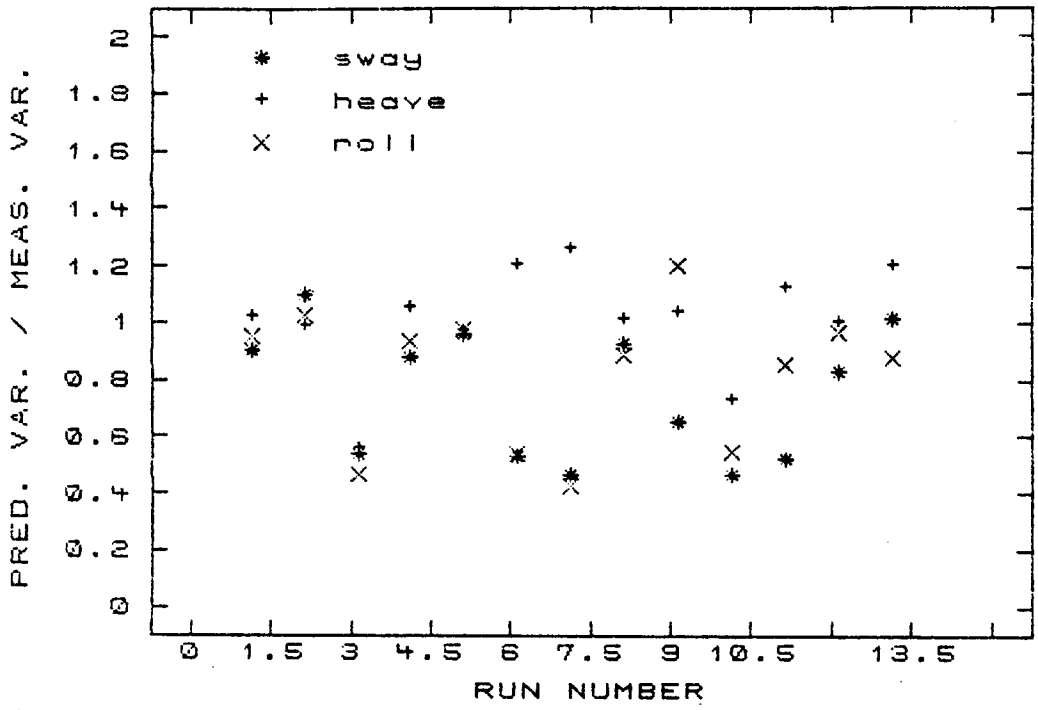

Figure 5.6 Summary of all Runs: Variance Ratios for all Three Degrees of Freedom

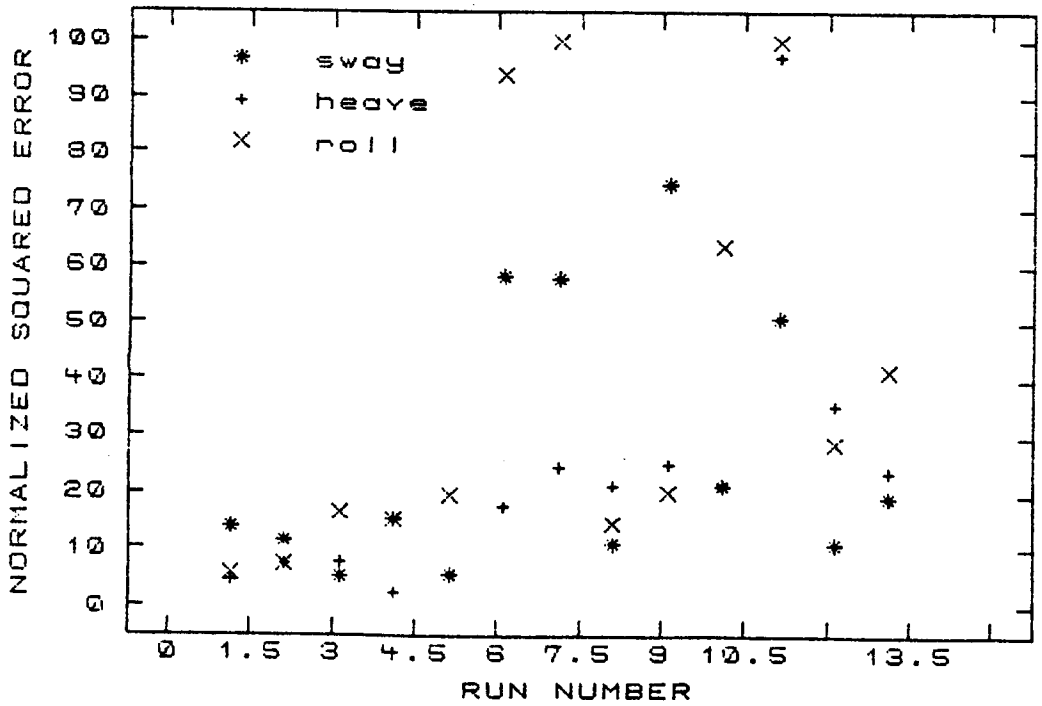

Figure 5.7 Summary of all Runs: Normalized Squared Error for all Three Degrees of Freedom

Date of Rec.	Run #	H_s	Mean Wind Angle	Unidir. Wind Dur.	1/WS	n	HEAVE		ROLL		SWAY	
							VR	E_n^2	VR	E_n^2	VR	E_n^2
		feet	degrees	hours	nd	nd	nd	sec^2	nd	sec^2	nd	sec^2
4/24/83	1	2.1	3.5	6	125	9	1.02	4.6	.95	5.7	.90	13.7
4/24/83	2	1.4	4.2	10	125	*	0.99	7.2	1.03	7.5	1.10	11.4
4/ 8/83	3	1.8	16.5	0	125	7	0.56	7.6	0.46	16.84	0.54	5.5
4/ 8/83	4	1.6	10.0	8	125	7	1.06	2.6	0.93	15.5	0.87	15.3
4/ 9/83	5	1.5	19.0	8	175	18	0.98	5.7	0.98	19.8	0.96	5.9
4/12/83	6	0.8	24.5	2	400	7	1.21	18.0	0.54	93.9	0.53	58.4
4/13/83	7	0.6	25.0	0	400	1	1.27	24.8	0.43	101.0	0.47	58.0
4/24/83	8	1.8	4.3	8	125	18	1.02	21.4	0.89	14.8	0.93	11.1
4/24/83	9	1.9	8.5	2	125	7	1.04	25.3	1.20	20.2	0.65	74.4
5/28/83	10	0.9	27.0	6	300	5	0.73	22.1	0.55	63.4	0.47	21.5
4/23/83	11	1.0	24.2	8	125	9	1.13	97.0	0.85	100.0	0.53	51.2
4/12/83	12	1.0	3.3	8	175	12	1.00	35.6	0.97	28.8	0.83	11.2
5/ 6/83	13	1.2	2.6	8	135	12	1.21	24.1	0.88	41.6	1.02	19.6

* unidirectional wave: n = infinity
nd = non-dimensional

Table 5.1 Summary Statistics for all Model Runs

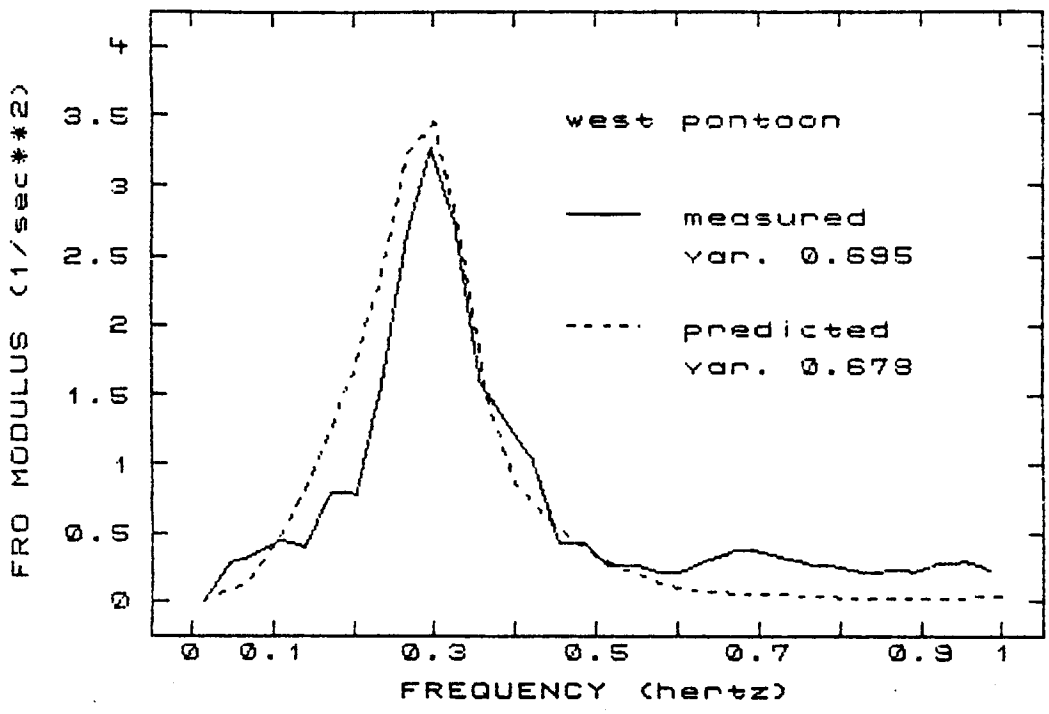

Figure 5.8 Measured and Predicted Heave Acceleration FRO Moduli for West Pontoon: Run 4

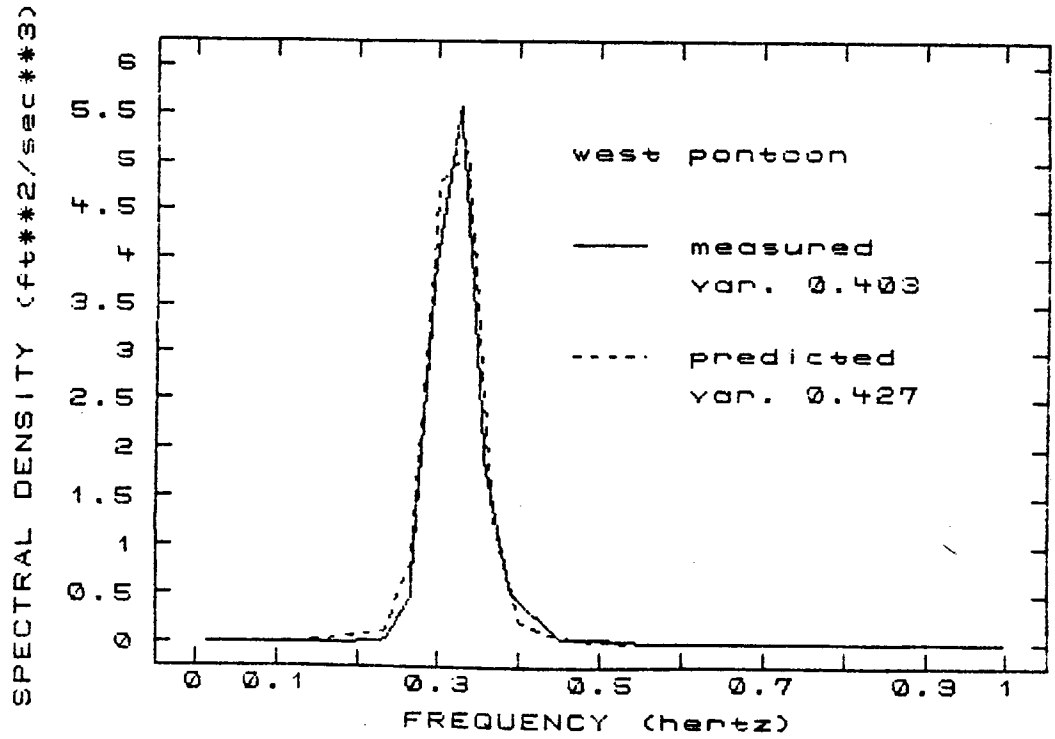

Figure 5.9 Measured and Predicted Heave Acceleration Autospectral Estimates for West Pontoon: Run 4

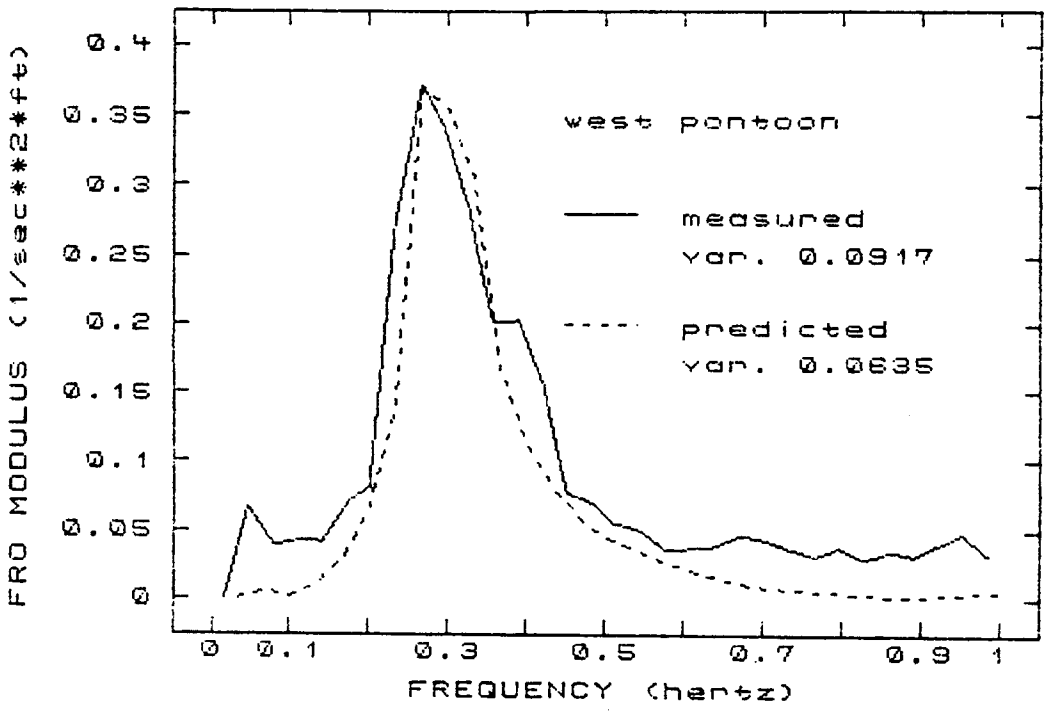

Figure 5.10 Measured and Predicted Roll Acceleration FRO Moduli for West Pontoon: Run 4

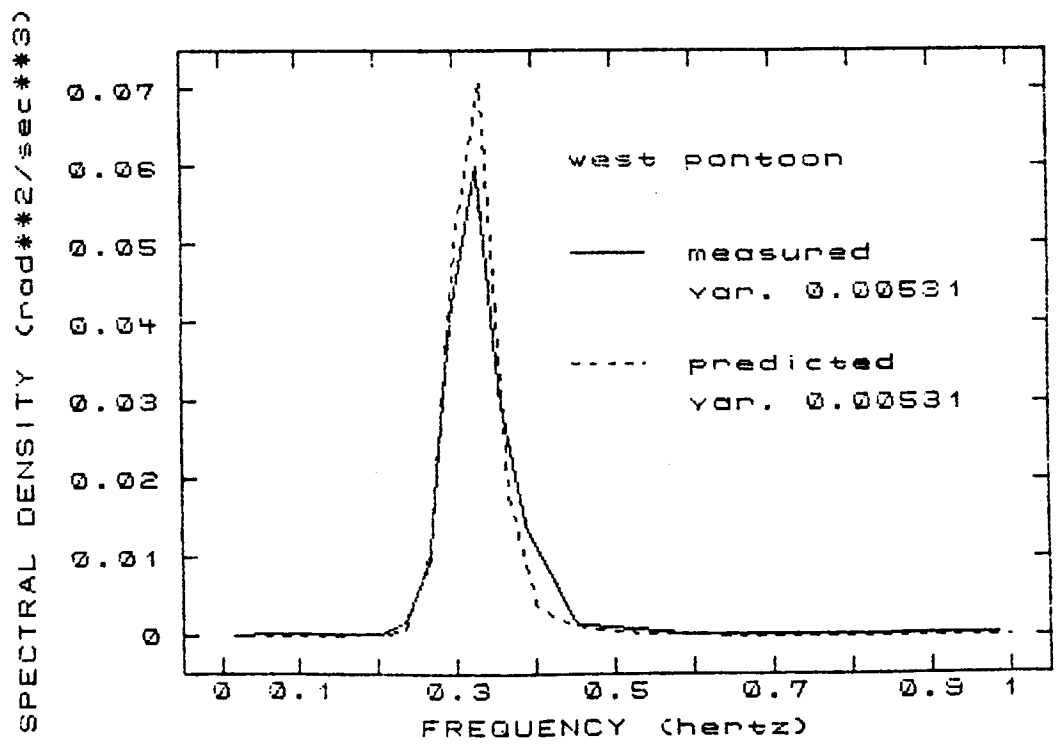

Figure 5.11 Measured and Predicted Roll Acceleration Autospectral Estimates for West Pontoon: Run 4

operators are computed is not at the center of mass of the breakwater but at the location of the accelerometers. This longitudinal offset from the center of mass produces a coupling of heave with pitch and sway with yaw. In addition, the transformation to body coordinates also couples certain modes, further reducing the likelihood of nulls.

An examination of typical acceleration frequency response operator modulus functions shows that the system under consideration acts as a band pass filter in all three degrees of freedom under discussion. Acceleration frequency response operators tend to be the largest in roughly the 0.2 to 0.5 hertz range (corresponding to b/λ of 0.125 to 0.80). Wave energy falling within this band therefore produces significant acceleration responses while wave energy falling outside of it does not have as much effect. Since most incident wave energy at the West Point test site falls within this band, the model need produce accurate operators in this frequency range only to provide good acceleration autospectral estimates under most conditions. In order to provide good estimates under the widest possible range of wave climates, however, it is desirable for the operators to be accurate outside this range as well, particularly in sway where lower frequency operators may not be of negligible magnitude.

A discussion of the results for each of the three degrees of freedom under consideration will now occur.

i) Heave

In general, more consistent results over a wider range of conditions were obtained for heave than for the other degrees of

freedom, particularly on the records examined which had short wind duration and those with recent wind directional shifts. Even when magnitude discrepancies occurred in heave such as run 3, the curve peaks in the correct place. This is not surprising in view of the fewer uncertain input parameters in heave, the relatively small stiffness provided by mooring restraints in this mode, and the absence of significant square law damping effects. Heave acceleration variance ratios ranged approximately from 0.55 to 1.25. The mean variance ratio averaged over all runs was 1.02 while the normalized squared error, E_n^2, in heave averages out to a respectable 22.77 over all runs. This value of E_n^2 is lower than for the other two degrees of freedom, and if the one outlier is discarded, it drops to 16.6.

The estimated natural frequency in heave is approximately 0.31 hertz which agrees well with the measured results. Although in many records the peak input wave energy occurred at or near the heave natural frequency, no need to include higher order damping terms in the model was apparent in this degree of freedom. This fact, a consequence of the predominant effect of free surface wave radiation over other types of breakwater motion-related energy dissipation in heave, has also found to be true for ship forms (Salveson et al., 1970; Ochi, 1974) and barges (Hutchison, 1977).

Some of the heave operator plots based on measurements exhibit values lower than predicted in the 0.18 to 0.25 hertz range (corresponding to deep water wavelengths from 80 to 160 feet or wave periods from 4 to 5.5 seconds). No apparent rela-

tionship is obvious between this phenomenon and wave attack angle, directional spreading power,n, significant wave height, H_s, or any of the parameters investigated. No parallel relationship of the same character appears to exist in the other two degrees of freedom considered. Since both breakwater acceleration response and input wave energy are low in this region, such differences are probably not significant.

ii) Roll

Historically, the accurate prediction of roll motions has been given a good deal of effort among the developers of ship motion theory. In direct opposition to the naval architect's desire for an aerodynamic hull shape looms the question of the stability of the vessel, the location of whose center of gravity might vary significantly under various loadings. While stability is generally not a problem for floating breakwaters, accurate predictions of roll accelerations are important for estimating internal torsional moments.

The general level of agreement obtained in predicting roll motions is quite good. If only records with fairly constant wind directions for at least four hours are considered, then the ratio of predicted to measured variances ranges from 0.85 to 1.03 with a mean of 0.93. A glance at Table 5.1 shows that a slight tendency toward underprediction exists overall. If only records are considered during which the breakwater underwent wave attacks within ten degrees of beam, then the mean variance ratio improves to 0.98.

The estimated roll natural frequency is approximately 0.3 hertz which agrees will with both model output and measurements. In runs 6,7 and 9 the measured peak roll response appears to be shifted slightly toward lower frequencies. Runs 6,7, and 9 are all of short unidirectional wind duration and records 6 and 7 both exhibit low significant wave heights and relatively large angles of wave attack with respect to beam. Oblique wave attack angles tend to shift the forcing functions to lower frequencies (see Figure A.9, Appendix II) but this should be correctly predicted by the analytical model. Perhaps the magnitude of the predicted wave excitation force for roll decays too rapidly as the principal attack angle shifts away from beam. An examination of the corresponding sway operators for these runs discloses a similar trend in all three cases. It therefore appears possible, given the short periods of steady wind direction in all records, that the principal wave attack angle was not coincident with that of the wind. It may be that a directional sea state with two principal directional components or other not easily inferred characteristics is the cause of this discrepancy. Since square law damping was only included in the model in a narrow frequency range (0.28 to 0.32 hertz) it is difficult to explain a shift of the entire operator curves by means of inaccurate estimation of square law damping parameters.

No tendency for response shifts toward lower frequencies with increasing significant wave height was evident. Field observations indicated the occurrence of nonlinear phenomena such as overtopping during storm events of comparable intensity to

some of those under analysis (Nelson et al., 1983). Hutchison (1977), based on his analysis of University of Michigan model tests, hypothesized that shifts in peak roll response toward lower frequencies could occur under extreme conditions due to water on the deck raising the value of the transverse metacentric height. While such an explanation appears quite plausible, direct comparisons between the two situations seem unwarranted due to the extreme loading and seakeeping conditions cited in the model tests and evidence of scaling problems.

While the general shape of the predicted autospectral plots for roll are quite reasonable, higher values were obtained for the normalized squared error, E_n^2 than for heave and sway. The mean value of E_n^2 in roll for all runs was 40.5, while if runs which do not have a directional wind duration of at least 4 hours are discarded, this figure drops to 33. If wind directions within ten degrees of beam only are considered, however, the mean E_n^2 drops to 19.5, exhibiting apparent dependence of accurate roll predictions on the principal angle of attack. The dependence of accurate roll predictions on wind direction is discussed more fully in Section C of this chapter.

Other phenomena of interest include unpredicted rises in the acceleration frequency response moduli, $/H_{\ddot{\eta},4}(w)/$ occurring in many records in the region of 0.4 hertz (see Figure 5.12) This occurrence is also manifested in the sway degree of freedom. The result of this local rise in the FRO is generally a wider banded measured response spectrum than predicted as illustrated by Figure 5.13. If a major portion of the incident wave energy

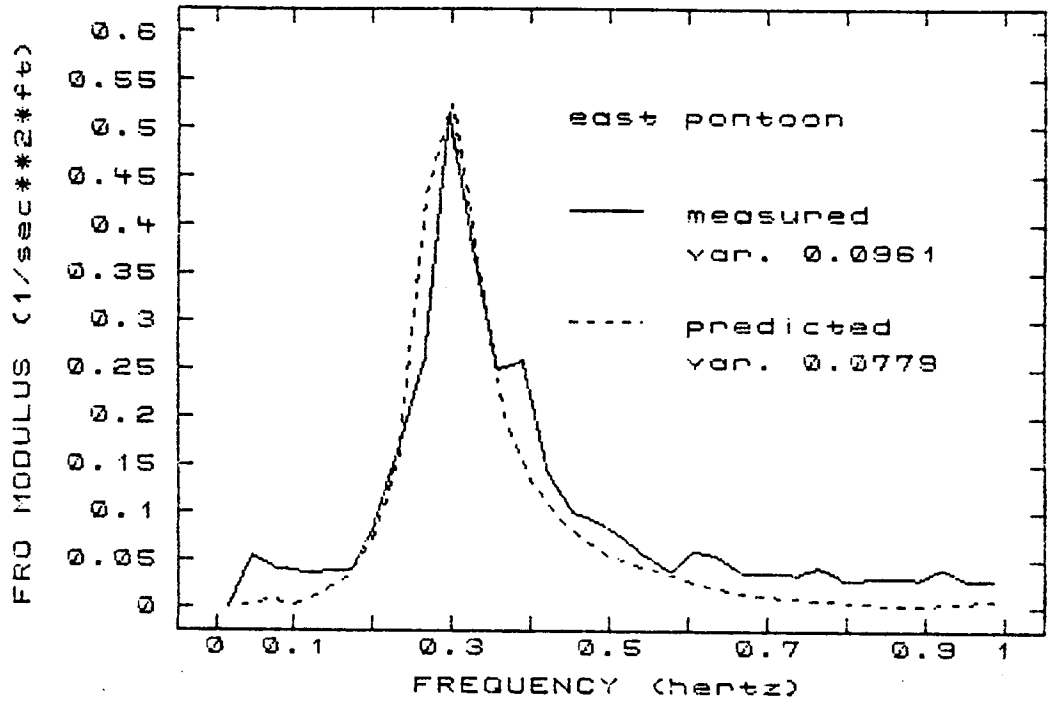

Figure 5.12 Measured and Predicted Roll Acceleration FRO Moduli for East Pontoon: Run 5

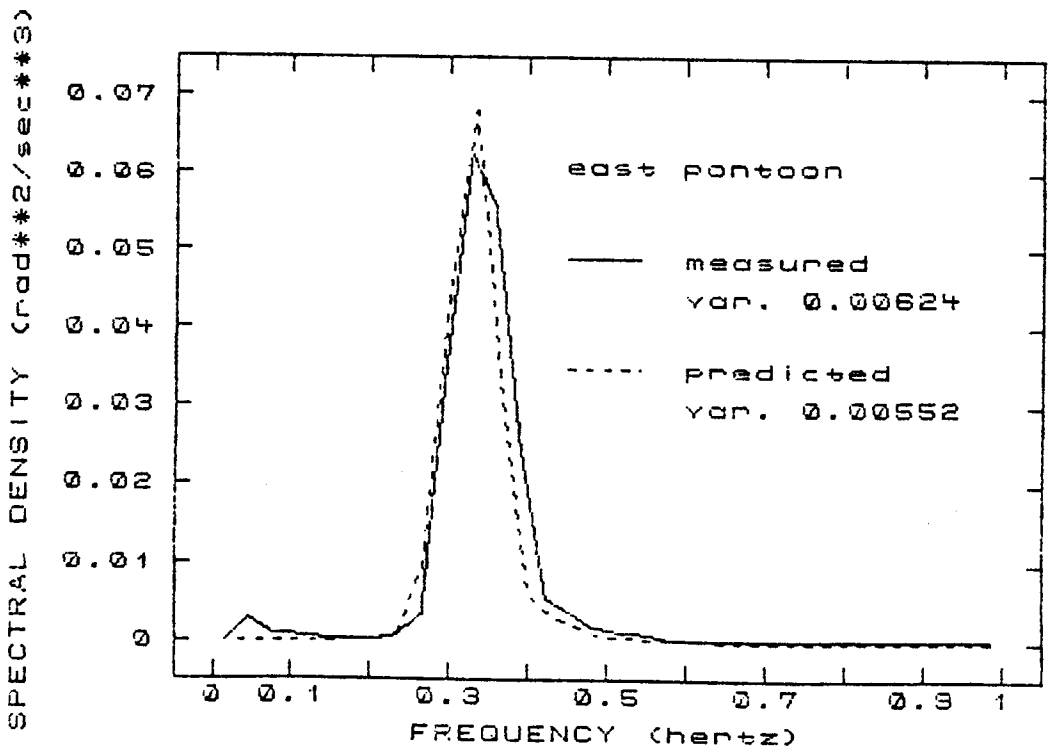

Figure 5.13 Measured and Predicted Roll Acceleration Autospectral Estimates for East Pontoon: Run 5

happens to be in this region, however, it may result in a significant underestimation of the response as illustrated by Figure 5.14.

The reasons for these locally heightened operator moduli in the sway and roll modes are not obvious. The increased prominence at smaller significant wave heights is probably a manifestation of the tendency for smaller seas to have higher percentages of their energy in the 0.4 to 0.55 hertz frequency range. The apparent lack of a consistent parallel trend in the heave mode points to the mooring system as a possible source of such increased excitations. In particular, on-site divers have observed oscillations of the clump weights attached to the mooring system at approximately this frequency. It is not unlikely that the influence of the motions of mooring components could become visible in the acceleration autospectra when the overall breakwater response was low and the incident wave spectrum had much of its energy at higher frequencies. If this explanation is valid, it could have an effect on the dynamic loading characteristics of the mooring system under such circumstances, possibly affecting the fatigue life of some of the mooring components.

In addition to exhibiting the problems just discussed, $/\hat{H}_{n,4}(w)/$ for runs 10 and 11 appeared to have smaller bandwidths overall than the measurement-derived counterparts. This fact is reflected in high E_n^2 values of 63 and 100 respectively for their responses. Both records have significant wave heights less than one foot and principal wave heading angles of about 25 degrees

off beam. It is possible that hydrodynamic damping is overestimated by the model in off-beam seas.

Proper treatment of square law damping in roll was important in obtaining reasonable peak roll amplitudes. Early runs made before the viscous damping model was coded had peak roll responses many times too large. Figure 5.15 shows the values for the reciprocal wave steepness, 1/WS which were found to yield the best results graphed against H_S. All of these values were used with a bilge radius of 0.3 feet. The general trend is certainly what might be expected. Square law roll damping calculations were included only near the roll resonant frequency since the results obtained elsewhere in the frequency domain were not found to differ appreciably either way.

Consideration of higher order effects increases the processing time required by a not inconsiderable margin. For this reason, iterations were performed with beam seas excitation forces and the resulting equivalent damping coefficent, B^*_{44}, applied at all other angles. Strictly speaking, the theory is developed for the beam seas case. While it is possible that this approach is partially responsible for the poorer results obtained for off-beam principal attack angles due to overdamping, the discrepancies obtained as the wave attack moved off beam were not localized near the roll natural frequency. Any overdamping which occurred outside this narrow window must therefore be due to overestimation of linear damping or other causes.

The value for the bilge radius, R_e, used in square law damping estimation was 0.3 feet. Since no guidelines for

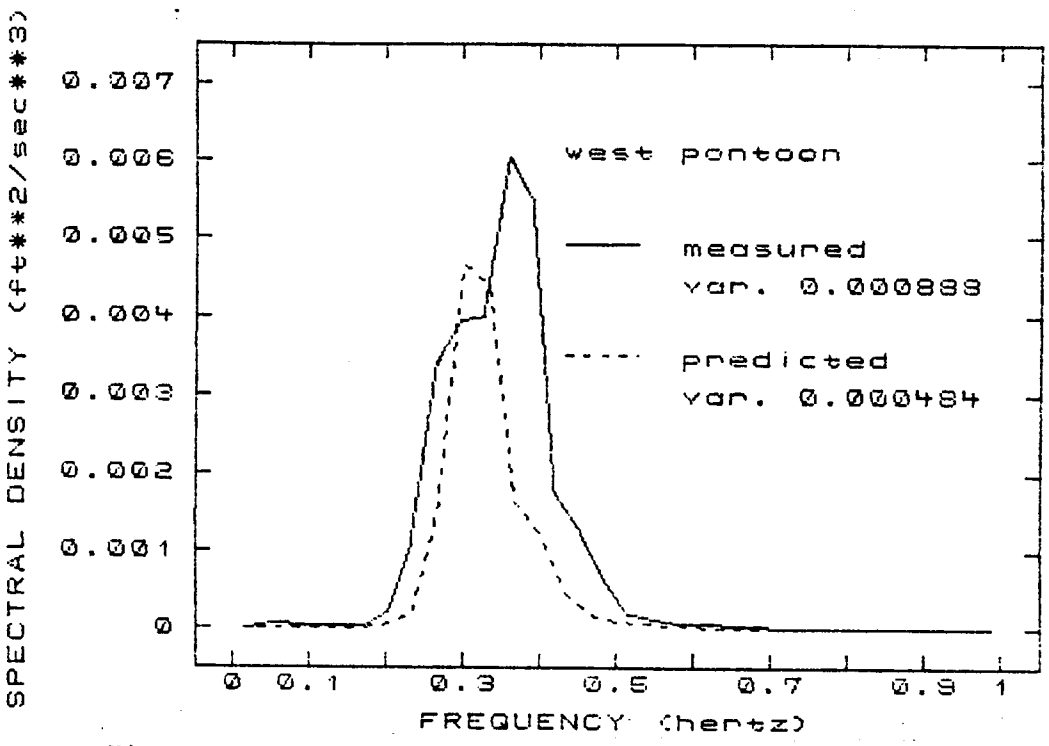

Figure 5.14 Measured and Predicted Roll Acceleration Autospectral Estimates for West Pontoon: Run 10

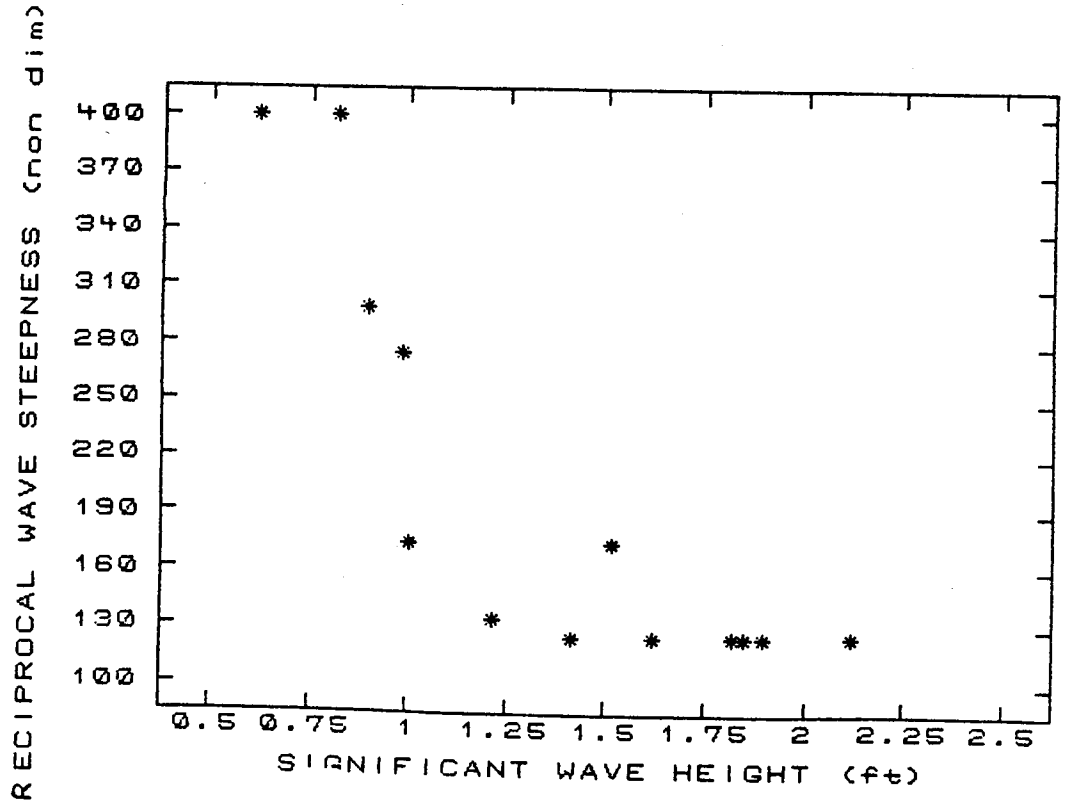

Figure 5.15 Roll Damping Input Parameter: Reciprocal Wave Steepness 1/WS versus Significant Wave Height

treating rectangular cross-sections were found in the literature, this value was obtained by means of the procedure described in Section A of this chapter.

The value of 1/WS is not a quantity which can easily be approached from a rational basis. Since both the incident sea spectrum and the roll response are continuous functions rather than "impulses" at discrete frequencies as assumed, it is not easy to specify a particular wave amplitude which correctly "lumps" the relevant characteristics of the frequency window under consideration. An attempt was made to use a wave steepness based on the significant wave height and peak wavwlength from $S_\zeta(w)$, but the result was overdamping. So that the empirical information gathered on roll damping coefficients may be of use to others, the source code for the roll damping routine is listed in Appendix III.

iii) Sway

Sway is only marginally a harmonic response mode due to the absence of a hydrostatic restoring constant. The mooring restraints do provide a small restoring force but this does not produce much effect on the acceleration of the body except in the low frequency range. The sway response, however, is harmonic in character due to the periodic nature of the wave excitation force and coupling with other truly harmonic degrees of freedom such as roll. Prediction of sway motions can be difficult because other causes such as wind, tides, and currents can produce significant sway excitations. Long period or steady drift-type forces may have a large effect on mooring stiffnesses which would certainly

influence the displacement response and can affect the acceleration response in the low-frequency range (Oppenheim, 1980; also see Section C, part v of this chapter).

It is therefore quite encouraging that the sway variance ratios do not appear to be seriously worse than those of heave or roll. Predicted variance ratios ranged from about 0.5 to 1.1 with a mean of 0.75 over all runs indicating a tendency toward underestimation, particularly as the wind direction veered away from beam. If only records are considered with a mean wind direction within 25 degrees of beam and at least four hours unidirectional wind duration, then the mean variance ratio improves to 0.89. The sway mode was generally more sensitive to input parameters relating to the state of the wave field than either heave or, to a lesser extent, roll. While these results indicate that a reasonable estimate may be made of the time-varying transverse horizontal inertial force on the body, it should be remembered that some of the considerations mentioned in the previous paragraph would have to be adequately addressed to correctly estimate the lower-frequency forces on the body due to mooring, current etc.

Measured sway accelerations showed a consistently lower variance on the east pontoon than on the west. The discrepency appeared to show little dependence on significant wave height or wind direction.

While systematic differences also occurred to a lesser extent in the measured roll results, in this mode the west pontoon variances appeared to be higher than those on the east. The

rotation vector for a rigid body does not change as the body undergoes small angle rotations and translations; therefore any true differential rotation would be due to torsional deformations. Other causes are more likely. This conclusion would seem to be upheld by the fact that no particular frequency range appears to account for the variation in roll, but rather the total response of the west accelerometer is slightly higher. A minor scaling or installation problem of some form is suspected. A slight misalignment of the roll accelerometer axes could create discrepancies of this order.

The sway or transverse accelerations, on the other hand, do vary with position of the body. The fact that the accelerometers on the west pontoon are located farther from the center of mass than those on the east (see Figure 3.2) would result in higher measured sway motions on the west pontoon if any yaw were occurring. This consideration, however, would be taken into account by the analytical model at the time the operators were transformed from the center of gravity to the position of the accelerometers. While slight differences between the two pontoons in the correct sense are predicted by the model, they are not of sufficient magnitude to account for the measurements. An alternative explanation is in order.

A closer examination of the acceleration FRO and response plots of records strongly exhibiting this phenomonon leads to the conclusion that the difference in the autospectral response occurs due to a slightly higher sway FRO for the east pontoon in the 0.3 to 0.45 hertz range, resulting in a wider response

bandwidth on the east pontoon than on the west. This portion of the frequency domain contains considerable wave energy in many cases. Figure 5.16 shows $/H_{\ddot{\eta},2}(w)/$ plots of both pontoons for run 8 superposed, while Figure 5.17 displays the corresponding acceleration response spectra.

While an explanation involving the mooring system is a temptation, the location in the frequency domain of the most prominent differences in the operators makes such reasoning questionable. Furthermore, from the juxtaposed plots of $/H_{\ddot{\eta},2}(w)/$ it may be seen that the low frequency spike directly attributable to mooring stiffnesses (see Section C part v of this chapter) is actually slightly higher on the west pontoon, where mooring anchor depths on the northern side of the breakwater are 10-12 feet deeper than their shoreward counterparts to the east. The expectation would be for mooring stiffnesses to be larger on the shoreward side, given a comparable level of pretensioning. The accuracy with which the 5000 pound pretension was applied to the cables was estimated by U.S. Army Corps of Engineers personnel to be approximately plus or minus 1000 pounds, so uncertainty in the level of pretension may override tidal effects for normal tidal variations. As a matter of interest, the ratio of the measured variances on the west to east sides, was plotted versus tide height and may be seen in Figure 5.18. While suggesting a trend, the results are not conclusive due to two dramatic outliers, which may indicate the influence of other parameters.

Another possible explanation of the larger sway accelerations at the west accelerometer location lies in the fact that

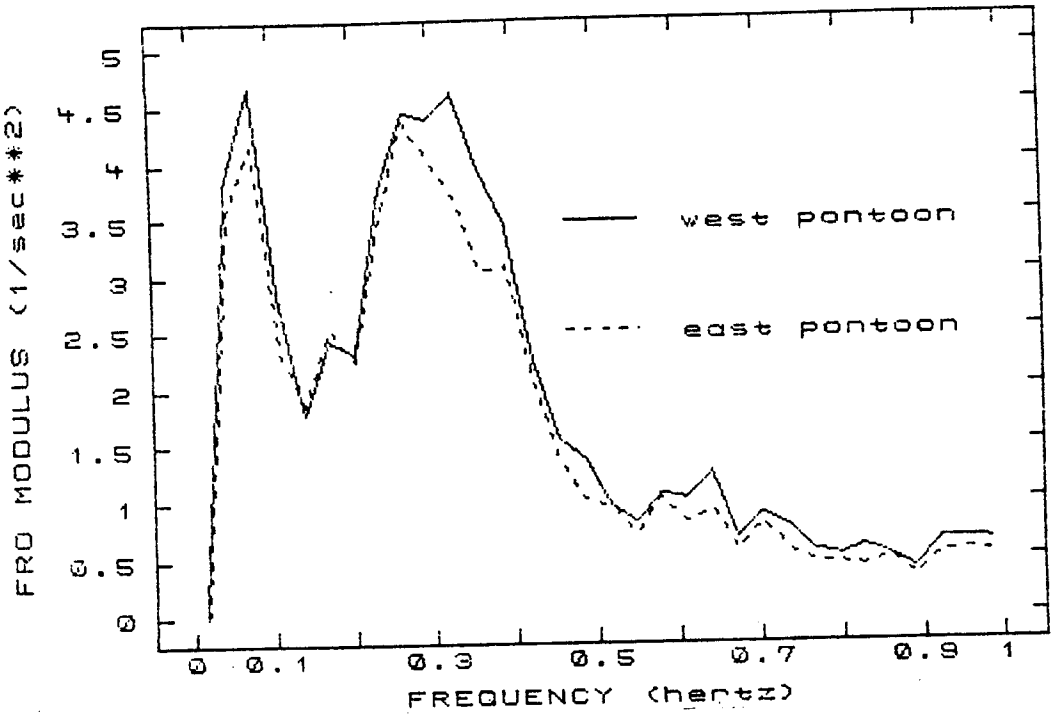

Figure 5.16 Measured Sway Acceleration FRO Moduli for both Pontoons: Run 8

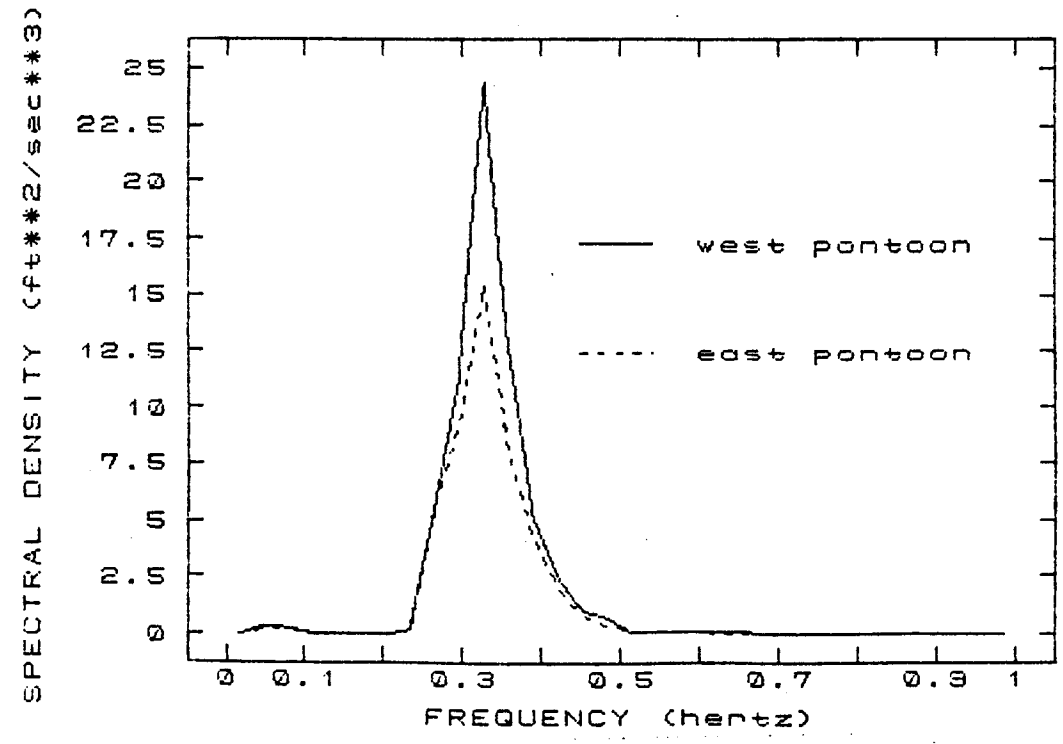

Figure 5.17 Measured Sway Acceleration Autospectral Estimates for both Pontoons: Run 8

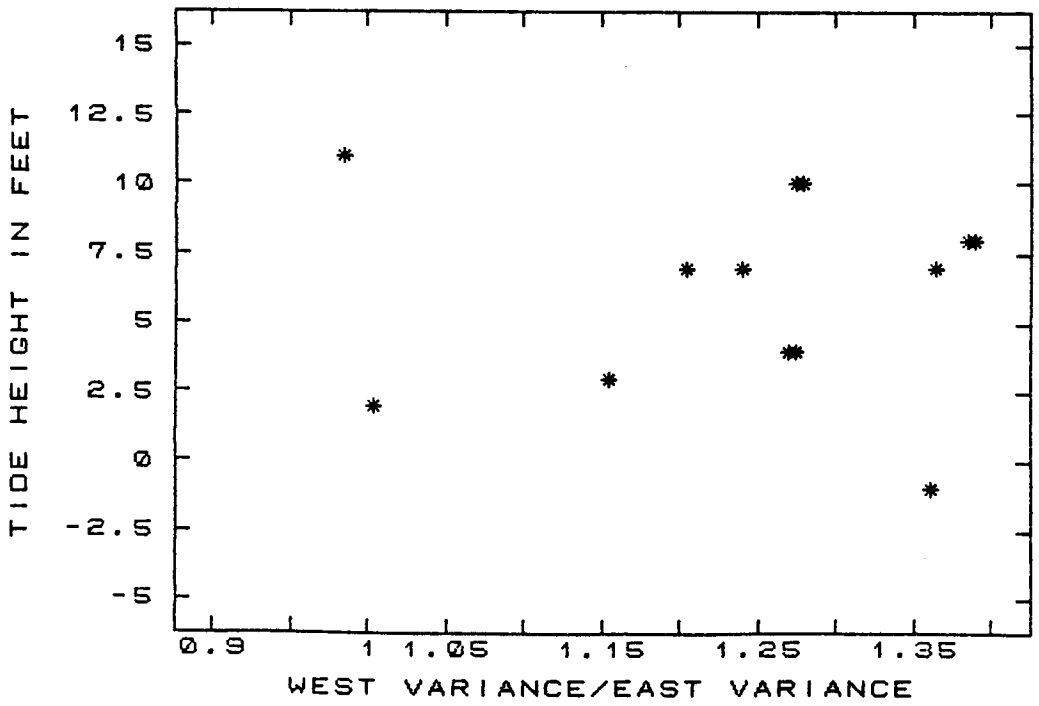

Figure 5.18 Ratio of Measured Sway Acceleration Variance (West Pontoon/East Pontoon) versus Tide Height for all Runs

the west pontoon sits approximately 2 to 3 inches lower in the water than the one on the east at the location of the accelerometers. These figures are based upon measurements made in August of 1983. Such an offset would slightly increase the coupling of sway with roll on the west, due to the higher value of Z_{cg} on the west end. A slightly greater vertical surface would be provided for wave pressures as well. The overall sensitivity of sway acceleration response to small increases in the submergence of the center of gravity can be investigated by artificially increasing the value of z_{cg}. Such an increase, however, does not account for changes in hydrodynamic quantities which might arise from a cross-section that is varying with longitudinal distance, x_b.

A model run was made with Z_{cg} arbitrarily increased by four inches, causing the predicted variances to increase by approximately 15%. While this is only about half of the increase required for agreement with the measured data, a comparison of the predicted operator plots of Figure 5.20, where this change was made, with those of Figure 5.19, in which z_{cg} was not altered, shows that some of the desired effects were attained. It appears possible that a more complete consideration of the increased hydrodynamic forces due to the larger wetted perimeter on the west end might help to account for some of the remaining difference.

Summary information presented in this report regarding agreement of sway predictions was calculated by averaging values for both pontoons together. While such a procedure lessens the

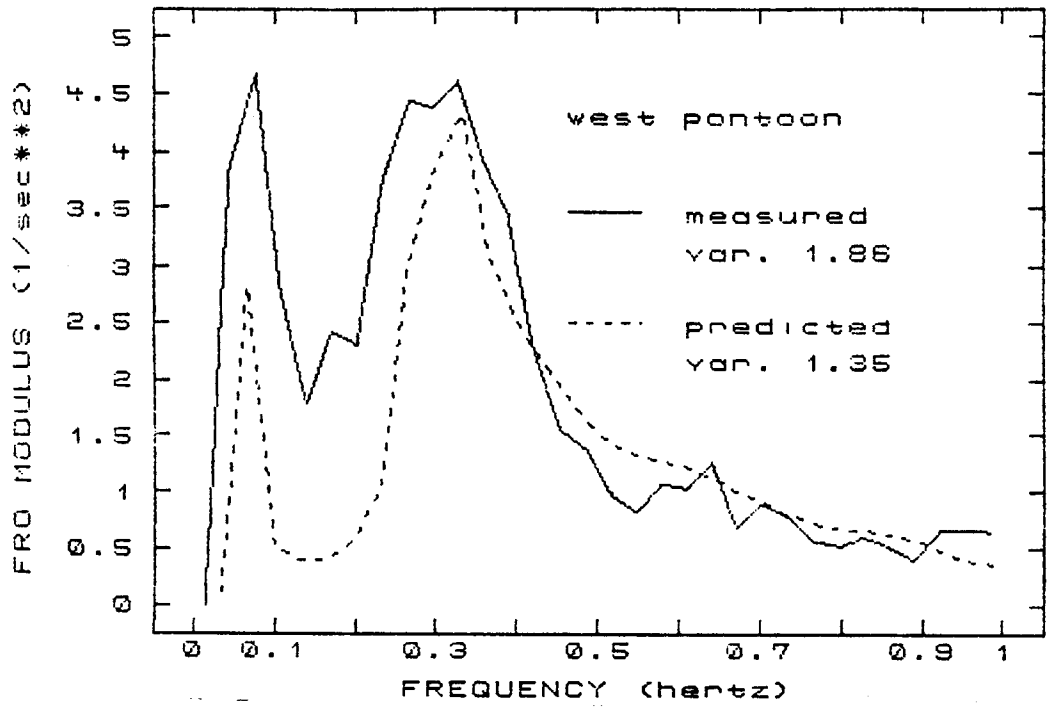

Figure 5.19 Measured and Predicted Sway Acceleration FRO Moduli for West Pontoon, Z_{cg} unaltered: Run 8

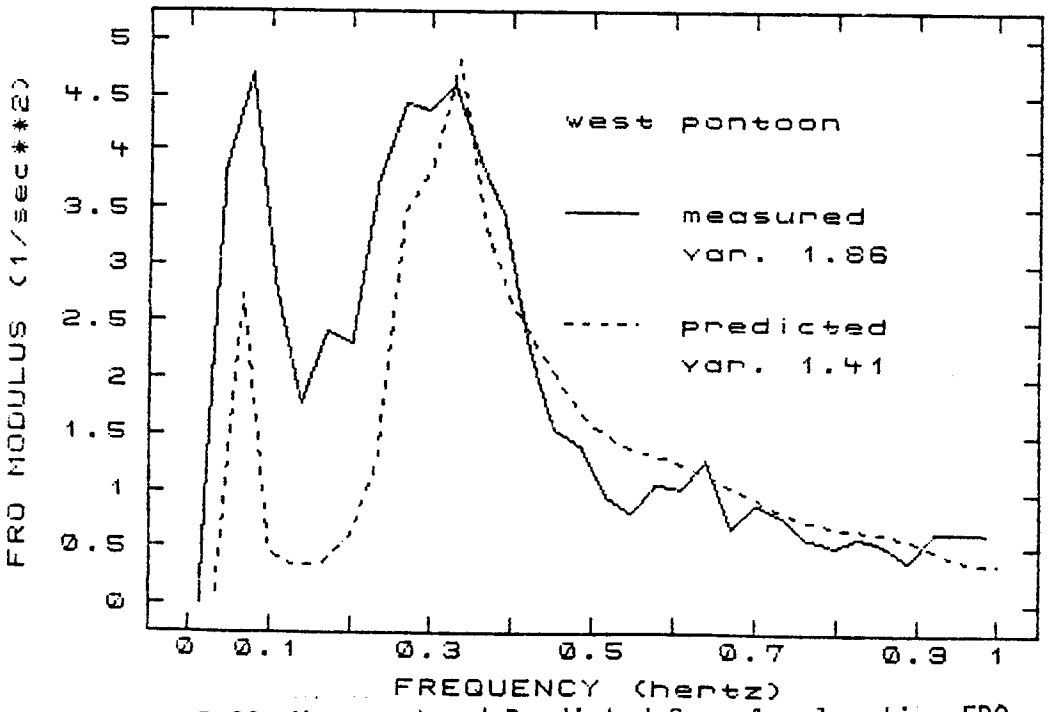

Figure 5.20 Measured and Predicted Sway Acceleration FRO Moduli for West Pontoon, Z_{cg} Increased by Four Inches: Run 8

agreement for one side and increases it for the other, results of this form may be considered valid for the center of mass of the entire breakwater.

Other systematic discrepancies between measured and predicted sway acceleration operators include a tendency for the measured sway operator to exceed the predicted values in the 0 to 0.28 hertz (b/λ = 0 to 0.25) range in many cases. A closer examination suggests two problems which may or may not appear concurrently: one from 0 to 0.2 hertz appearing in runs 1, 2, 3, 8, and 9 and one from 0.2 to about 0.28 hertz which is evident in runs 1, 3, 4, 9, 12, and 13. The first problem tends to occur at higher significant wave heights and is believed to be related to mooring forces. A further discussion occurs in Section C part v.

The second problem is of a more serious nature, since it involves the peak sway operator response. A problem in the coupled roll-sway added mass and damping may be indicated, since quite different results were obtained from program NSRDC in the frequency range in question simply by varying the manner in which points on the breakwater cross-section were specified even though the same cross-section resulted when the points were connected by lines. Figures A.7 and A.8 in Appendix A show that the values of A_{24} and B_{24} vary quite rapidly in this region. In order to investigate the influence of these coefficients, a model run was made which set these coefficients to zero in the frequency range from 0 to 0.3 hertz. Figures 5.21 and 5.22 show the sway acceleration operator plots which resulted, which should be compared to the plots of Figure 5.23 and 5.24 where the cross-coupling is

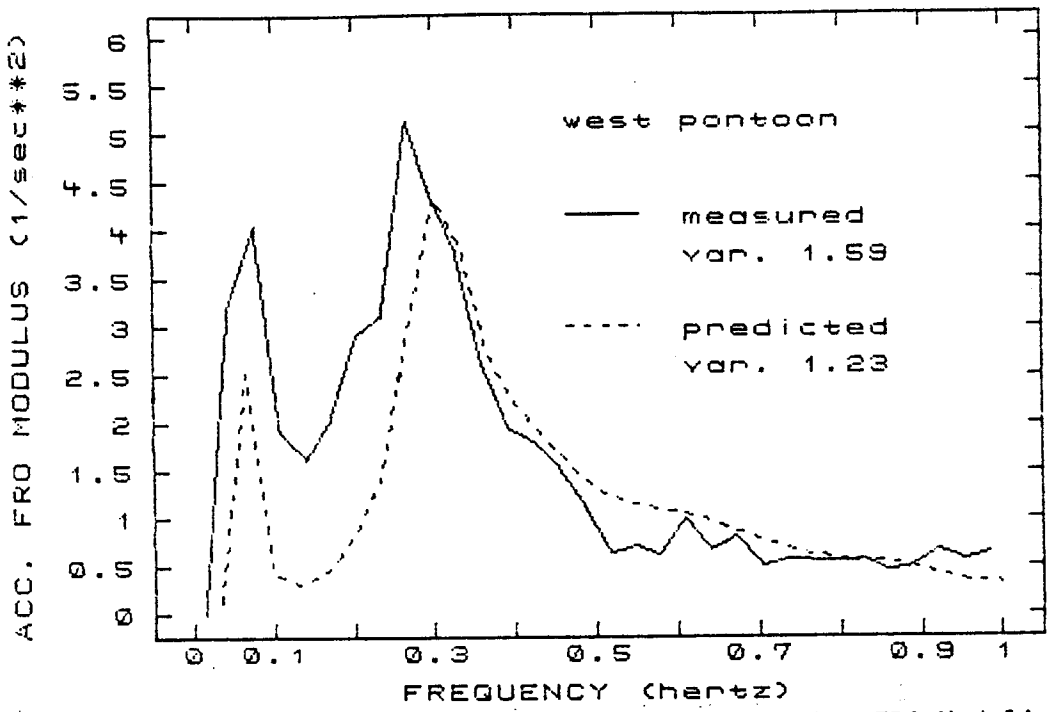

Figure 5.21 Measured and Predicted Sway Acceleration FRO Moduli for West Pontoon: no Sway-Roll Cross-Coupling Terms Below 0.3 Hertz (Run 1)

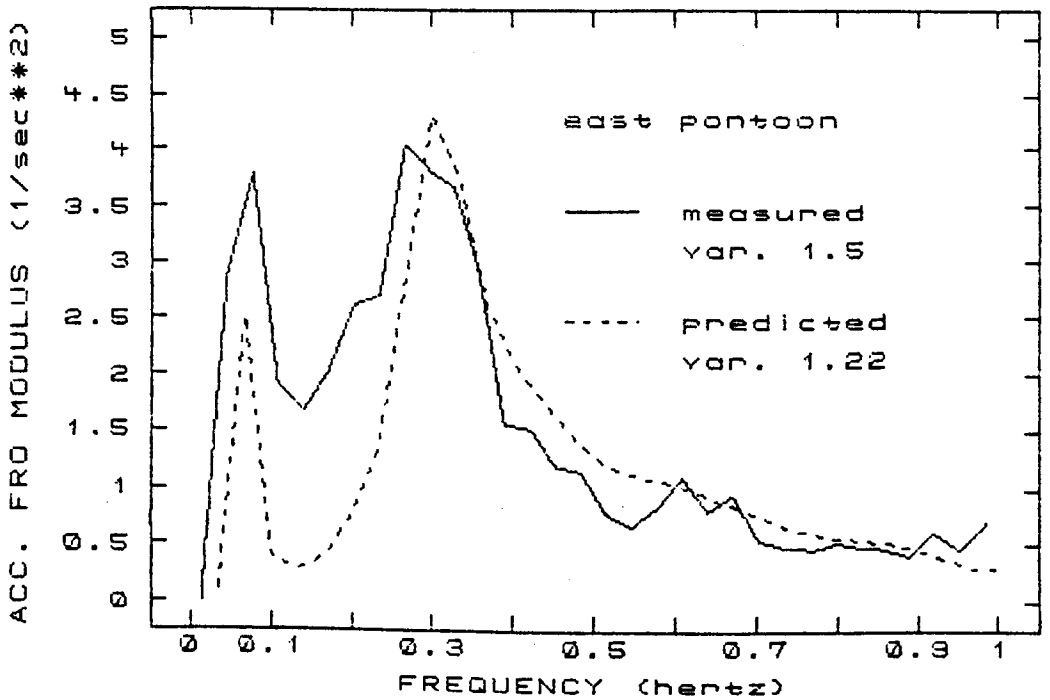

Figure 5.22 Measured and Predicted Sway Acceleration FRO Moduli for East Pontoon: no Sway-Roll Cross-Coupling Terms Below 03. Hertz (Run 1)

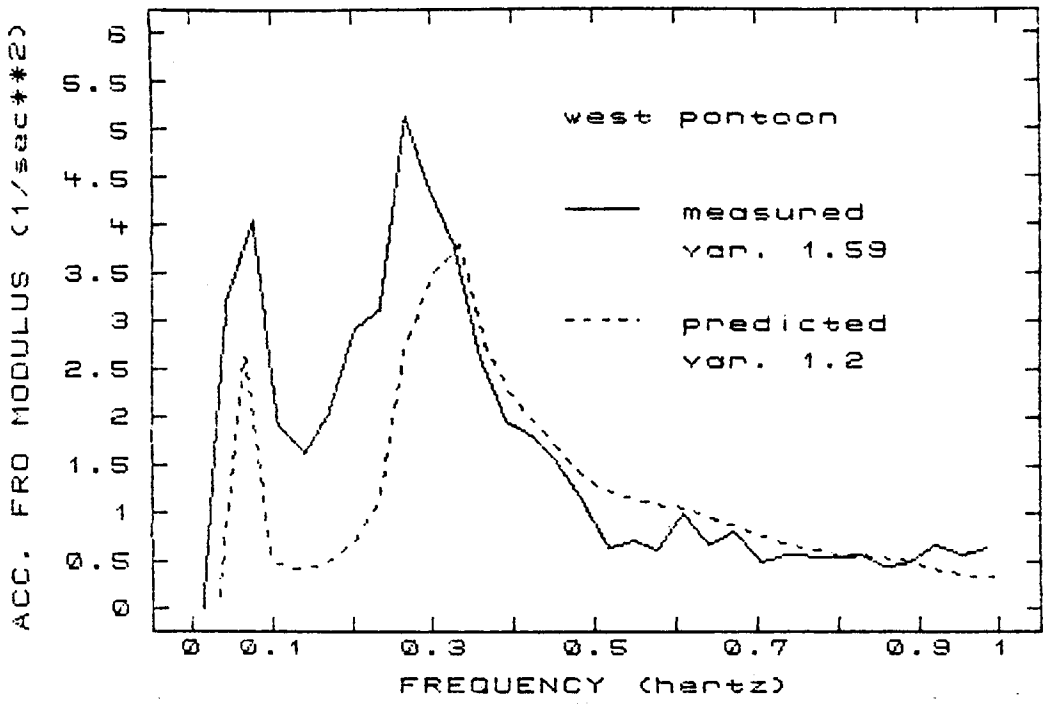

Figure 5.23 Measured and Predicted Sway Acceleration FRO Moduli for West Pontoon: Sway-Roll Cross-Coupling Calculated by Program NSRDC (Run 1)

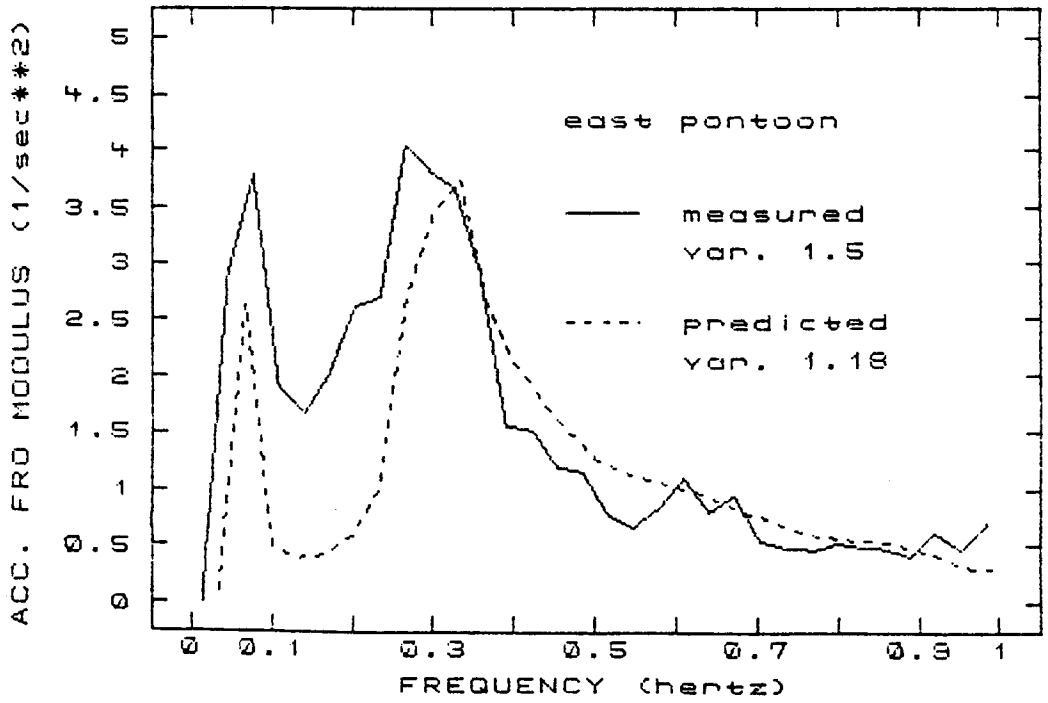

Figure 5.24 Measured and Predicted Sway Acceleration FRO Moduli for East Pontoon: Sway-Roll Cross-Coupling Calculated by Program NSRDC (Run 1)

included. Indeed, better agreement between predicted and measurement-based sway acceleration operators may be noted in the region in question, although the problem is not entirely corrected. The predicted roll operator also appeared to benefit from this alteration, manifesting slightly larger operators in this same frequency range which brings it into slightly better agreement with measurements. The magnitude of the peak operator response at 0.3 hertz, however, increased noticeably as well, indicating a recalibration of roll damping parameters might be required if the roll-sway coupling terms are altered. The need for excising the relevant portion of program NSRDC or recodin of the hydrodynamic calculations iss indicated, so the parameters affecting accurate calculations of the cross-coupling terms can be more economically investigated. The values these quantities assume appear to have a noticeable influence on the outcome of the predictions, and simply ignoring them would not, therefore, seem prudent.

Although the variance ratios obtained for sway showed poorer agreement than in roll or heave, the mean sway normalized squared error, E_n^2, averaged over all runs was 25.8. This is only slightly higher than for heave (24.5) and significantly lower than roll (40.5). If only those records are considered with four hour or greater unidirectional wind durations and principal attack angles less than 25 degrees off beam, the mean E_n^2 drops to 17.9 which is actually lower than the corresponding heave statistic. The agreement between measured and predicted shapes of the resultant sway autospectral estimates (as evidenced by

small values of the normalized squared error), therefore, appears to be quite good under the proper conditions. Underestimation of magnitudes accompanied by good agreement of shape could indicate an underestimation of the forcing functions in the frequency range of maximum wave energy. Such an underestimation would not severely affect the shape of the response curves if the underestimation was consistent over attack angles and frequencies of interest, but would cause a depression of the response magnitude.

C) Discussion of Important Paramters

The verification of analytical models, always a difficult task, is particularly challenging when attempting to use the "real world" as a laboratory. Yet the validity of any model is open to question until it has withstood this test. The recognition, isolation, and evaluation of the important parameters affecting a process is not just a matter of making a few measurements. Indeed, realizing precisely what to measure is undoubtedly the most important decision of all.

One might think that given a full year's worth of data, there would be little trouble in finding ample records suitable for this analysis. The West Point prototype floating breakwater, however, was in a configuration consistent with a rigid body assumption for only about six months. Of this time, lack of storm events (and hence timeseries), failure of certain key data channels (such as accelerometers), or temporary inoperability of the entire data acquisition system further decreased the amount of suitable data. Ideal tests isolating quantities hypothesized to affect breakwater response were therefore impossible and a

certain degree of coupling between the parameters of interest was inevitable. A discussion of the effects of some of the more important parameters affecting acceleration response follows.

i) Significant Wave Height

Variations in significant wave height would not affect the accuracy of the predictions for a truly linear system. At large significant wave heights, the expectation would be for agreement to fall off at some point as the effect of physical nonlinearities (e.g. deck overtopping or flooding of pontoons) became more predominant. Unanticipated coupling between motions due to mooring restraints, relatively larger amounts of higher order damping, unaccounted increases in mooring stiffnesses, more severe geometry changes in the position of the body with respect to the global origin, and other possible events not considered by the analytical model all might be expected to reduce the accuracy of predictions. Under extremely severe conditions, overprediction of accelerations might be anticipated as more energy becomes dissipated in reality by the breakwater than is accounted for by a linear or quasi-linear model. Actual stiffnesses greater than estimated could cause an overestimation of displacements at lower frequencies and hence of the forces imparted on the body by the mooring system. Unfortunately, such extreme events are of greatest interest to a designer.

Similarly, while less severe sea states would appear to be more in keeping with a "small amplitude" assumption, such conditions could be expected to increase the signal to noise ratio for both the wave staff and the accelerometers. Spectral density

estimates based on incident wave height measurements are used as inputs into the model. Output from the model is compared directly to spectral density estimates based upon measured acceleration timeseries. It is not clear, therefore, whether predicted or measured acceleration spectral density estimates would be most affected by noise in the data, although the level of agreement between the two might be expected to decrease under such circumstances.

VR and E_n^2, the quantitative measures of closeness, are compared with significant wave height in Figures 5.25 through 5.30. A distinction was made between the data records in which the unidirectional wind duration was four hours or greater and those in which it was not.

The accuracy of the heave response predictions shows no particular dependence upon H_S. The records which had low unidirectional wind durations did not to result in markedly poorer agreement, except in one case where the response magnitude was underpredicted.

Both roll and sway accelerations, on the other hand, had noticeably poorer agreement at smaller significant wave heights. There may be a tendency for milder sea states to have a more complex directional character due to the higher frequency components and shorter time periods required for them to arise. Such a situation would affect roll and sway more than heave due to their greater sensitivity to the directional parameters of the distribution of wave energy. Some of the apparent decline in accuracy, however, is undoubtedly due to the fact that the re-

cords with the four smallest significant wave heights all have wind headings of about 25 degrees off beam, so it is unclear which parameter had the greatest effect in reducing agreement. This topic is briefly discussed again in part ii of this section.

No tendency is evident for agreement to lessen for more severe sea states. The period when the rigid connection between the two pontoons was in place was April 1983 through September 1983, and the violent storms of the preceding autumn did not occur during this time. Although the breakwater is designed to withstand a six-foot wave, no waves approaching this size occurred during the period mentioned. It is likely that the scatter on Figures 5.25 through 5.30 would increase with increasing H_s if such data were available.

ii) Wind Duration

The site of the West Point prototype floating breakwater has an unrestricted fetch of approximately 15 miles to the south and 6-7 miles to the north. Using the relationship

$$C_g = \lambda / 2T$$

where C_g is the group speed of the water wave train in deep water and T is the period it can be shown that a 3-second wave travels at approximately 5.25 miles per hour. A wave train being generated at the southernmost point of the fetch would require approximately 3 hours to arrive from the south; the corresponding time is about 80 minutes from the north. These figures can be considered a lower bound on the time required for a sea state to become "fully arisen." The reason that this concept is important

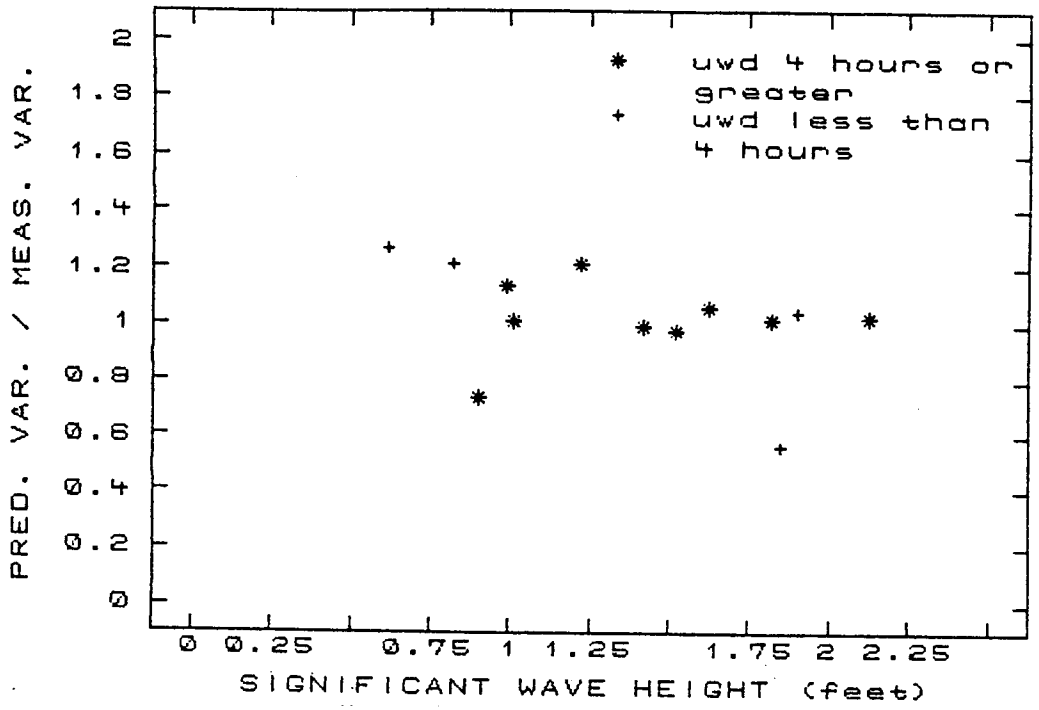

Figure 5.25 Variance Ratios in Heave Mode versus Significant Wave Height for All Runs

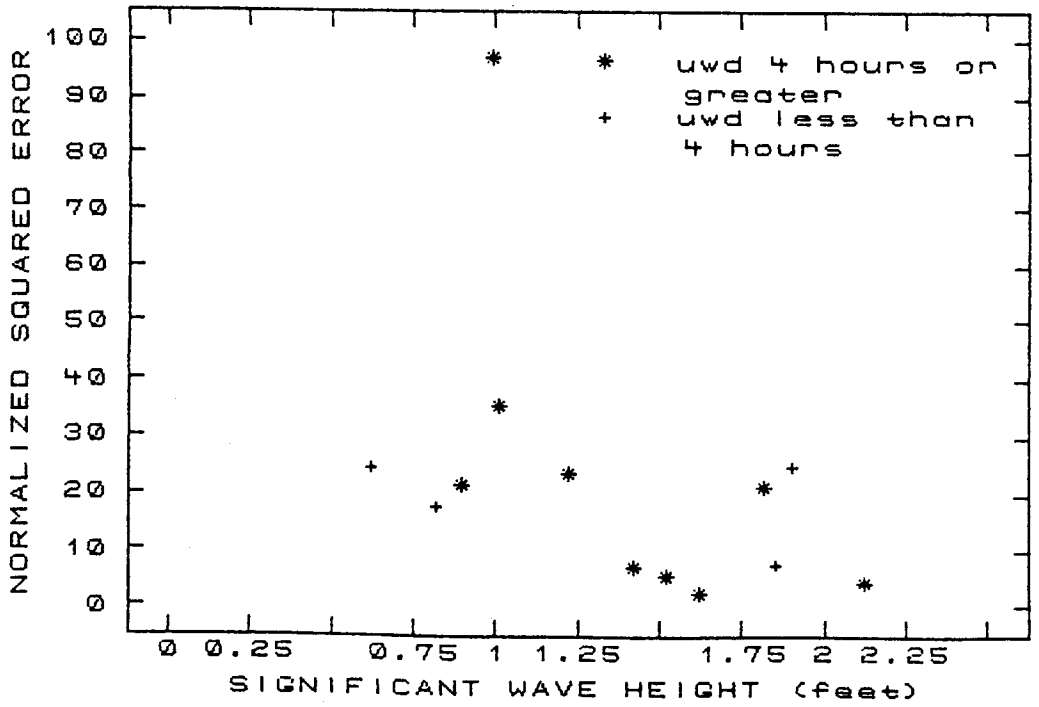

Figure 5.26 Normalized Squared Error in Heave Mode versus Significant Wave Height for All Runs

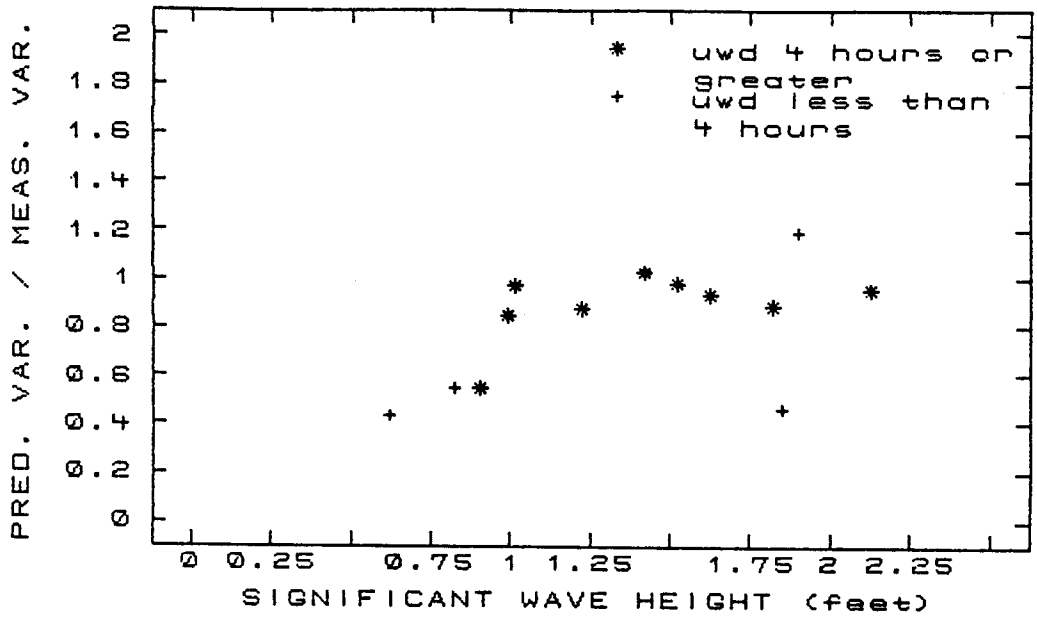

Figure 5.27 Variance Ratios in Roll Mode versus Significant Wave Height for All Runs

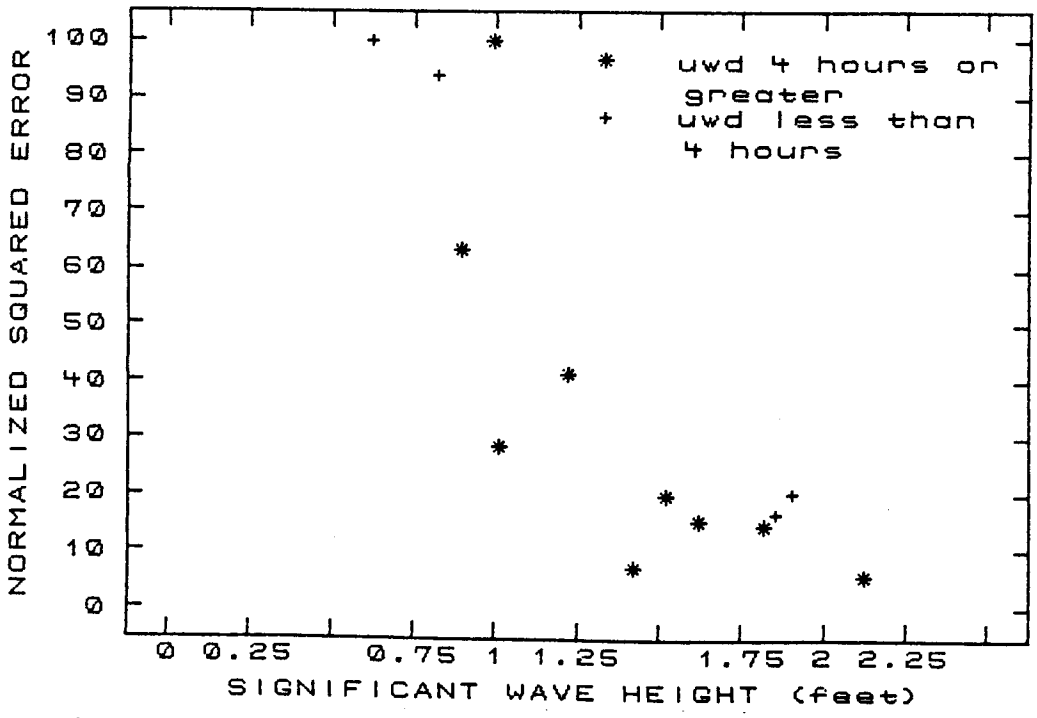

Figure 5.28 Normalized Squared Error in Roll Mode versus Significant Wave Height for All Runs

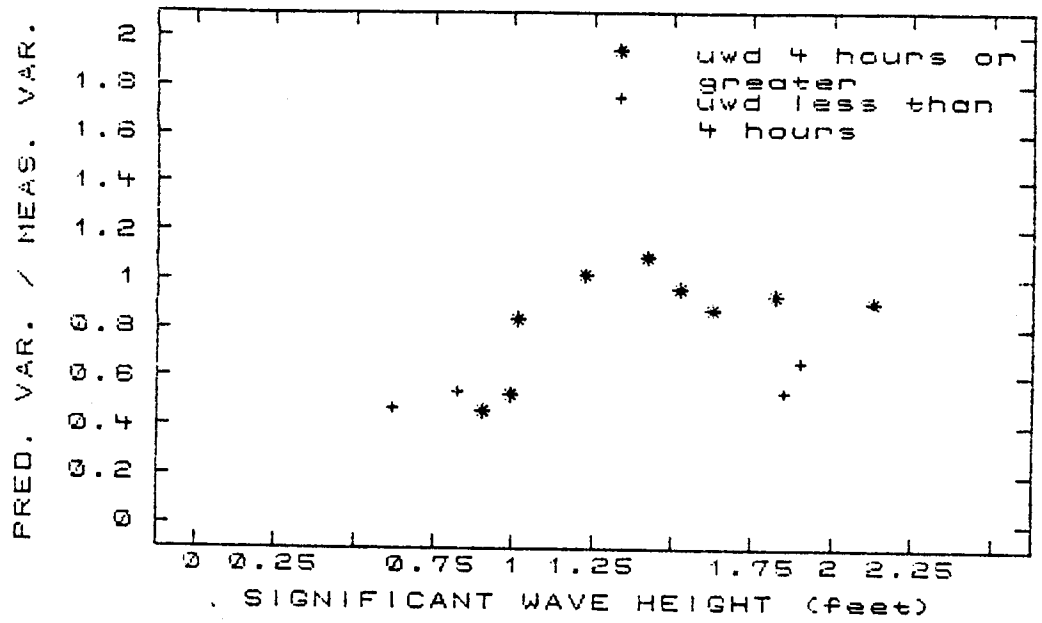

Figure 5.29 Variance Ratios in Sway Mode versus Significant Wave Height for All Runs

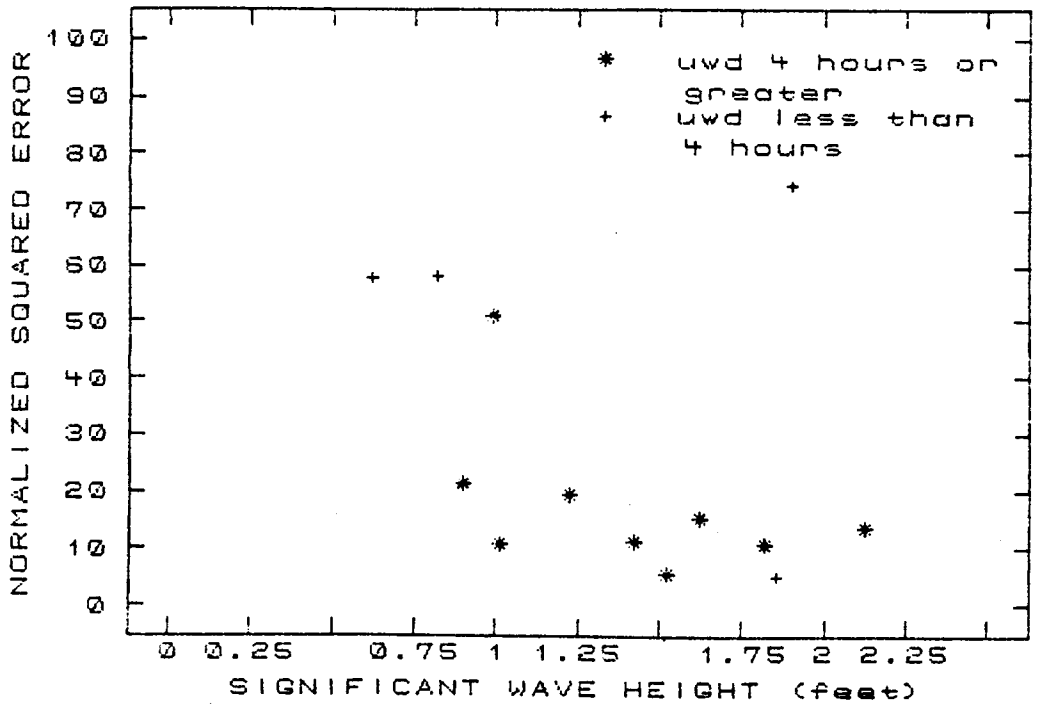

Figure 5.30 Normalized Squared Error in Sway Mode versus Significant Wave Height for all Runs

is that the methods used in this analysis assume both stationarity and ergodicity of the wave field not only to produce accurate incident wave spectral density estimates but to justify the use of a linear breakwater model. Strictly speaking, a wave field would not be stationary and ergodic unless a wind had been blowing at the same speed over an infinite fetch for an infinite period of time (Kinsman, 1965). In practice the conditions under which the ergodic hypothesis may be justified must be established empirically.

The directional wind durations mentioned in this report were assessed in the following manner: if the wind direction as measured in the previous statistical records did not vary more than 25 degrees either way from the mean of the timeseries for a specific number of hours, then the wind was assumed to be of constant directional duration over that period of time.

The statistical results appear to show scatter with respect to duration of the wind direction. No significant trends are obvious other than lower variance ratios in sway and roll for records in which the directional wind duration was less than four hours. It seems likely that other parameters such as H_s exert more influence. The normalized squared error did not seem to show a significant trend toward increase for winds of short directional durations, except in sway. The duration of the wind direction did not appear to noticeably affect either statistical parameter for the heave degree of freedom.

The failure to accurately predict breakwater response under conditions of recently shifted winds would not be a serious flaw

in the method, since design assumptions would normally assume a fully arisen sea.

iii) Wind Direction

Much mention has already been made of the influence of the wind direction on the accuracy of the response predictions. The purpose of this section will primarily be to summarize and discuss these results.

Figures 5.31 through 5.36 show effects of wind direction on the statistical results. Reductions in the accuracy of both the predicted magnitudes (as quantified by the variance ratios) and shapes (as indicated by E) in the sway and roll degrees of freedom occurred as the wind direction moved off beam. It is a little surprising, however, that 20 or 25 degree shifts would produce such noticeable effects, although Hutchison (1977) mentions poorer agreement in roll for quartering seas ($\theta_0 = 45^o$) than beam seas ($\theta_0 = 0$), but no such effect for heave. The explanation suggested by Hutchison relating to mooring force coupling between pitch, heave, and roll in quartering seas would be more plausible for displacement response (such as he examined) than for accelerations.

The poorer agreement of some of the records which relate to the higher frequency range (around 0.4 hertz) previously discussed might be explained as follows: mooring force coupling due to off-beam wave attacks could be responsible for producing clump-weight oscillations. The hydrodynamic and inertial forces engendered by such oscillations might then influence the frequencies of predominant acceleration responses. The data seem to

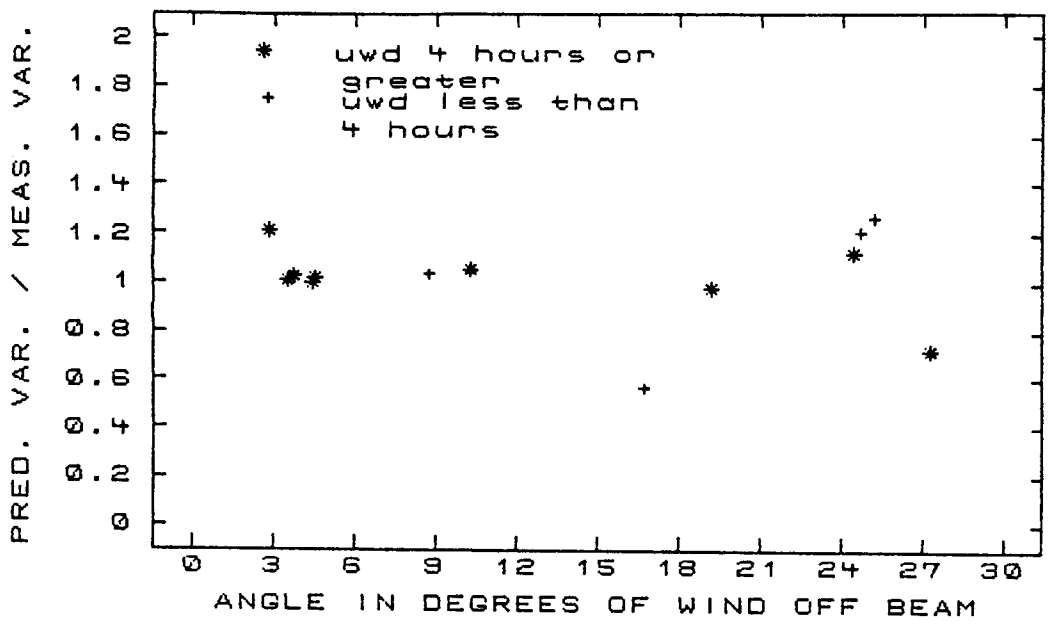

Figure 5.31 Variance Ratios in Roll Mode versus Mean Wind Direction for All Runs

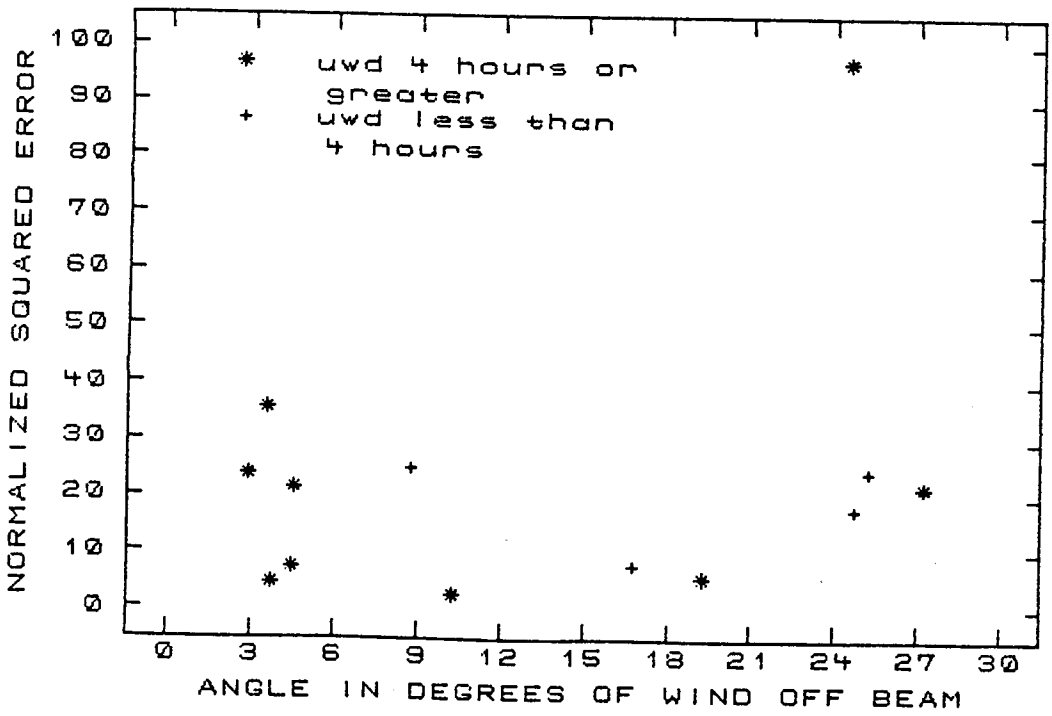

Figure 5.32 Normalized Squared Error in Heave Mode versus Mean Wind Direction for All Runs

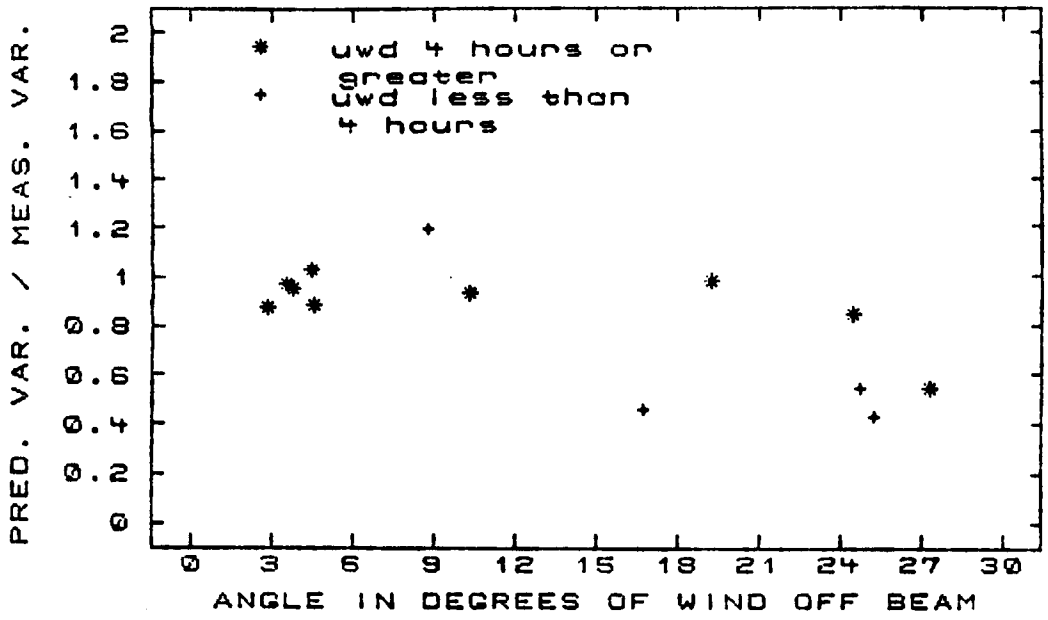

Figure 5.33 Variance Ratios in Roll Mode versus Mean Wind Direction for All Runs

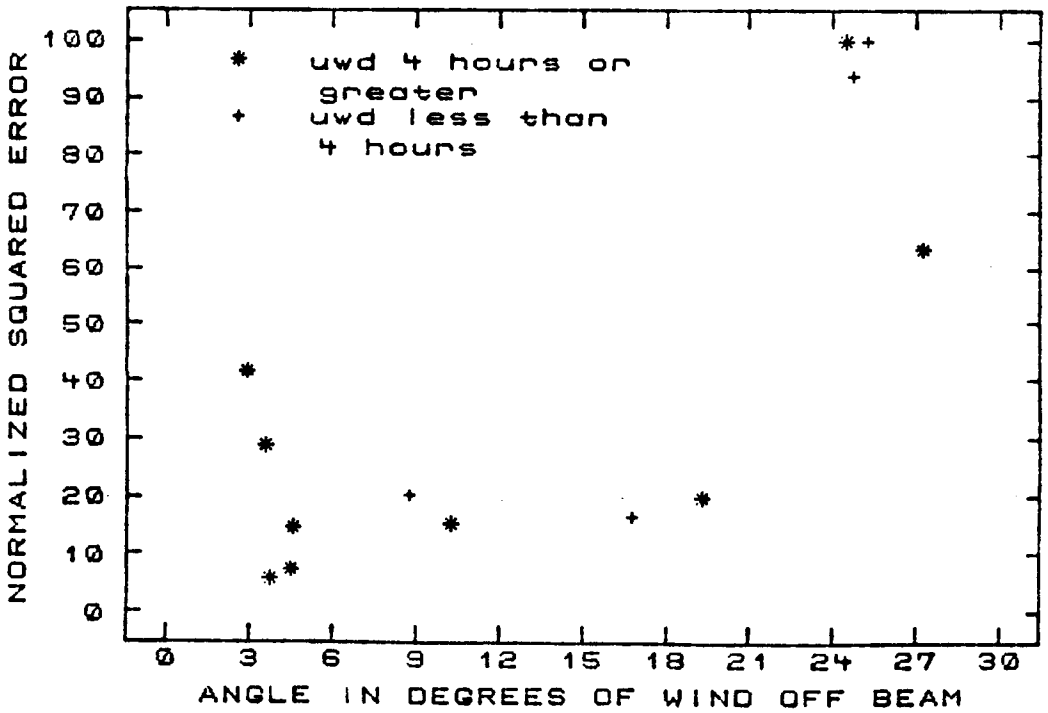

Figure 5.34 Normalized Squared Error in Roll Mode versus Mean Wind Direction for All Runs

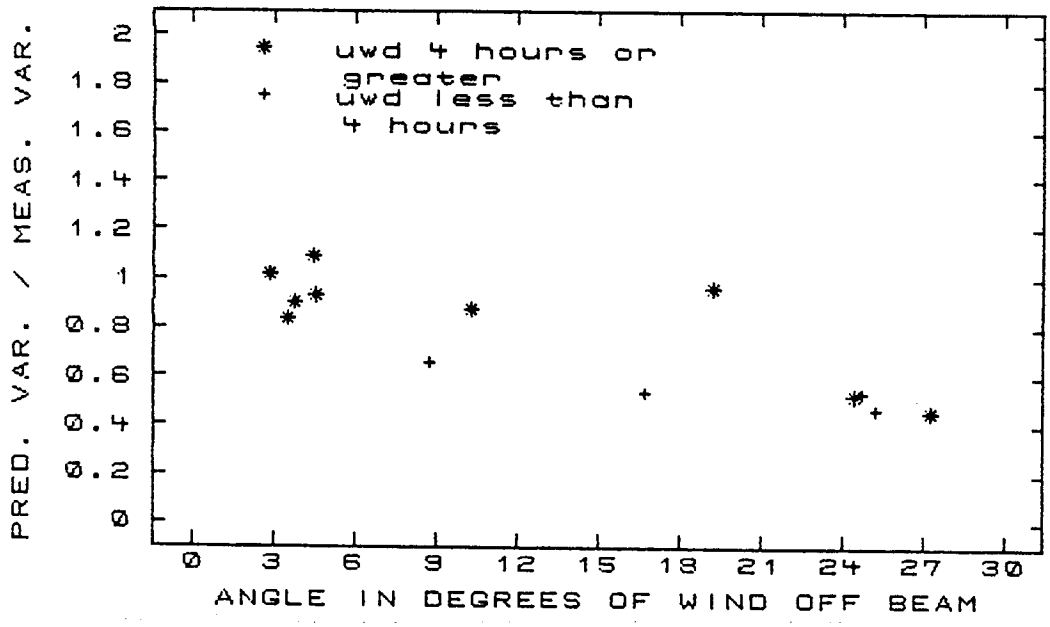

Figure 5.35 Variance Ratios in Sway Mode versus Mean Wind Direction for All Runs

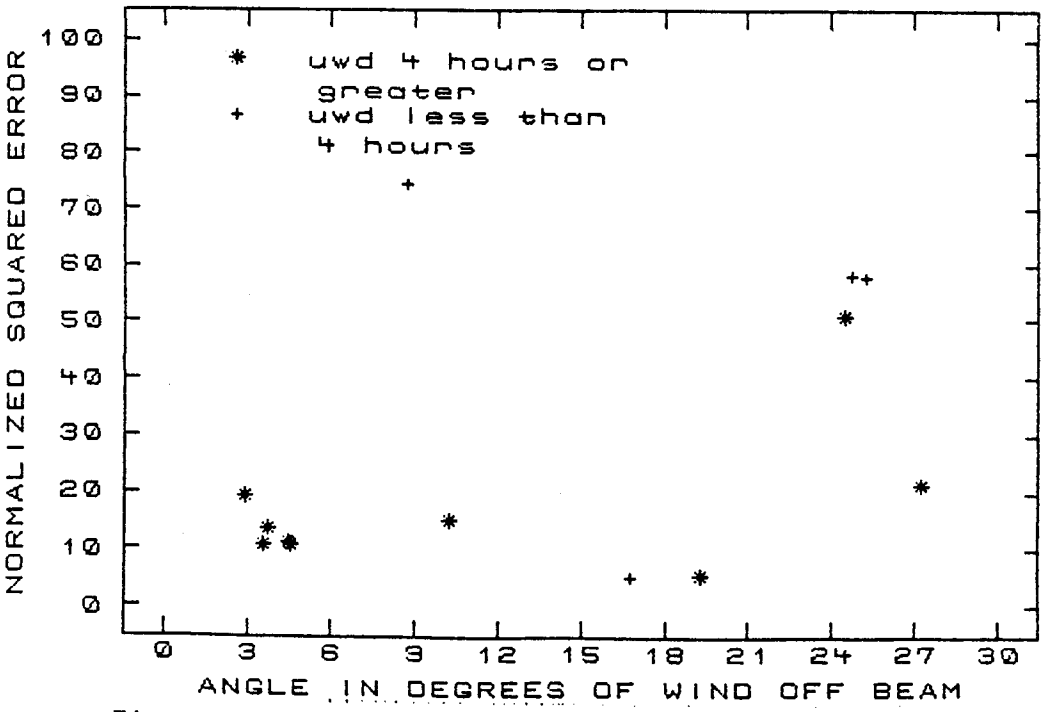

Figure 5.36 Normalized Squared Error in Sway Mode versus Mean Wind Direction for All Runs

support this hypothesis. The heightened "lump" in the $/H_{\eta,2}(w)/$ (see Figures 5.3, 5.4, 5.10, 5.12) plots tends to become more prominent in records of larger θ_0. The lower variance ratios occur in records of smaller H_s due to a tendency for a higher percentage of the wave energy to appear in this higher frequency (around 0.4 to 0.5 hertz) band when the wave climate is less severe.

A possible explanation for the overall reduced agreement in roll and sway with shifts of θ_0 off beam (aside from the higher frequency problem just discussed) relates to the manner in which the model was implemented. A glance at Figure A.9 in the Appendix I suffices to demonstrate that, to a large extent, the sway response is a function of the amount of wave energy coming directly at beam. Even a shift of ten degrees causes a drop in the magnitude of the sway excitation force. This is also true to a lesser extent in roll and heave. In fact, some models estimate the response at all wave attack angles by means of the product of the response in beams seas with a retarding function (Hutchison, 1983). The present model used 10 degree increments for calculation of the excitation forces. Finer divisions would have been more appropriate, but this was not done due to funding constraints. In retrospect, better modeling would have been obtained with the same number of attack angles by using graduated spacings. The increments of $\Delta\theta$ would start out smaller near the beam and gradually get coarser as head seas were approached.

Since breakwaters are primarily designed with wave attenuation in mind, the fact that results were the best for larger

waves in beam seas is encouraging. The problem suggested in the preceding paragraph, however, may well have had repercussions other than merely reducing the agreement at oblique attack angles with respect to beam, as the following discussion suggests.

iv) Directional Spreading Function

The directional characteristics of the limited-fetch short-crested seaway is a subject for which only a very limited amount of data are available. While various methods for modeling this phenomonon exist, the presence of only one node in this analysis made a long-crested approach by far the most straightforward. Controversy exists as to whether long-crested superpostion results in a valid representation of the short-crested seaway, but since it is the usual technique employed in seakeeping theory, it was also used in the current analysis.

In this technique, the directional distribution of the wave energy is determined by the exponent, n, in equation 4.39. Opinions differ as to appropriate values for n in the Puget Sound region. Langen (1981) states that in general powers from 2 to 10 are justified and goes on to quote Weigel in "Hood Canal Floating Bridge: Phase I Report. Determination of the Causes of Failure," as indicating that a power of 7 is appropriate for Hood Canal, based upon measured data. The assumption that the directional distribution of energy is independent of frequency appears to be based upon convenience rather than fact. High frequency waves are generated and decay more rapidly than waves of lower frequency. Frequency independence of the directional wave energy

distribution would be a doubtful assumption for a sea state which is not yet fully arisen, or one in which wind directions had recently changed. To obtain accurate response predictions, the appropriate value of n for the frequencies of maximum breakwater response must be found. If this value is not correct outside the 0.2 to 0.5 hertz range (for the West Point Breakwater), the predicted accelerations will not be greatly affected.

Some of the values of n found to result in the best agreement between measured and predicted autospectra are higher than can be justified in the literature. Powers of 18 were used twice and on one occasion a unidirectional wave was used. The sway response was the most sensitive to the power of n employed, followed by roll, and heave to a much lesser extent.

Such high cosine powers may have been required partially as a result of the inadequate increments in the attack angles used to generate the excitation forces. Each forcing function was effectively applied at an increment of wave attack equal to five degrees on either side of the value for which it was explicitly calculated. This procedure creates step functions which approximate the cosine curve, with the ordinates of the step functions occurring at the calculated value of the cosine curve being used. For curves or regions of curves which do not have large slopes, such an approximation is fairly good. For curves which are quite steep, the approximation is poor. Cosine curves of large powers become very steep, although as the power gets higher, less and less steepening effect is attained for a given increment in n. Regardless of how steep the curves become, however, they must

have zero slope on top. For a certain range of n, a portion of the area of such a curve near θ_0 would be shifted away from θ_0 by this approximation (see Figures 5.37 and 5.38). If θ_0 is near beam as was the case in many model runs, then acceleration response would tend to be inhibited somewhat by this transformation as another look at Figure A.9 in Appendix II emphasizes.

There is nothing sacred about the cosine spreading function; it is merely a convenient way to distribute wave energy about a range of directions. The way in which this function was discretized in the current analysis, however, might have hindered a direct comparison with the values obtained for n from other sources. A linear interpolation to every five degrees might have helped remedy this situation, but large fluctuations in the phases of some of the forcing functions near resonance made the advisability of this procedure questionable. It is not likely, however, that such an explanation can fully account for the high powers needed to attain adequate response levels in some of the model runs.

Despite these problems, some interesting trends emerged. A graph of n versus unidirectional wind duration (Figure 5.39) demonstrates a trend toward higher powers as the wind blows longer in the same direction.

While one might think that longer wind durations would imply a more unidirectional wave energy spectrum, this should not be the case for a fully arisen sea. Wave energy is not transmitted only in the direction of wave propogation, but also along the crests as the phenomenon of diffraction clearly demonstrates

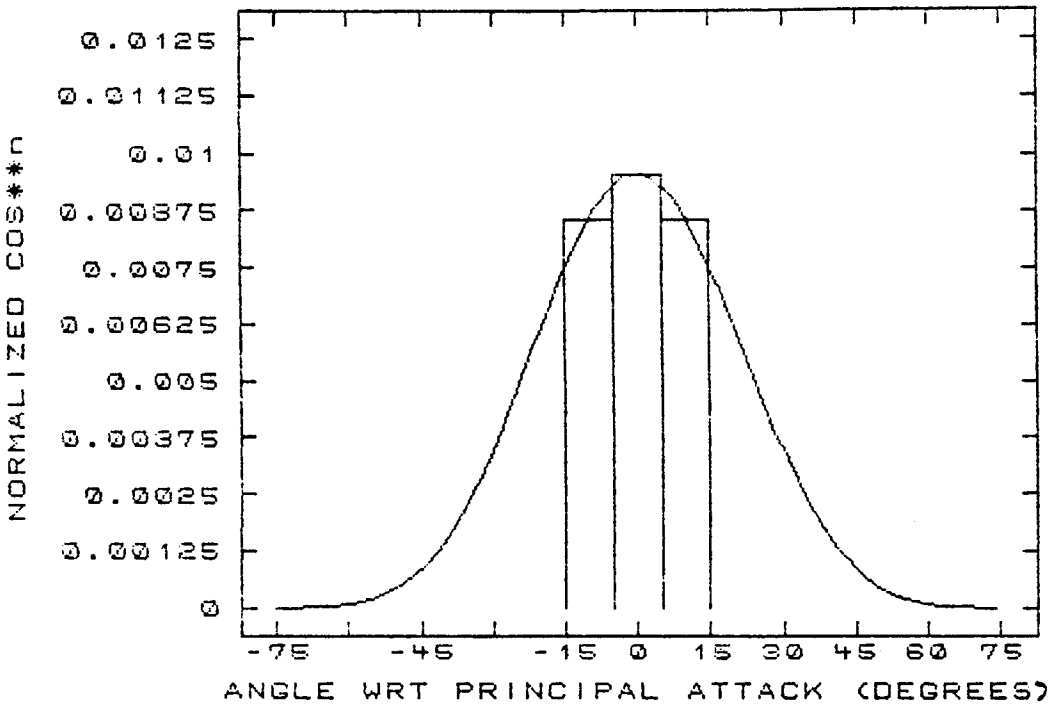

Figure 5.37 Cosine Power Spreading Function Discretization for n = 7 and its Effect on Wave Energy Distribution near Principal Attack Angle

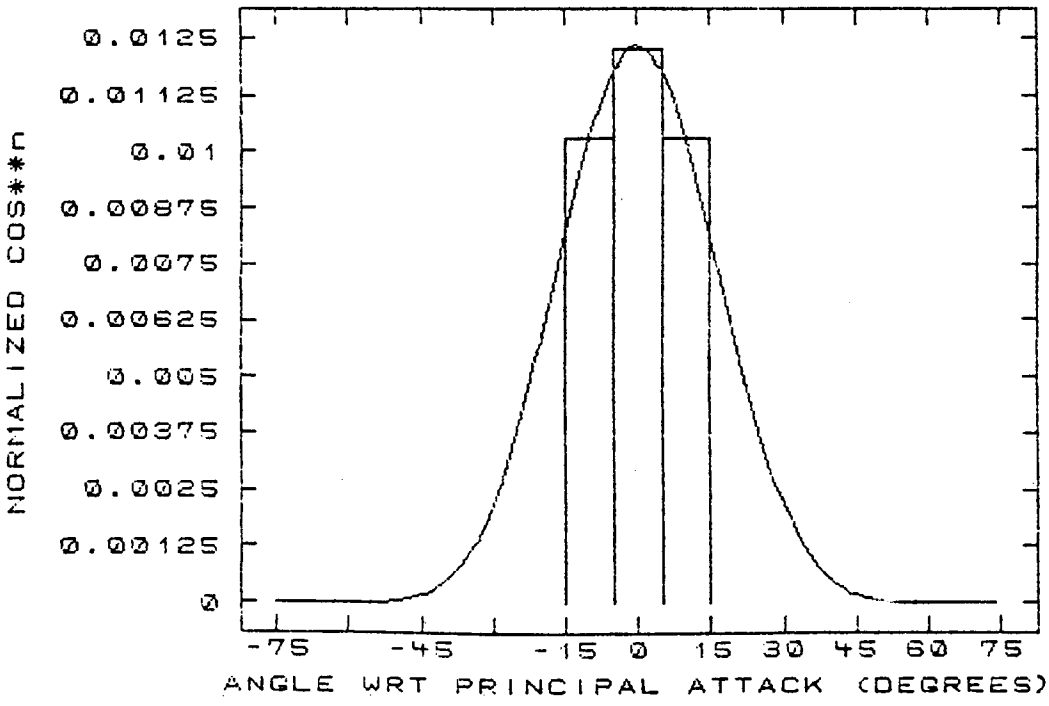

Figure 5.38 Cosine Power Spreading Function Discretization for n = 12 and its Effect on Wave Energy Distribution near Principal Attack Angle

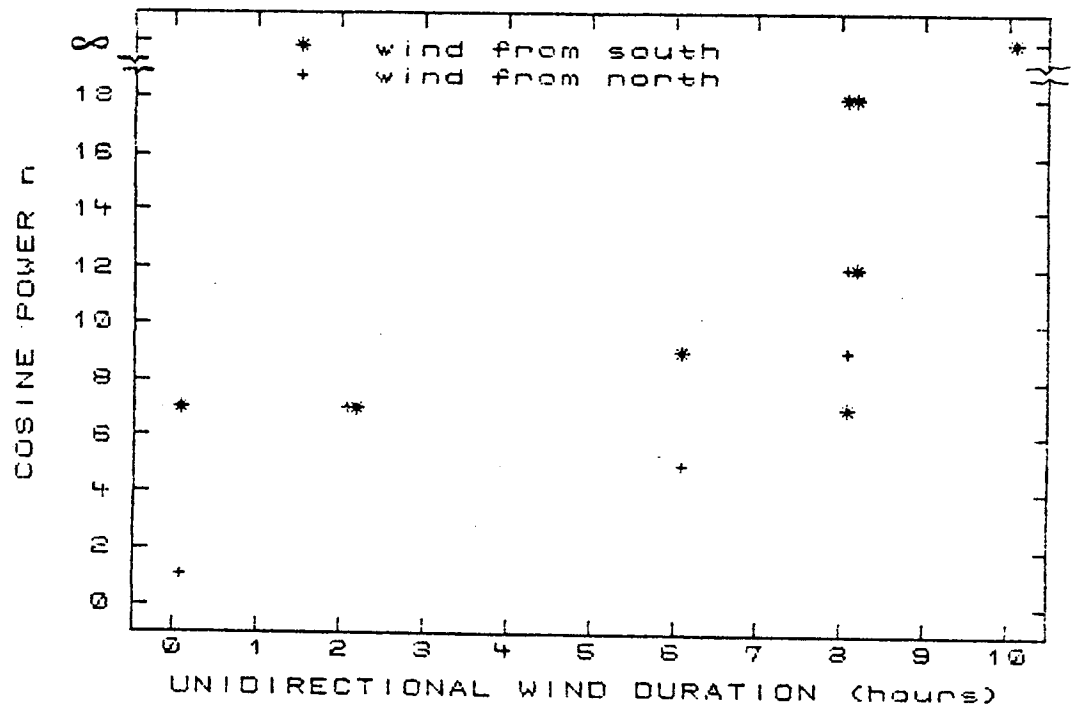

Figure 5.39 Spreading Function Cosine Power, n, Found to Give Best Agreement versus Unidirectional Wind Duration

Note: Unrestricted fetch from North ≃ 7 miles.
Unrestricted fetch from South ≃ 15 miles.

(Shore Protection Manual, 1977). This is also true for sound and light waves and is sometimes referred to as Huygen's Principle in elementary physics texts. A directional sea is not necessarily generated by wind components in different directions but by the fundamental mechanics of waves in a fluid medium. The dispersion occurs more rapidly at higher frequencies. It is possible that during the generation phase the dispersion effect has not had time to fully take effect for the longer period waves and that higher values of n would occur than for shorter period waves which are relatively more dispersed. Precisely what would correspond to the generation phase in the records examined is not clear, although calculations above indicate that three hours would be a lower bound for a southerly storm. The need for more research on wind-wave generation in restricted fetch areas is apparent.

v) Mooring Forces

The procedure whereby mooring forces are modeled in a frequency domain analysis is a weakness of the method. It is well known that the forces exerted by a non-taut hanging cable are not a linear function of displacement. The question is not so much whether such forces respond linearly to displacements, but over what range of conditions is the error incurred by making such an assumption acceptable.

Mooring dynamics in deep water can be separated into two problems: a high frequency problem caused by high frequency hydrodynamic forces at zero mean, and a second order hydrodynamic force which has a mean value (Oppenheim, 1980; Standing et al,

1981). The high frequency forces are approximately proportional to wave amplitude while the second order or drift force is approximately proportional to wave amplitude squared. Low frequency excitations are small; large horizontal motions result because damping and restoration are also small in sway. Larger damping and restoration terms and hence smaller responses occur at low frequencies in the heave and roll modes.

An example of corresponding sway displacement (Figure 5.40) and acceleration (Figure 5.41) spectral density estimates for the same timeseries appears on the following page. The displacement spectrum was derived from the measured acceleration spectral estimate by dividing through a factor of w^4. This relationship may be derived from equations 4.27 and 4.40. The factor of w^4 becomes a weighting factor which heavily weights the low-frequency end of the spectrum. It is common in Fourier analysis to set a certain number of the lowest frequency Fourier coefficients to zero. In the case of the integrated acceleration autospectrum just mentioned, failing to do so would result in significant calculated sway displacements in the hundreds of feet. Problems appear to exist, therefore, in looking at displacements by means of integrating acceleration spectral density estimates, unless more sophisticated spectral analysis techniques are used. A time domain integration might be preferable but these are not nearly so straightforward. Nevertheless, integration in the frequency domain may provide useful information about the frequencies of peak spectral displacements and their relative magnitudes.

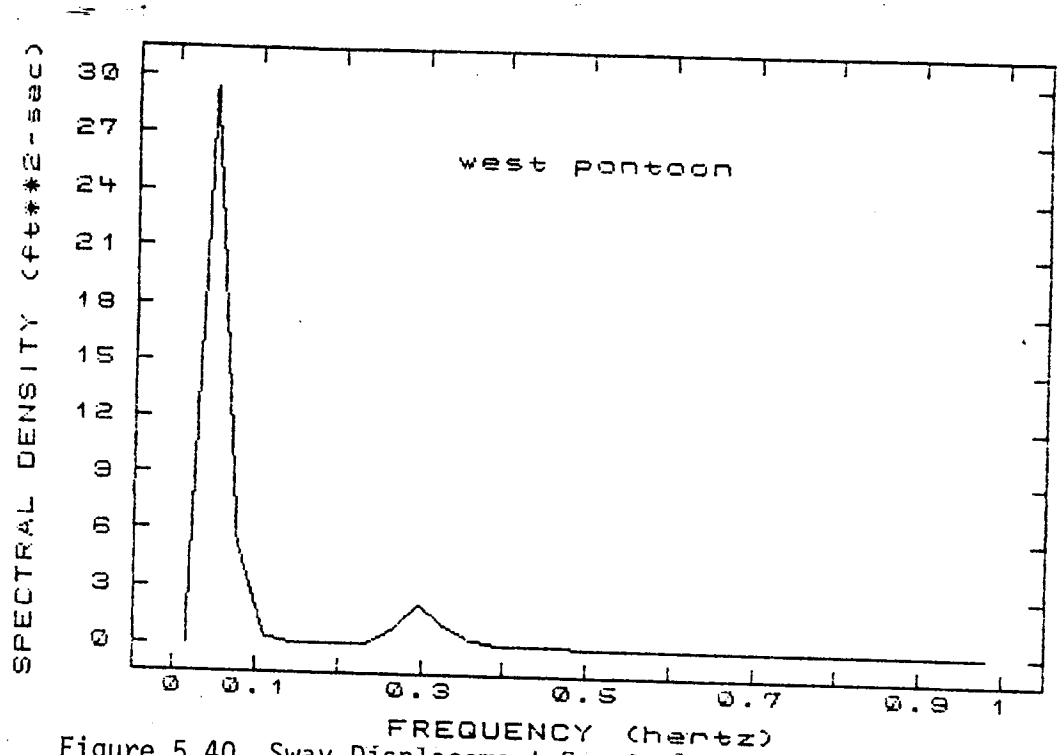

Figure 5.40 Sway Displacement Spectral Density Estimate Drived by Integrating Acceleration Data: Run 1

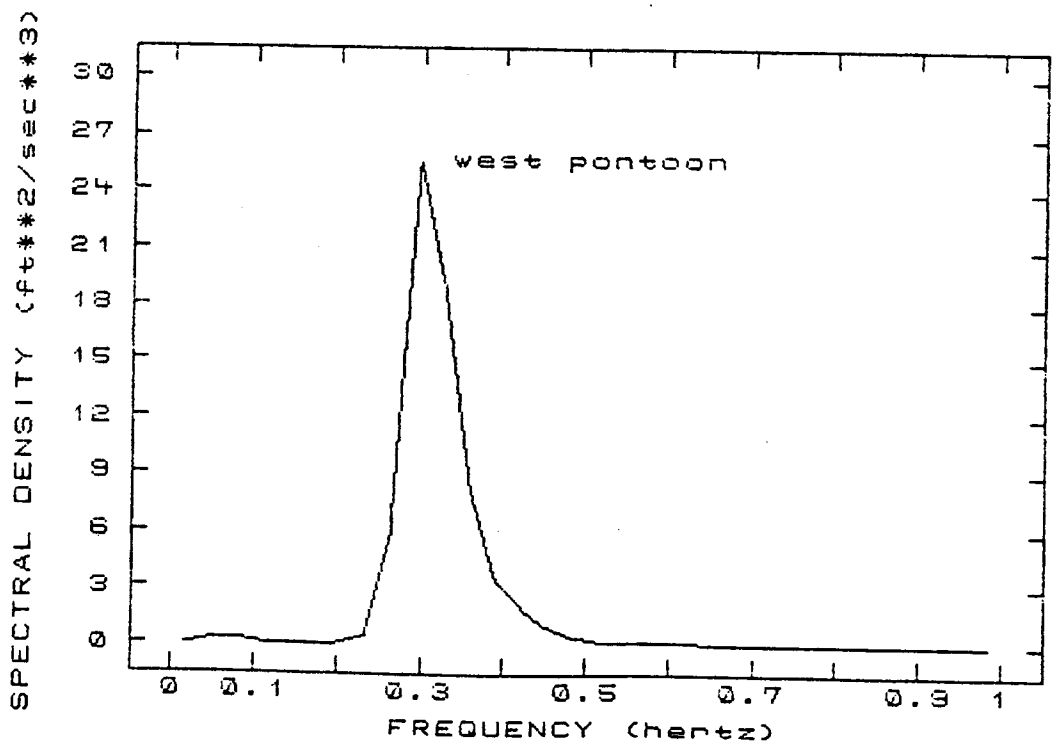

Figure 5.41 Acceleration Spectral Density Estimate: Run 1

Sway acceleration operator plots show a different character in the low-frequency range than those of heave and roll. Some problems exist with the measurement-based operator plots in the low-frequency range due to the division of a small acceleration spectral density estimate by an incident wave height spectral density estimate (see equation 5.1) which is also quite small. Since all degrees of freedom in a given run are divided by the same small numbers, consistent trends between them are still informative. Direct comparison of the very low frequency measurement-based operators with those predicted, however, should be undertaken with caution. An analysis of the effects of the mooring input data upon the accuracy of response prediction will now be made.

The disagreement between predicted acceleration FRO's in the low-frequency range for the heave and roll degrees of freedom are small enough that they do not appear important. This does not appear to be the case in sway, where predicted operators fell short of their measured counterparts in runs 1,3,8, and 9 in the low-frequency range. Although final predicted acceleration auto-spectra are not greatly affected, the corresponding spectral displacement estimates (if they were calculated) would significantly underpredict the low-frequency components of the displacment under these circumstances. Such underprediction would lead to underestimation of mooring forces as well.

Obtaining better low-frequency agreement for the sway operator moduli is not simply a matter of trying different values for the mooring constants. As an example, the sequence of Fi-

gures 5.42 through 5.45 demonstrates the effect of varying the amount of linear restoration introduced by the model into the sway mode. In Figure 5.42, no restoring constant was used, while in Figure 5.43 a value of about one kip/foot was used per cable pair as calculated by program BRKMOOR. The first spike appearing at about 0.067 hertz is the only noticeable effect of the stiffness introduced, but the effect on the acceleration autospectrum would be only barely discernable. Doubling the stiffness (Figure 5.44) does little besides shift the spike to a higher frequency while a factor of five (Figure 5.45) shifts it and increases its magnitude to the point of dominating the plot. The values supplied by program BRKMOOR seem to do as good a job as any. In some cases the predicted plots agree much better with those based on measurements such as those in Figure 5.46.

No obvious reasons are evident for the differences in levels of agreement at low frequencies in the sway operators. Perhaps a low frequency analysis of the type mentioned above would provide a better insight. The fact that the poorest agreement in the 0 to 0.2 hertz range occurs at the higher significant wave heights suggests that drift forces might have an effect. What is clear is that estimates of total sway displacements and any parameters which heavily depend upon them (such as mooring forces) should only be made with great caution if the current technique of analysis is the only tool being used. It is possible that a quasi-linear analysis of the type described by Vassilopoulos (1971) could increase the level of agreement, but since no second

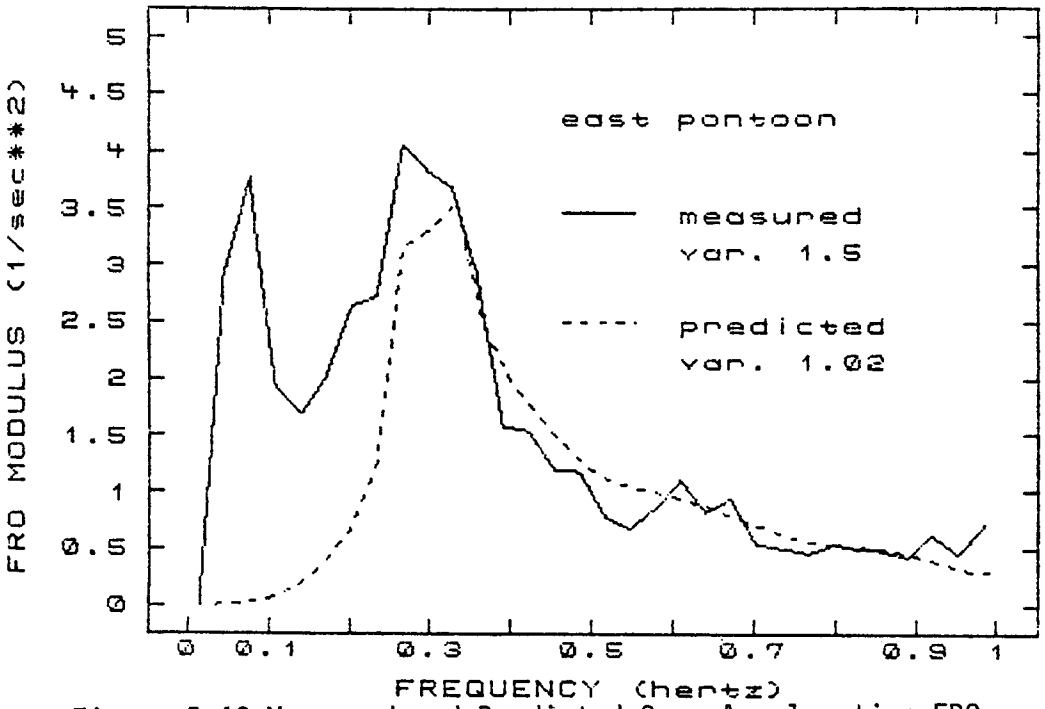

Figure 5.42 Measured and Predicted Sway Acceleration FRO Moduli for West Pontoon, Run 1: No Mooring Stiffnesses Assumed in Predictions

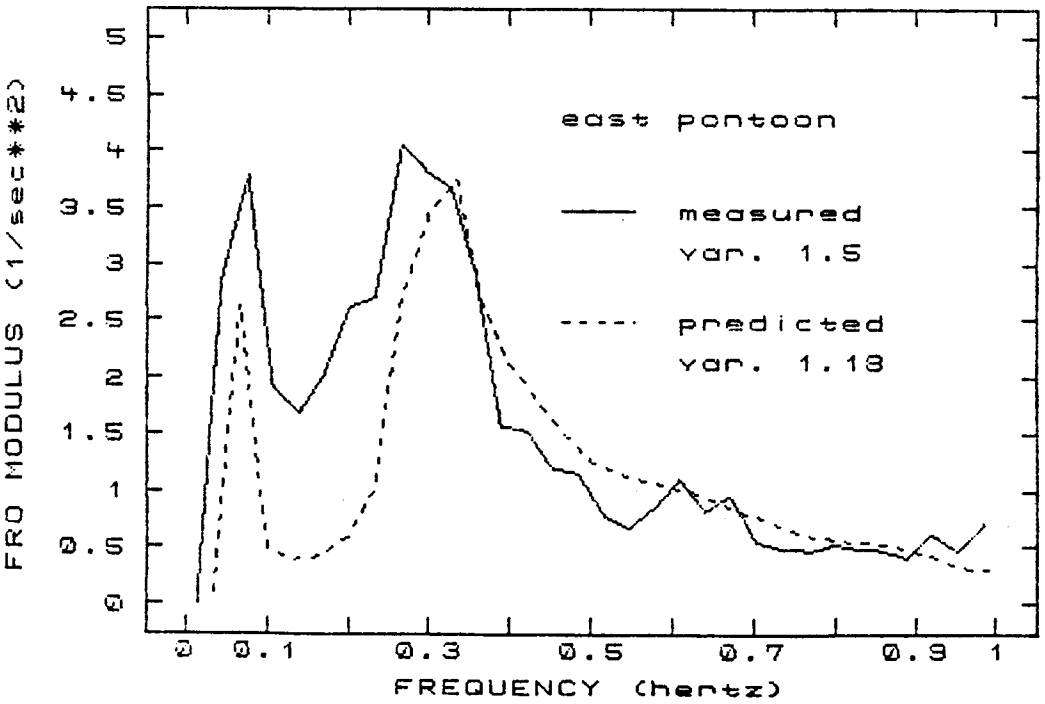

Figure 5.43 Measured and Predicted Sway Acceleration FRO Modlui for West Pontoon, Run 1: Mooring Stiffnesses from Program BRKMOOR

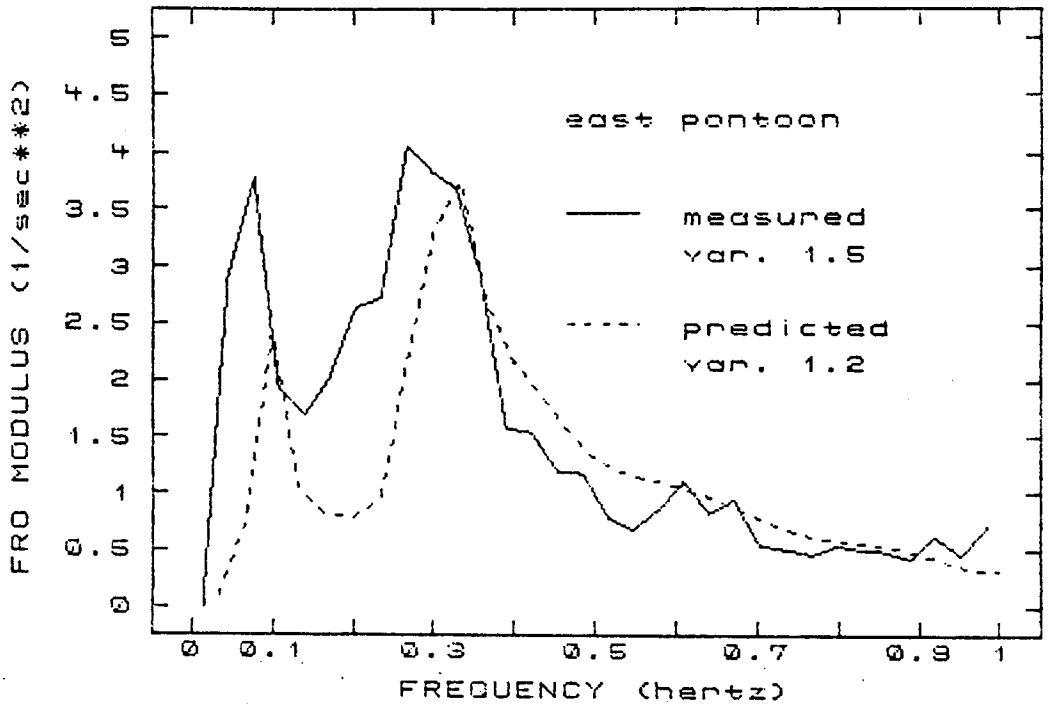

Figure 5.44 Measured and Predicted Sway Acceleration FRO Moduli for West Pontoon, Run 1: Program BRKMOOR Stiffnesses Arbitrarily Doubled

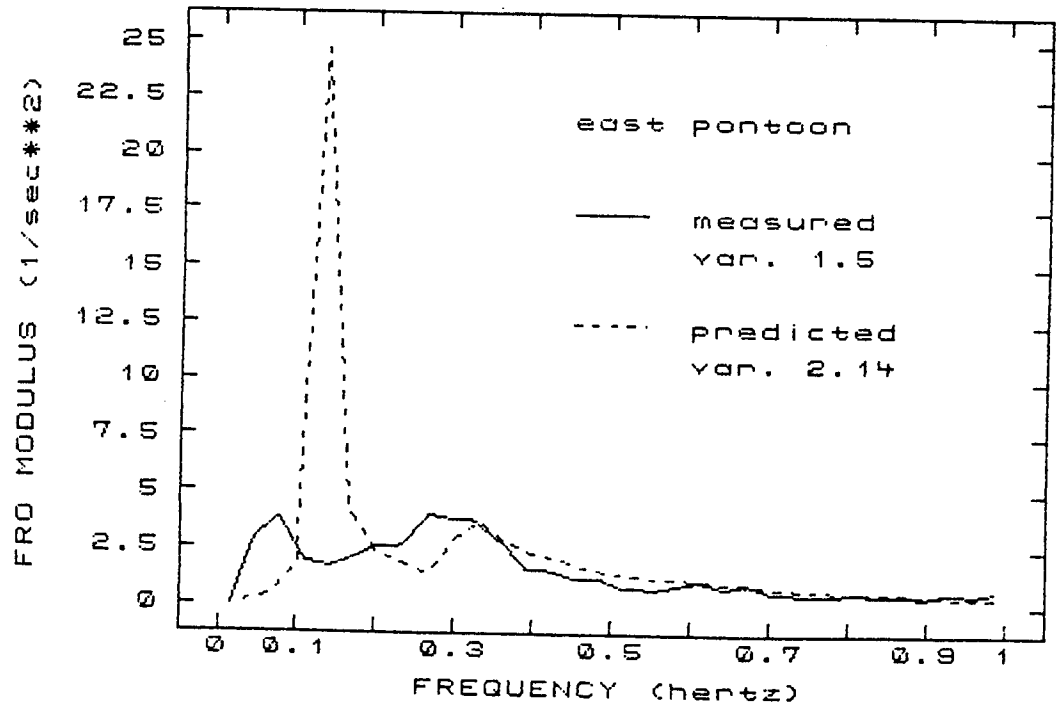

Figure 5.45 Measured and Predicted Sway Acceleration FRO Moduli for West Pontoon, Run 1: Program BRKMOOR Stiffnesses Arbitrarily Multiplied by 5

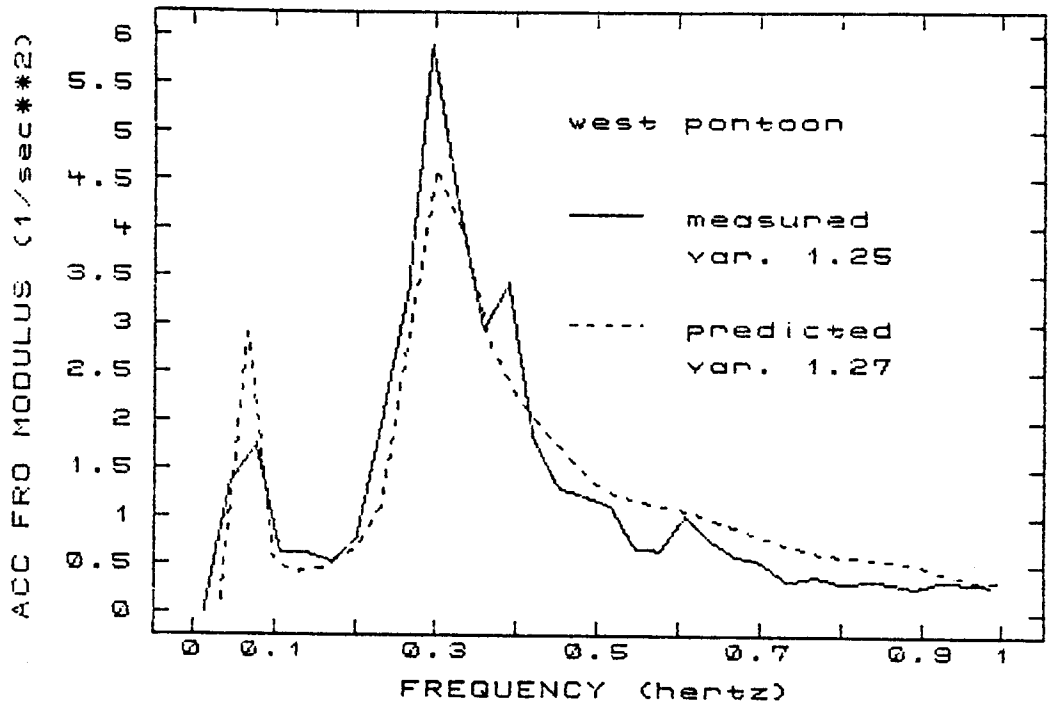

Figure 5.46 Measured and Predicted Sway Acceleration Autospectral Estimates for West Pontoon: Run 5

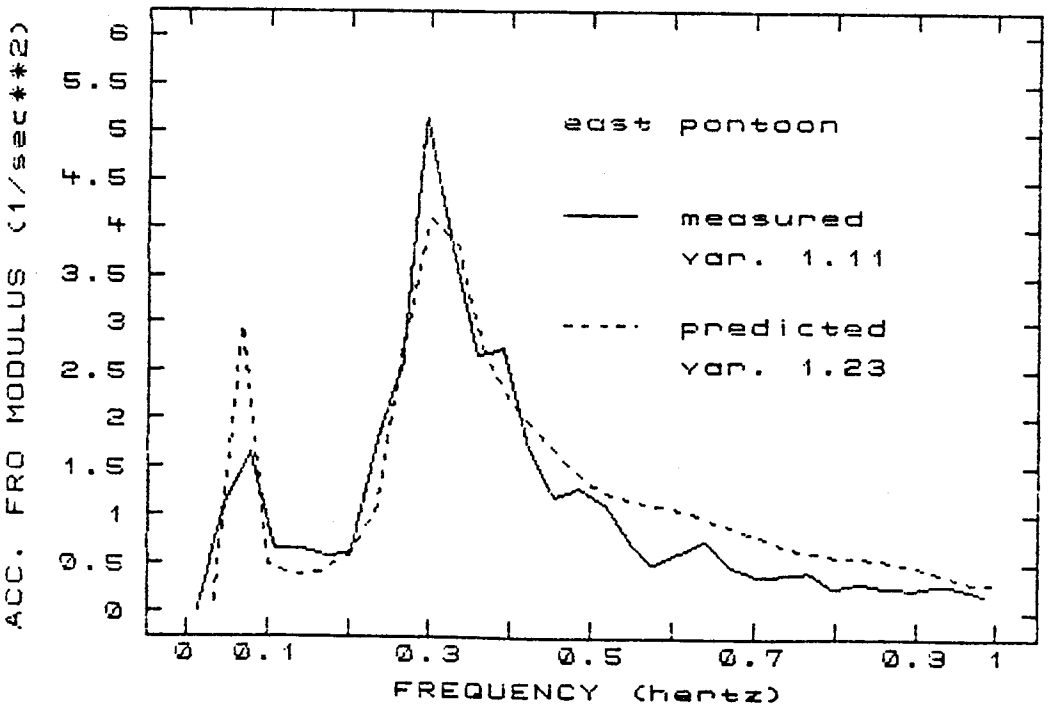

Figure 5.47 Measured and Predicted Sway Acceleration Autospectral Estimates for East Pontoon: Run 5

order hydrodynamic forces would be included, the potential for improvement is limited.

The statistics, figures, and discussions of the preceeding pages have established that the current theory is quite suitable, however, for providing accurate autospectral acceleration (and hence inertial force) estimates in all three degrees of freedom discussed. It also should suffice to provide good estimates of the lateral shear and other internal forces and moments on the body as the following discussion will attempt to demonstrate.

As a rough investigation of the relative orders of magnitude of the contributions to the dynamic horizontal shear, the following simplified analysis is offered. For the records with incident significant wave heights of 1.5 to 2.0 feet, the significant sway acceleration is about 5.0 feet/sec^2. The significant sway displacement will be assumed to be about four feet. This value should be conservative, being double that mentioned as the maximum horizontal excursion observed in the field under comparable conditions (Nelson et al, 1983).

The peak of the narrow-banded sway acceleration autospectrum is at about 0.3 hertz for the records of larger values of H_S, while from Figure 5.41 it is clear that the peak displacement response occurs at much lower frequencies, say 0.033 hertz.

An appreciation of the relative magnitudes of the contributions to the horizontal shear may be obtained by considering a simplified unidirectional beam sea with all time-varying forces lumped at the two frequencies just mentioned (0.3 and 0.033 hertz). Such a visualization is useful because both the accele-

ration and displacement spectra are relatively narrow-banded. The transverse horizontal shear may be calculated at any location simply by making a cut, summing all external forces including hydrodynamic, inertia, and restoring forces, and equilibrating the section with an internal shear force. If this is done at both frequencies (see Appendix D for calculations) two sets of phasor diagrams may be made, one for each frequency (Figures 5.48 and 5.49). These figures should be imagined as superposed upon one another and rotating at the frequencies indicated. The dynamic shear at a section would be the force required to equilibrate the sum of the projection of all pictured forces along the real axis.

As the diagrams are pictured, equilibrium is always maintained and no shear is required because the total mooring force on the body has been converted into a force per unit length. In actuality, since there are five pairs of mooring attachments on the West Point floating breakwater, these restoring forces take on the character of step functions at the points of cable attachment. Even for only two frequencies, directional seas would cause the amplitudes of all force vectors pictured to vary with time and space due to wave pressure coherencies of less than one along the face of the body.

The current description is sufficient to appreciate, however, that mooring forces are not likely to be the dominant contributor to maximum shears in the breakwater itself, being of significantly smaller magnitude than forces due to waves or inertia. This is not to say that forces related to the mooring

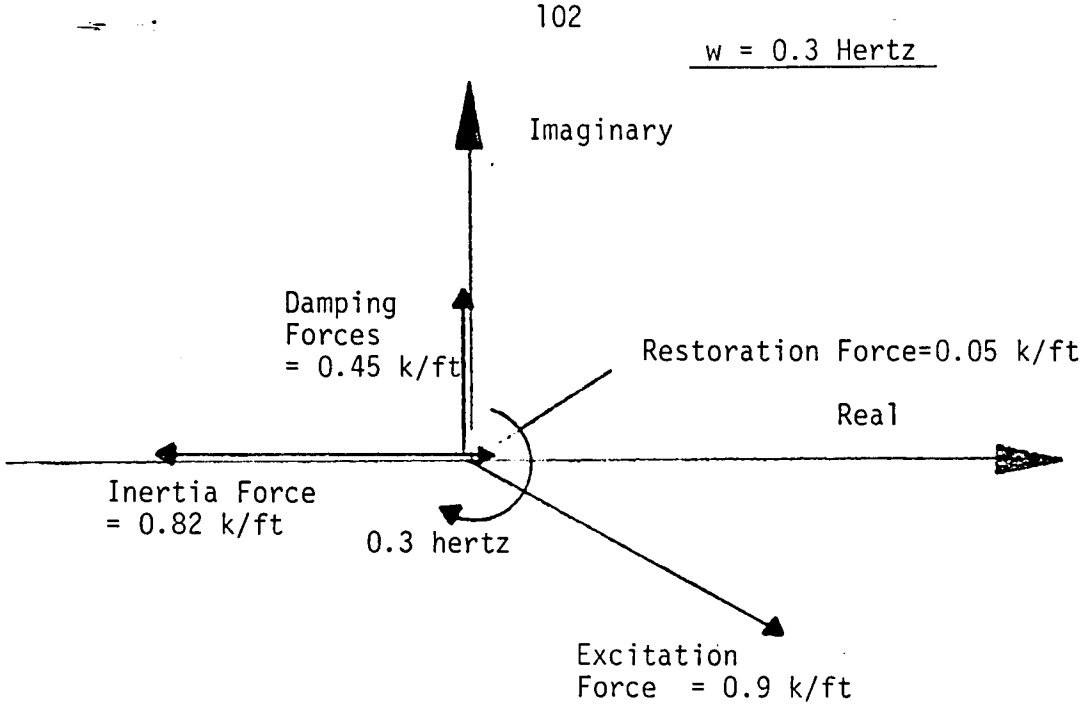

Figure 5.48 Phasor Diagram Showing Magnitude Estimates of Forces Acting at Arbitrary Section on Breakwater: 0.3 hertz

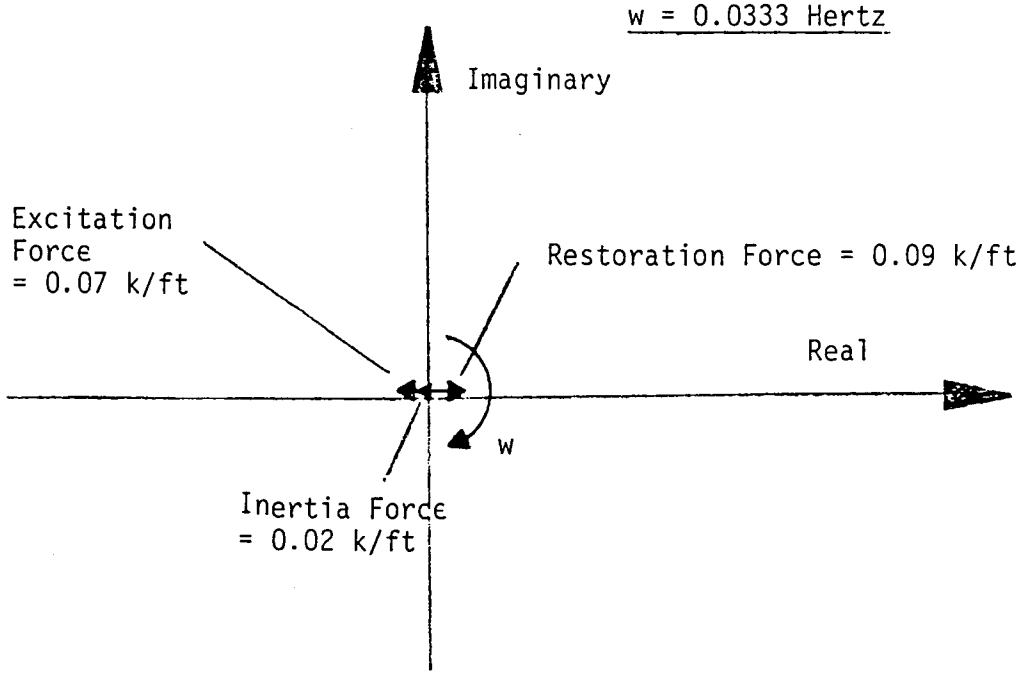

Figure 5.49 Phasor Diagram Showing Magnitude Estimates of Forces Acting at Arbitrary Sections on Breakwater: 0.033 hertz, Same Scale as 5.48

system would not be important near the points of attachment of the cables. In fact, at the ends of the breakwater they would be equal to the shear, provided mooring attachments were located precisely at the ends.

This analysis would seem to suggest that reasonable estimates of maximum dynamic shear stresses in the major portions of the pontoons themselves might be made despite the rough nature of the mooring force estimates provided by a method of analysis such as the one contained in this report. Economical design of the mooring system itself, as well as local reinforcement detail in the pontoon near the points of attachment, however, might be better pursued with the aid of a supplementary low-frequency analaysis such as described by Oppenheim (1981) or Standing (1981).

CHAPTER VI

CONCLUSIONS AND RECOMMENDATIONS

A) Conclusions

Reasonable estimates of rigid body accelerations of the West Point prototype floating breakwater in short crested seas using seakeeping theory were obtained for the three degrees of freedom (sway, heave, and roll) extensively examined. Agreement appeared to be the best at higher significant wave heights although H_s = 2.1 feet was the most extreme sea state for which good data was available.

The predicted results in heave or the vertical degree of freedom showed the best agreement with the data over the widest range of sea states, exhibiting less sensitivity to wave height and angle of wave attack. Predicted acceleration variances ranged from 0.55 to 1.25 of those measured.

The agreement in shape between the predicted and measured acceleration spectra (as quantified by the normalized squared error) in the sway or lateral mode was nearly as good as for the heave degree of freedom. A tendency toward underprediction of the magnitude became evident, however, at lower significant wave heights and for angles of wave attack exceeding twenty degrees off of beam. The coincidence of low significant wave heights and larger principal angles of wave attack in the records analyzed made determination of the major causes of the disagreement difficult. Predicted variances in sway ranged from 0.5 to 1.1 of those measured.

The magnitude of the predicted roll or longitudinal angular acceleration also tended to fall short under the same circumstances as in sway, only to a lesser extent. Predicted variances were from 0.5 to 1.2 of those measured. The shape of the predicted roll acceleration autospectra, however, generally exhibited the poorest agreement with measurements. This was because the bandwidth of the predicted spectrum was smaller than the measured estimate in a small number of model runs. Both roll and sway showed markedly poorer agreement for records where the wind direction had not been steady for at least four hours. This may be due again to sensitivity to the principal angle of wave attack or to a seastate with complex directional properties.

Unpredicted rises in the acceleration frequency response operators occurred in the sway and roll modes near 0.4 hertz. Such behavior was more prominent in less severe sea states where larger percentages of the incident wave energy occurred at this frequency and when the principal attack angle was farthest from beam. Oscillations of the clump weights and/or mooring lines were suspected.

Accuracy of sway acceleration predictions might become significantly poorer in sea states containing wave energy below 0.28 hertz ($b/\lambda = .25$) due to a lack of consistent agreement of the predicted sway frequency response operators with those derived from measurements. Problems with hydrodynamic coefficients in the 0.2 to 0.28 hertz frequency range are a possible cause. The incident wave spectra examined generally contained little energy

at these wavelengths, so overall analytical predictive ability was minimally affected.

Under more severe sea states, seakeeping methods may have trouble adequately accounting for the influences on the sway mode of the mooring restraints at frequencies below 0.2 hertz. A low frequency dynamic mooring analysis appears advisable as a supplement to the current approach to adequately account for nonlinear drift forces if accurate estimates of mooring forces are desired at high significant wave heights. If reasonable estimates of internal forces and moments in the breakwater itself are required, then the methods presented are probably sufficient provided such estimates are made far enough away from the local influence of mooring attachments.

In some cases, questionably high powers of a cosine spreading function were required to obtain responses of sufficient magnitude. Powers of 18 and in one case a unidirectional sea state were found to give the closest agreement. A lack of closely enough spaced wave excitation calculations was shown to be a possible contributing factor although probably not the only one. It was also noted that different portions of the frequency domain would have required different degrees of cosine spreading for optimum agreement of the predicted linear operators with those based on measurements. A need for accurate directional wave data became apparent.

In summary, seakeeping theory appears to adequately predict floating breakwater accelerations in beam seas in the regions of

maximum acceleration response. It appears to be well suited for use as a design tool if its limitations are recognized and accurate input quantities are available.

B) Recommendations

Recommendations stemming from this report fall into two categories: suggestions pertaining to future data acquisition efforts and fruitful directions for work on extending the capabilities of this type of analysis.

i) Suggestions for Future Data Acquisition Efforts

The biggest unknown present in any dynamic analysis occurring in limited fetch environments is accurate information regarding the character of the sea state. Whether the short-crestedness of the seaway is explicitly modeled or treated as a superposition of long crested waves as is usually assumed in seakeeping theory, a knowledge of the characteristics of the seaway is a must if proper coherencies are to be established between spatial locations. The profession currently must supplement scanty data measured at a very few locations with suppositions. The net result is more uncertainty in the analysis and overdesign. An ideal scenario would involve pressure measurements on the face of a floating bridge or breakwater made concurrently with those by a wave array located at some distance away. In this way, some idea of the interaction between the structure and the incident wave field might be obtained.

The current analysis could have benefited from more extreme events, as the level of agreement had not yet begun to fall at the largest incident wave heights available in the data. Before

the limitations of this method can truly said to have been found, it must be carried into the range where nonlinearities clearly become significant. What is needed are data in which the motions of the breakwater are so severe that clear evidence of nonlinear coupling and frequency shifts are seen. In short, the profession could greatly benefit from more projects of this type.

In order to accurately extend the type of analysis detailed in this report to the maximum possible number of situations, data on the load-displacement relationships of interpontoon connections is a necessity. The connection at the West Point site during the period of the data analyzed by this report was rigid, but the U.S. Army Corps of Engineers also experimented with flexible connectors of butyl rubber. The results of this report indicate that accurate predictions can be made for a single module. There is no reason such an analysis could not be carried to multiple nodes provided the stiffnesses between modules could be adequately defined. Since modules interconnected in this manner would tend to respond together to long-period waves and separately to shorter period waves, accurate estimates of the forces in the connectors could be made for practical incident wave climates provided suitable linearizations of the load-displacement characteristics of the connectors were feasible. This is a question which only controlled testing can properly answer.

ii) Suggestions for Extending Analysis Capabilities

A version of the Frank Close Fit method for calculating hydrodynamic coefficients should be obtained or coded. The

version contained within program NSRDC is too thoroughly integrated into the program to be easily excised, and the program itself is extremely inefficient for breakwater analysis. By experimenting with the way in which contours are input, better results in sway and roll could very likely be achieved. It is possible that some of the problems cited in the Analysis and Discussion section of this report are not really limitations of the general theory at all. Unless guidelines for the reliable use of such an algorithm can be documented, its usefulness is severely hampered.

The measured rigid body accelerations should be transformed to the locations of the strain gages on the West Point breakwater and internal forces calculated. The level of agreement could then be investigated with the strain gage data available. If the results were good, the technique used in this report could be used with more confidence in the prediction of such forces.

A low frequency mooring analysis package of the type frequently referenced in the body of this report should be obtained and run. The level of agreement at the displacement level should be noted when the results are combined with an analysis similar to the one used in this report. Predicted mooring forces from such an analysis should be compared with the mooring force measurements made on the West Point breakwater. If the results are sufficiently promising, the method could be integrated with a more traditional seakeeping model into a complete breakwater

analysis package. Such a tool would be invaluable in the hands of a designer.

BIBLIOGRAPHY

1. Adee, B.H., Richey, E.P., and Christensen, D.R., "Floating Breakwater Field Assessment Program, Friday Harbor, Washington," U.S. Army Corps of Engineers Coastal Engineering Research Center, Fort Belvoir, Virginia, Technical Paper No. 76-17, October 1976.

2. Bhattacharyya, Rameswar, Dynamics of Marine Vehicles, New York: John Wiley and Sons, Inc., 1978.

3. Frank, W., "Oscillation of Cylinders in or Below the Free Surface of Deep Fluids," Naval Ship Research and Development Center Report 2375, Wash. D.C., 1967.

4. Georgiadis, Constantinos and Hartz, B. J., A Computer Program for the Dynamic Analysis of Continuous Floating Structures in Short Crested Waves, Harris Hydraulics Laboratory Technical Report No. 4, University of Washington, April 1982.

5. Georgiadis, Constantinos, Wave Induced Vibrations of Continuous Floating Structures, Doctoral Dissertation, University of Washington, 1981. (Unpublished)

6. Gerald, Curtis F., Applied Numerical Analysis, Philippines, Addison-Wesley Publishing Company, Inc. May 1980.

7. Geshkinli, Nezih and Yavuz, Davras, Discrete Fourier Transformation and Its Applications to Power Spectra Estimation, New York, Elsevier Scientific Publishing Company Inc., 1983.

8. Hartz, B. J., "Notes on the Spatial Correlation Factor," University of Washington, unpublished, 1983.

9. Hutchison, Bruce L., The Prediction and Analysis of the Motions of Offshore Deck Cargo Barges, MS Thesis, University of Washington, 1977.

10. Hutchison, Bruce L., "Impulse Response Techniques for Floating Bridges and Breakwaters Subject to Short-Crested Seas," presented at Pacific Northwest Section, Society of Naval Architects and Marine Engineers, 1982.

11. Hutchison, Bruce L. and Bringloe, J. Thomas, "Application of Seakeeping Analysis," Marine Technology, Vol 15, No. 4, Oct. 1978, pp. 416-431.

12. Jenkins, Gwilym M. and Watts, Donald G., Spectral Analysis and Its Applications, San Francisco, California, Holden-Day, August, 1969.

13. Kinsman, Blair. Wind Waves, Englewood Cliffs, New Jersey: Prentice-Hall, Inc. 1965.

14. Langen, Ivar, On Dynamic Analysis of Floating Bridges, Division of Structural Mechanics, The Norwegian Institute of Technology, The University of Trondheim, Norway, Report No. 81-1, May 1981.

15. Meyers, W.G. et al, "Manual: NSRDC Ship-Motion and Sea-Load Computer Program," Naval Ship Research and Development Center Report 3376, Washington D.C. February 1975.

16. Nelson, Eric, Christensen, Derald, and Schuldt, David A., "Floating Breakwater Prototype Test Program," Presented at A.S.C.E. Coastal Structures Conference, 1983.

17. Ochi, Michel K., "Review of Recent Progress in Theoretical Prediction of Ship Responses to Random Seas," Seakeeping 1953-1973, SNAME T & R Symposium S-3, June 1974, pp. 129-191.

18. Oppenheim, B.W. and Wilson, P.A., Low-Frequency Dynamics of Moored Vessels, Giannotti and Associates, Inc. February, 1980.

19. Orr, Walton Alburtus, Random Motion Response of a Model in A Natural Seaway Environment, Doctoral Dissertation, University of Washington, 1975.

20. St. Denis, Manley and Pierson, Willard J. Jr., "On the Motion of Ships in Confused Seas," Trans. SNAME, Vol. 61, 1953, pp. 280-357.

21. Salveson, N., Tuck, E.O., and Faltinsen, O.M., "Ship Motions and Sea Loads," Trans. SNAME, Vol. 78, 1970, pp. 250-287.

22. Schmitke, &Rodney T., "Ship Sway, Roll, and Yaw Motions in Oblique Seas," presented at Annual Meeting, SNAME, New York, N.Y., November 16-18, 1978.

23. Sergev, &S. S., Rigid Body Acceleration of an Ocean-Going Towed Barge, MS Thesis, University of Washington, 1972.

24. Shore Protection Manual, U.S. Army Coastal Engineering Research Center, Washington D.C., 1977.

25. Standing, &R.G., et al., "Slowly-Varying Second-Order Wave Forces: Theory and Experiment", National Maritime Inst., Feltham England, 1981.

26. Sutko, A. A. and Haden, E. L., "The Effect of Surge, Heave and Pitch on the Performance of a Floating Breakwater," Floating Breakwaters Conference, Newport, Rhode Island, 1974.

27. Vassilopoulos, Lyssimachos, "Ship Rolling at Zero Speed in Random Beam Seas with Nonlinear Damping and Restoration," Journal of Ship Research, December 1971, pps. 289-294.

28. Vugts, Jan Hendrik, "The Hydrodynamic Coefficients for Swaying, Heaving, and Rolling Cylinders in a Free Surface," Shipbuilding Laboratory Report No. 112 S, Technological University of Delft, Netherlands, 1968.

29. Vugts, Jan Hendrik, The Hydrodynamic Forces and Ship Motions in Waves, Doctoral Dissertation, Technological University of Delft, Netherlands 1970.

APPENDIX A

DESCRIPTION OF COMPUTER MODEL

Rather than attempt to formulate a comprehensive computer program which would perform a breakwater analysis from start to finish, the author elected to allow the software to remain in several separate programs. This format allowed more flexibility, both in permitting different programs to be run on different computers, based on such considerations as memory, processing time, cost etc., but also simplified the task of making software modifications. By simply ensuring that a program wrote files which were compatible with the next processing step, changes and corrections in logic were limited in scope. Except for Program NSRDC, all processing was done on an Intel 8085/8088 based microcomputer.

A) Program NSRDC

Hydrodynamic coefficients and excitation forces were calculated using a sophisticated ship motion package produced by the David Taylor Naval Ship Research and Development Center (Meyers et al.,1975). The program uses the Frank Close-Fit method to compute the hydrodynamic coefficients and forcing functions and then goes on to calculate the motion frequency response operators for six degrees-of-freedom in a unidirectional sea for up to 40 discrete frequencies at any specified wave attack angles. Program NSRDC does not calculate the response to an input wave spectrum, either in a unidirectional or short-crested seaway but the frequency response operators are output for use by post-processing programs. The computer model developed for this re-

port does not make use of these operators, however, since no account of stiffnesses due to moorings is made and no convenient input avenue exists for supplying them. Even if such an avenue existed (or could be developed), program NSRDC is extremely expensive to run (requiring up to 250 processing seconds for 30 frequencies and 10 attack angles) on a CDC 6400 and would be difficult to modify so as to avoid redundant recomputation of many of the hydrodynamic quantities. The expense of running the program was increased somewhat by specifying a larger frequency range than was really necessary.

Figures A.1 through A.8 show the values of the hydrodynamic mass and damping coefficients obtained from program NSRDC which were used. In general the results in sway and heave are in very close correspondence with those of Vugts (1970). The roll added mass coefficient is somewhat higher than that obtained by Vugts for non-dimensional frequencies greater than 0.75. The magnitude of the roll hydrodynamic damping coefficient calculated by program NSRDC is also a little larger than that of Vugts, but it peaks at the same frequency. The sway-roll cross-coupling mass, while exhibiting a similar overall shape as that of Vugts appears to take on more extreme values. This could be the cause of some of the problems mentioned in the body of this report with regard to sway predictions; program NSRDC appears to be somewhat sensitive to the precise way in which the section contours are entered. As mentioned in Chapter V, different values for A42 and B42 were obtained for contours which differed only in the exact location of the points specified, although the outline was the

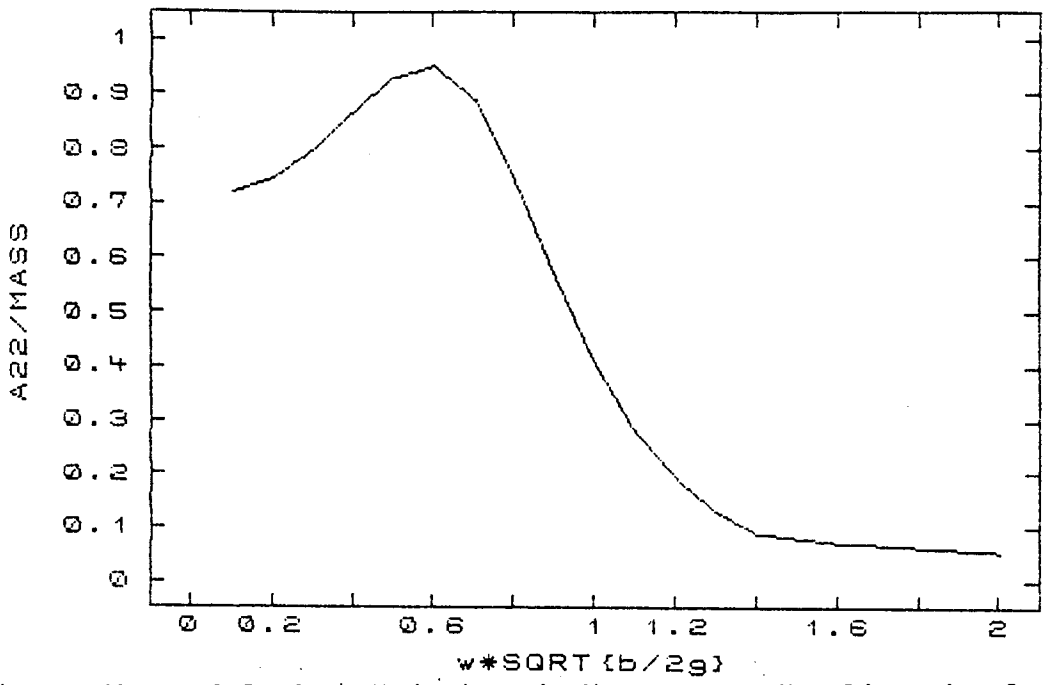

Figure A.1 Sway Hydrodynamic Mass versus Non-Dimensional Frequency as Calculated by Program NSRDC

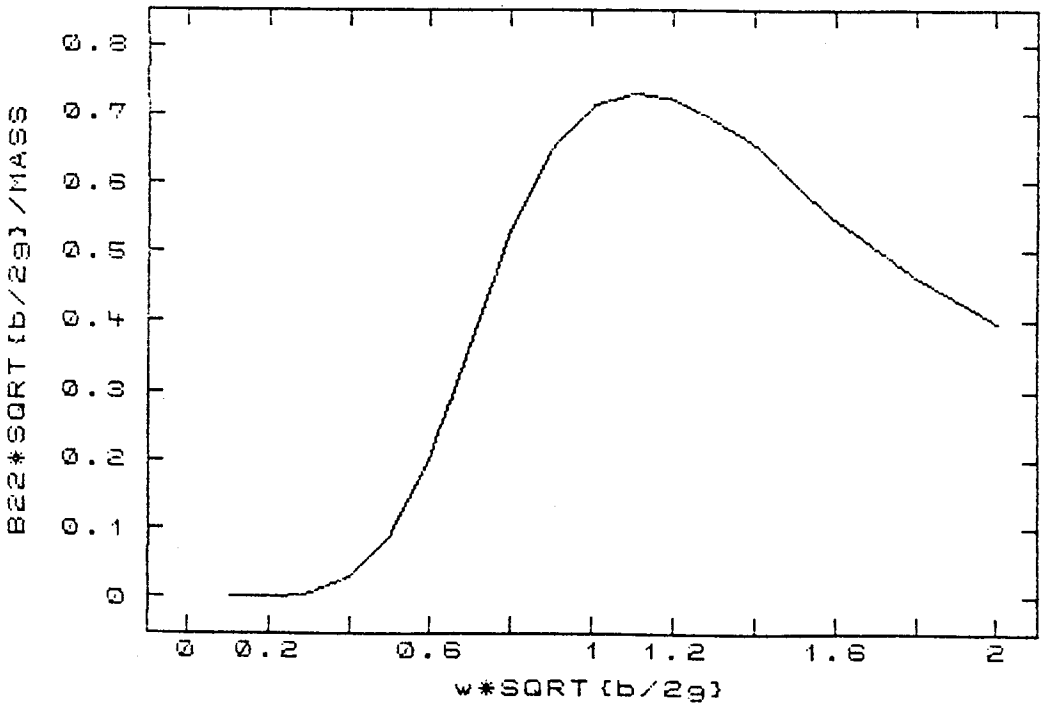

Figure A.2 Sway Hydrodynamic Damping versus Non-Dimensional Frequency as Calculated by Program NSRDC

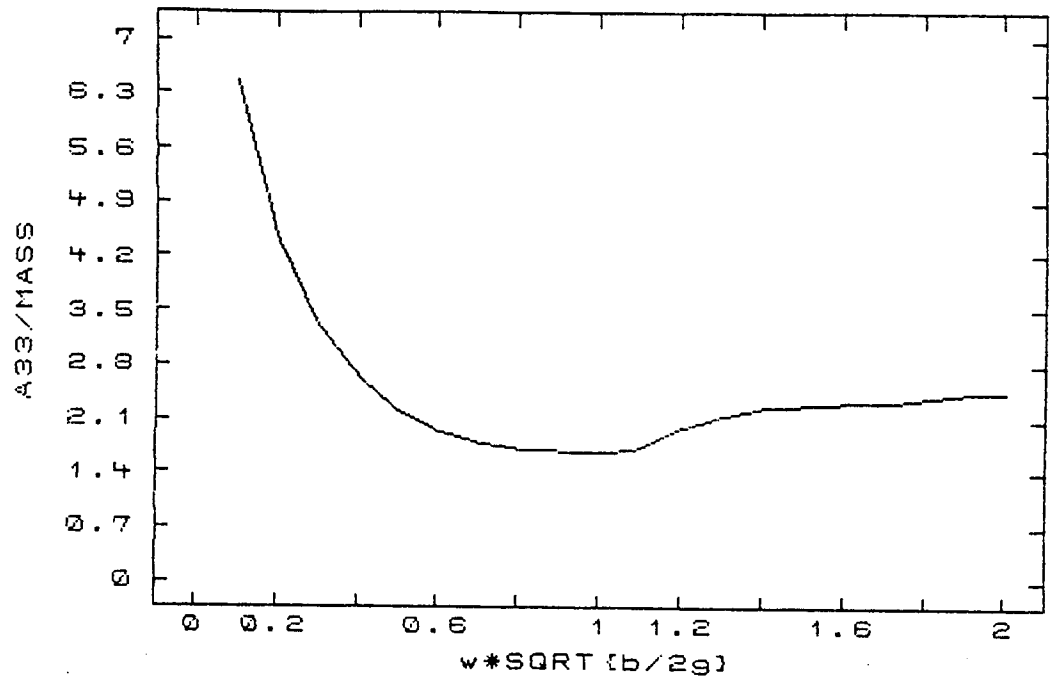

Figure A.3 Heave Hydrodynamic Mass versus Non-Dimensional Frequency as Calculated by Program NSRDC

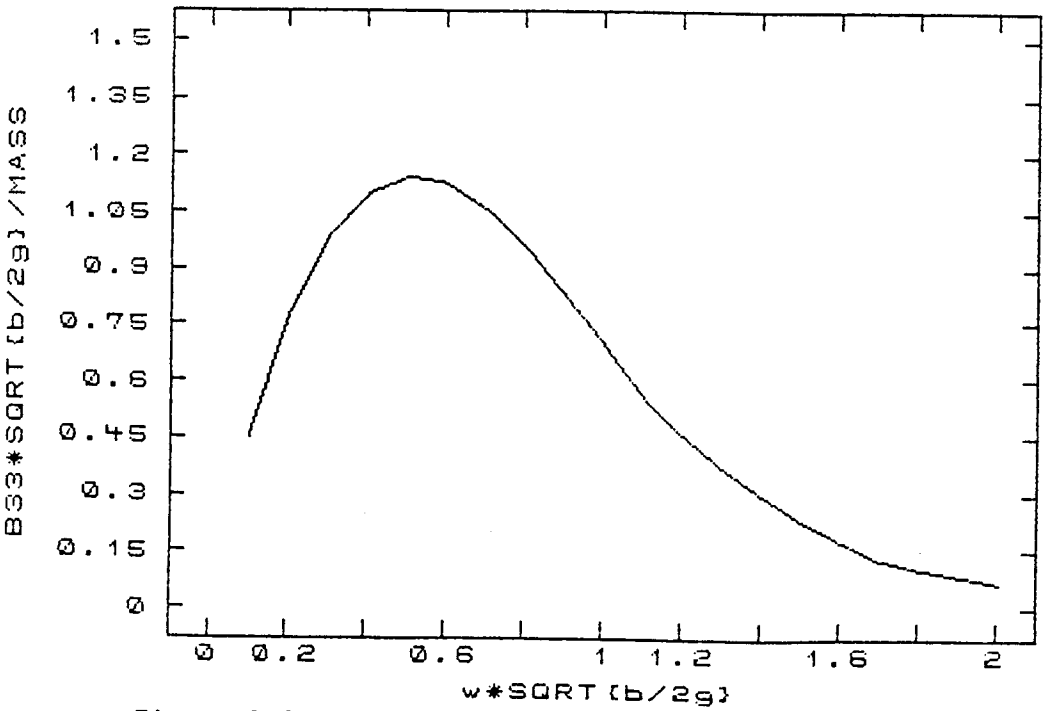

Figure A.4 Heave Hydrodynamic Damping versus Non-Dimensional Frequency as Calculated by Program NSRDC

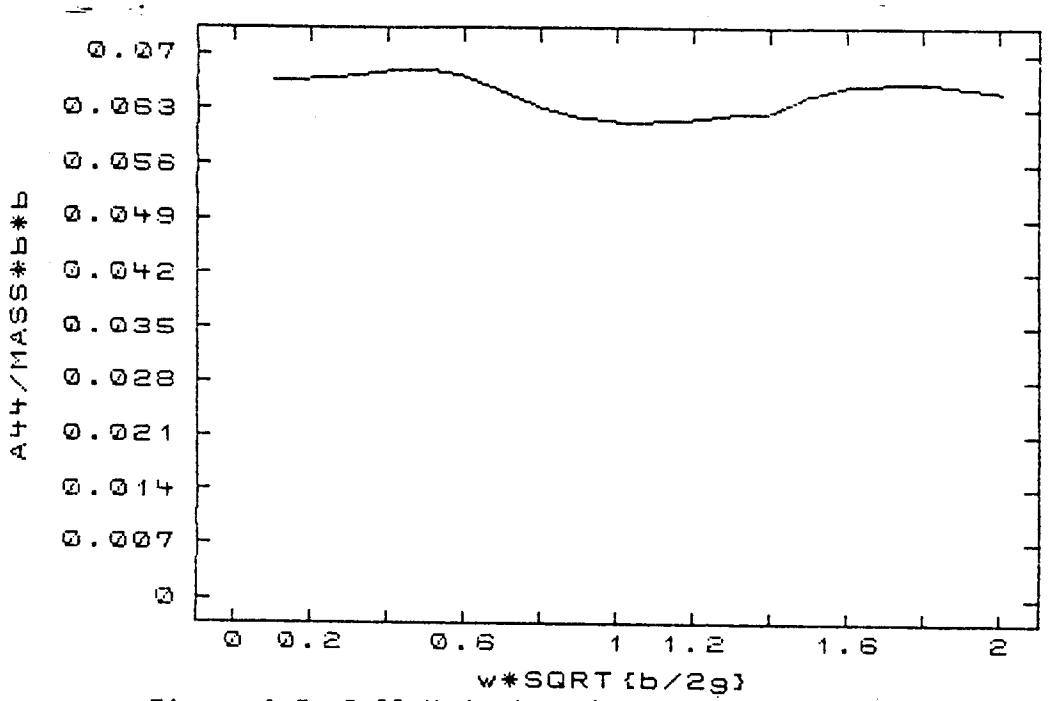

Figure A.5 Roll Hydrodynamic Mass versus Non-Dimensional Frequency as Calculated by Program NSRDC

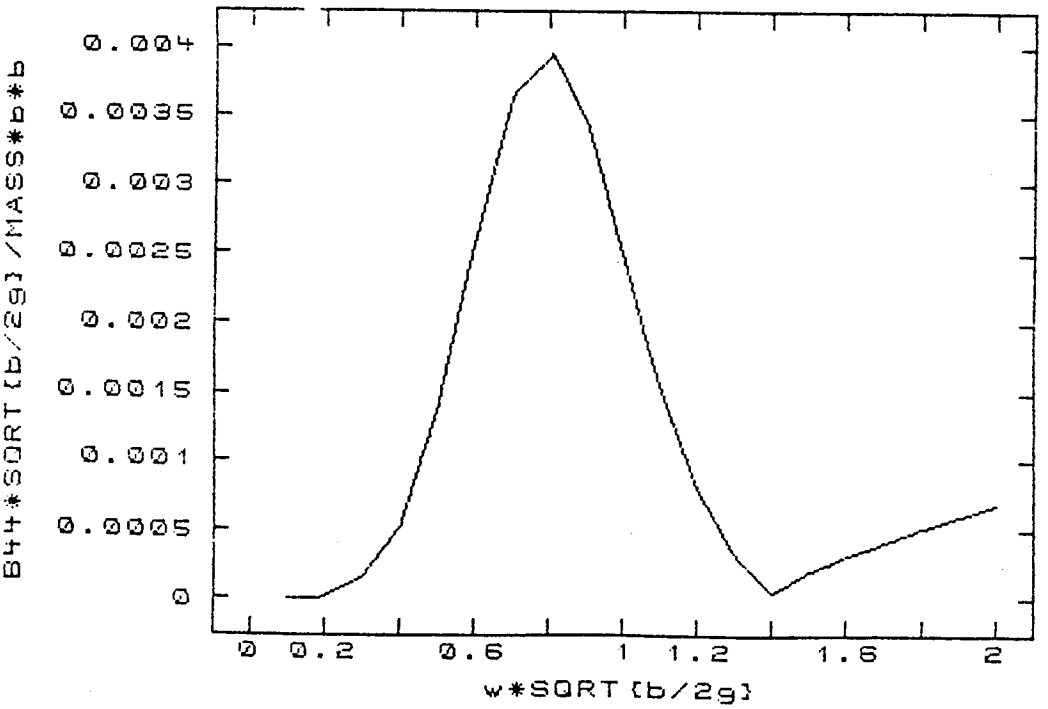

Figure A.6 Roll Hydrodynamic Damping versus Non-Dimensional Frequency as Calculated by Program NSRDC

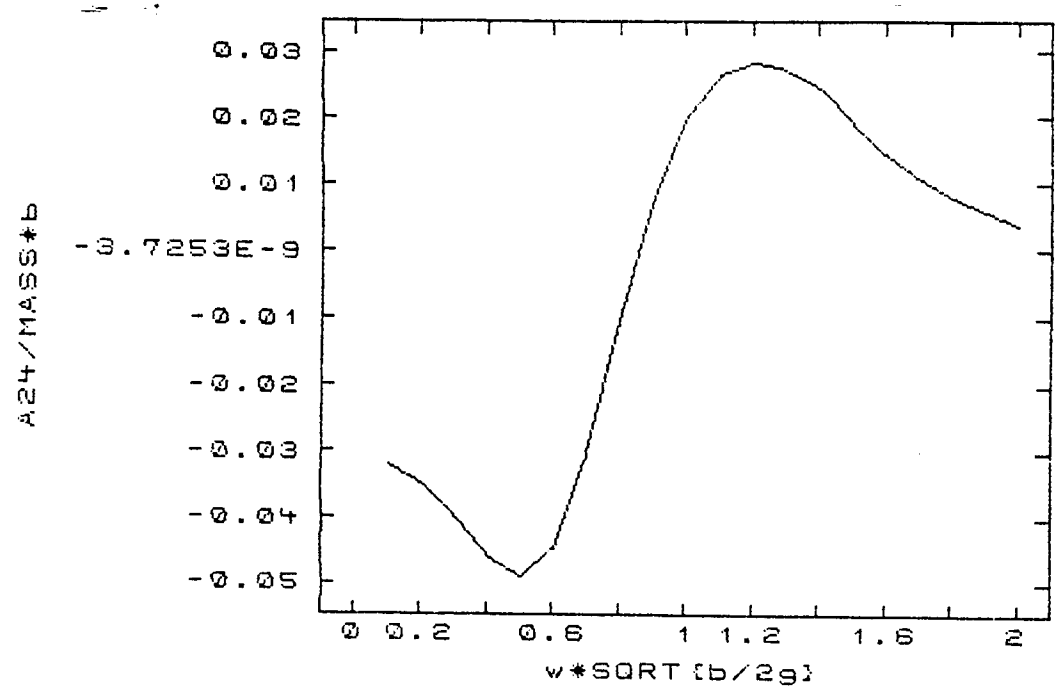

Figure A.7 Sway Coupled into Roll Hydrodynamic Mass versus Non-Dimensional Frequency as Calculated by Program NSRDC

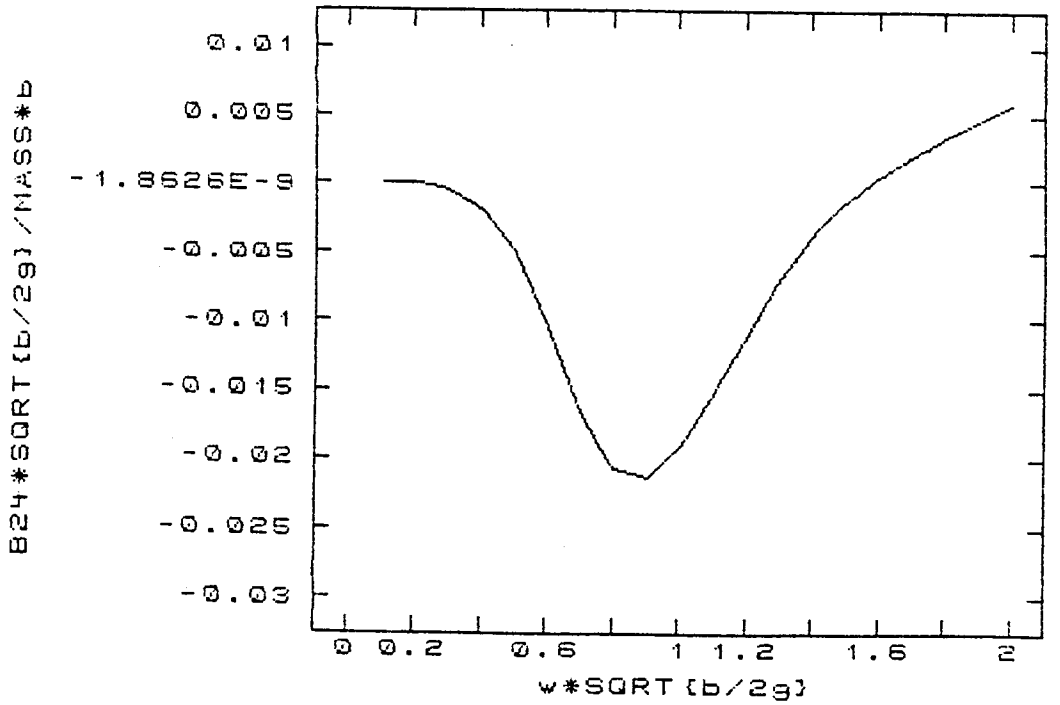

Figure A.8 Sway Coupled into Roll Hydrodynamic Damping versus Non-Dimensional Frequency as a Calculated by Program NSRDC

same. Figures A.9 through A.13 show the wave excitation forces obtained from program NSRDC with the exception of the surge force.

A point regarding Program NSRDC's treatment of the surge forcing function: since slender-body strip theory is used, it is assumed that no sharp discontinuities occur in the contour of the body. The ends of the breakwater, however, are examples of severe discontinuities in the breakwater profile. No account is made by the program of the wave forces which might act against these end surfaces. The surge exciting force that is calculated arises from the unit normal in the x direction due to the change in contour between two adjacent sections. For a rectangular prismatic body, this force would properly be zero since there is no normal in the x direction. The surge excitation forces supplied by Program NSRDC appear to be entirely the result of inexactitudes in numerical integrations etc. which explains their extremely small magnitudes and the fact that the surge force is calculated to be the greatest at an attack angle of zero degree (beam) seas. Surge motions are often considered negligible and since the surge equation of motion is entirely uncoupled from the others, no attempt was made in this analysis to account for surge. While a thorough examination of the coordinate transformations discussed in Chapter IV would include a surge component in the normal (heave in vessel coordinates) acceleration, the smallness of both the surge motion itself and the pitch angle make this contribution negligible.

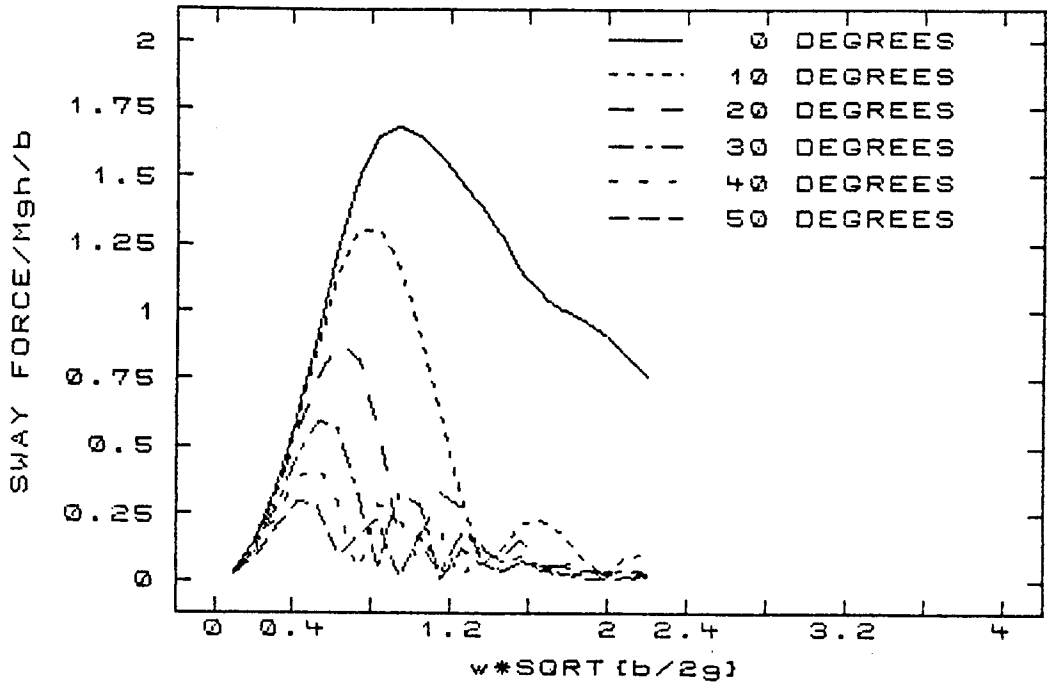

Figure A.9 Sway Excitation Froce Magnitude for Various Attack Angles as Calculated by Program NSRDC

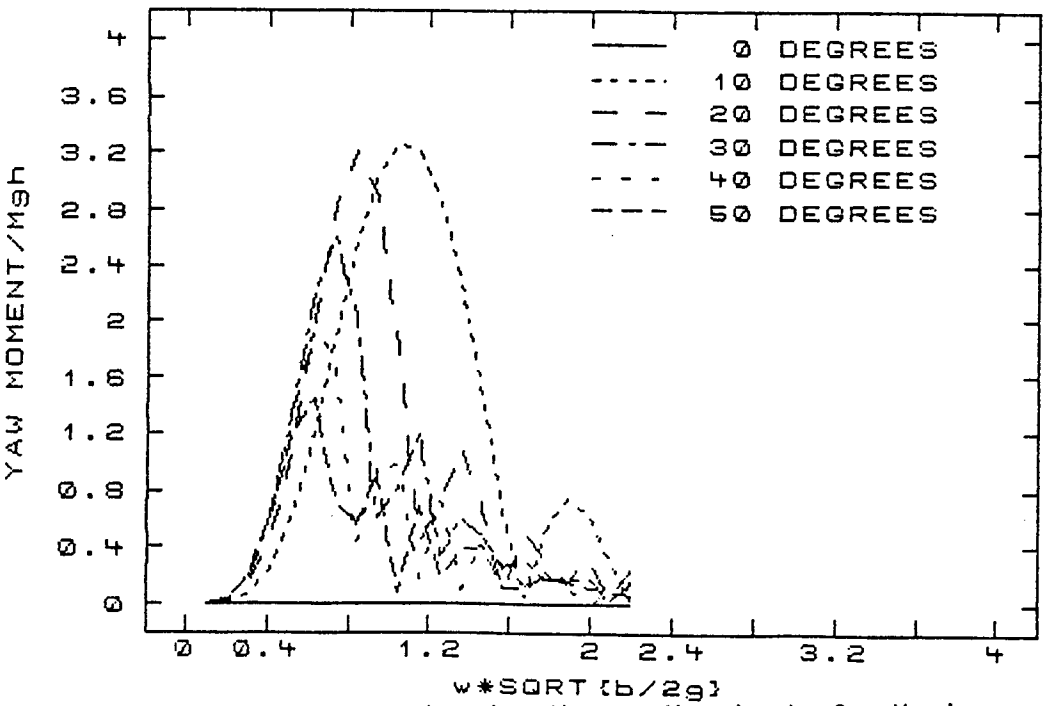

Figure A.10 Yaw Excitation Moment Magnitude for Various Attack Angles as Calculated by Program NSRDC

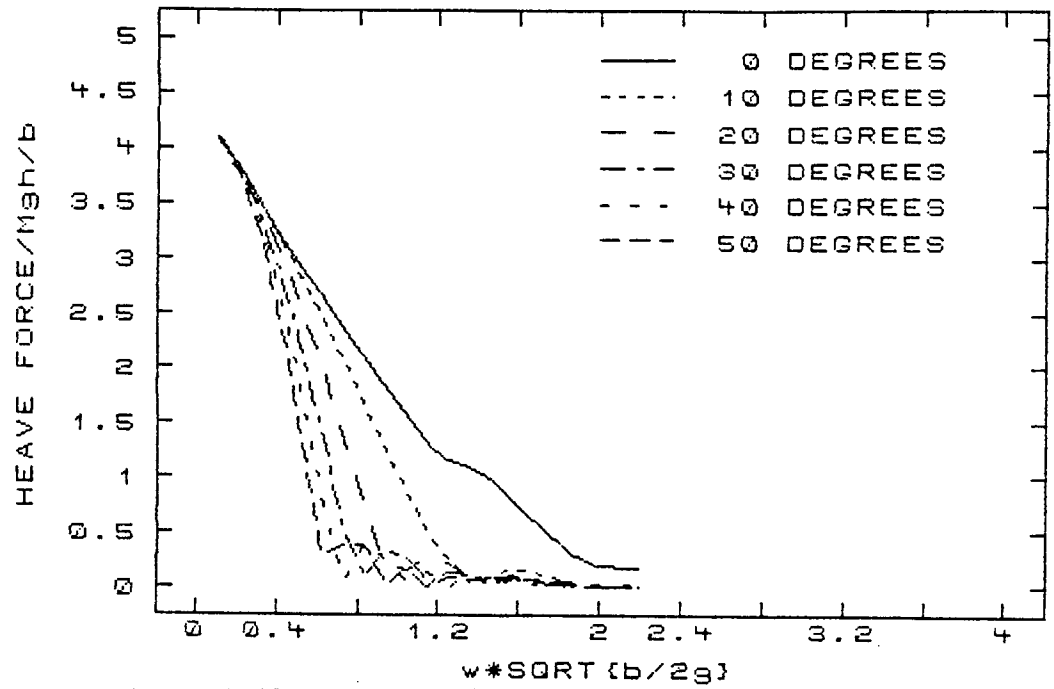

Figure A.11 Heave Excitation Force Magnitude for Various Attack Angles as Calculated by Program NSRDC

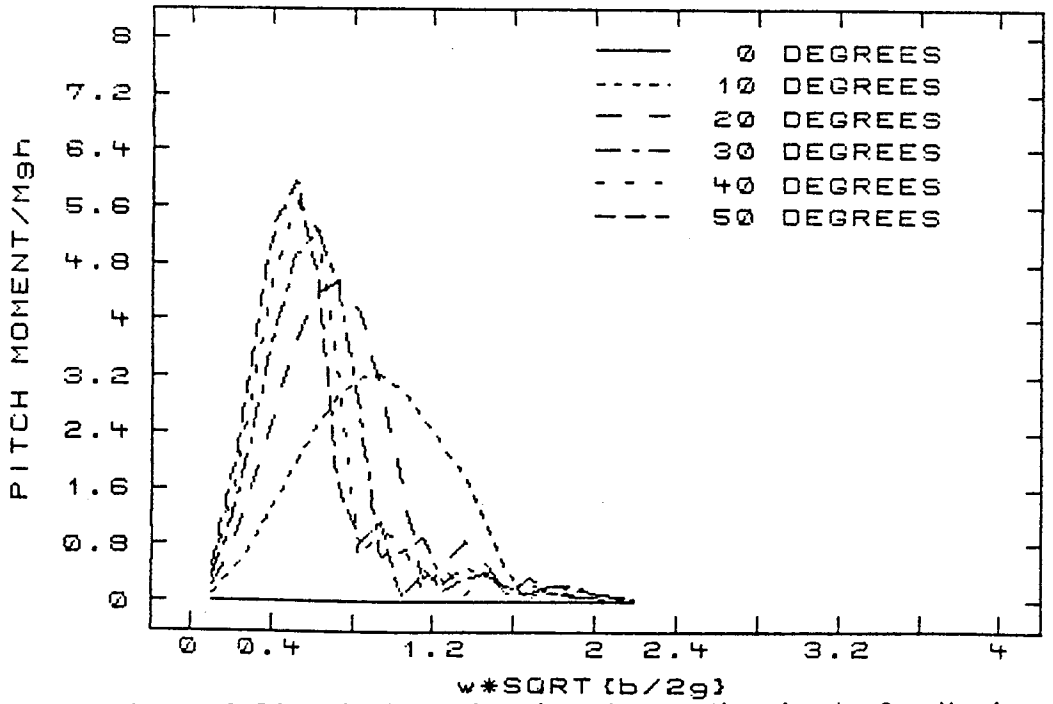

Figure A.12 Pitch Excitation Moment Magnitude for Various Attack Angles as Calculated by Program NSRDC

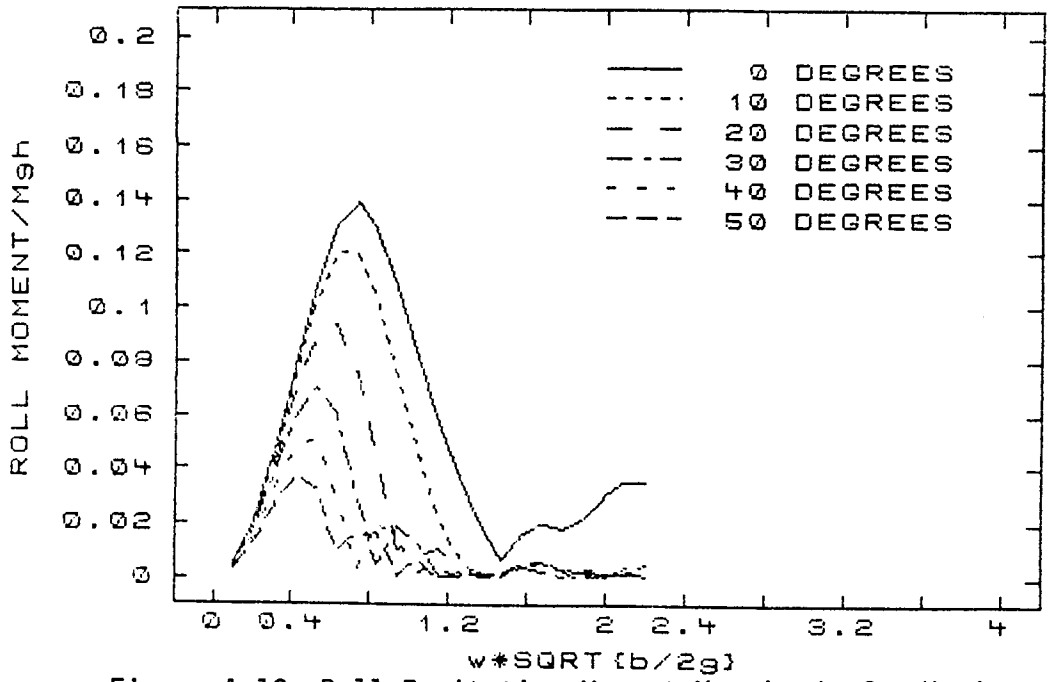

Figure A.13 Roll Excitation Moment Magnitude for Various Attack Angles as Calculated by Program NSRDC

B) Program BRKMOOR

Mooring stiffnesses were calculated by Program BRKMOOR, the listing and documentation of which occur in (Adee et al., 1976). The program determines the breakwater equilibrium condition by dividing the cable into elements, connecting the nodes with straight but elastic segments, and iterating until both equilibrium and cable geometry are sufficiently satisfied. Spring constants are then determined by perturbing the breakwater from equilibrium and calculating the changes in tension which result.

Two-dimensional output is then converted into a full 3-dimensional mooring stiffness matrix by a short post-processing program written by the author which is capable of considering differences in depths, cable lengths, and other asymmetries in the mooring system. It was quickly apparent that the precision with which the input quantities were known did not justify this extra refinement.

C) Program EOMSOL

Program EOMSOL assembles and solves the equations of motion for all wave attack angles specified and considers square law roll damping effects over any user-specified frequency band. Since useful results for the roll degree-of-freedom depend upon proper input constants for bilge radius and wave steepness, it was decided to include a listing of the subroutine that performs the viscous roll-damping calculations so information presented in this report might be of use to others.

D) Program RESP

The post-processing program used was initially based upon program CARGO (Hutchison, 1977), although few similarities remain. Program RESP takes the motion FRO's from program EOMSOL, integrates them to produce acceleration FRO's, transforms them to any specified location on the body and forms their response spectra.

APPENDIX B

DEFLECTION AND VIBRATIONAL FREQUENCY ESTIMATION

The following calculations relate to the West Point Prototype Floating Breakwater:

A conservative support condition to use in calculation of maximum vertical deflection would be to simply support the breakwater longitudinally on the crests of three waves. Such a situation would correspond to a 3.8 second wave, which is slightly larger than the peak wave energy of any incident wave autospectra measured during the course of the monitoring. Furthermore, for the breakwater to reach anything resembling this configuration would require the wave crests to be propogating in almost a due East or West direction, both of which have very limited fetches.

The values used for the moment of inertia and modulus of elasticity are taken from (Georgiadis and Hartz, 1982) and were calculated for breakwater pontoons almost identical to those under consideration here. It is easily seen from the symmetry of the loading that the deflection desired would be that of a beam clamped at one end, simply supported at the other, and with a span of half the total length of the West Point breakwater. The maximum deflection under this loading would then be

$$\Delta_{max} = q_o L^4/185EI \qquad B1.1$$

where Δ_{max} is the maximum deflection in feet = 0.02 ft

L is 1/2 the breakwater length = 75 feet

q_o is the load per foot = 3.6 k/ft

E is the modulus of elasticity = 417,000 k/ft^2

and I is the moment of inertia about the transverse axis

= 75 ft^4

This small deflection represents less than 1/2 of 1 percent of the depth of the breakwater.

In estimating the natural frequency of vibration, the mass will be doubled as a rough accounting of the added mass of water. In this case,

$$f_{nat} = C[EI/2mL^4]^{1/2} \qquad \text{B1.2}$$

where C = 3.56 for a free-free bar

m = mass per unit length = .112 kslug/ft

L = total length of body = 150 feet

f_{nat} = natural frequency of vibration = 1.87 hertz

This frequency is well above the main region of energy in the incident wave spectrum. Any stiffness imparted by the mooring system or other causes would raise this value further.

APPENDIX C

LISTING OF SQUARE LAW ROLL DAMPING SUBROUTINE

The following is the source code to the square law or viscous roll damping routine referred to in the body of the report. It is provided in the hopes that some of the input values found to yield reasonable response estimates might be of some use to others. A listing of the main program EOMSOL will be provided upon request as well.

```
C   SUBROUTINE TO ITERATE CONSIDERING ONLY ROLL AND SWAY DEGREES OF FREEDOM
C   ATTEMPTING TO FIND REASONABLE LINEAR 'VISCOUS' DAMPING COEFFICIENT
C   FOR USE BY MAIN EQUATIONS
C   FOR RELEVENT EQUATIONS, SEE PPS. 4 & 5 OF "SHIP SWAY, ROLL AND YAW
C   MOTIONS IN OBLIQUE SEAS" BY RODNEY T. SCHMITKE, SNAME
C
C
C
C   PROGRAMMED BY ROBERT MILLER, UW
C   REQUESTS FOR INFORMATION ON THIS ROUTINE OR THE MAIN PROGRAM THAT
C   CALLS IT SHOULD BE ADDRESSED TO ROBERT MILLER
C   C/O DERALD CHRISTENSON
C   FX 10
C   DEPARTMENT OF CIVIL ENGINEERING
C   UNIVERSITY OF WASHINGTON
C
C
C   DUM(4,4)=COUPLED SWAY & ROLL EQUATION SYSTEM WHICH IS A SUBSET OF
C     COEFF: COEFF IS NOT WRITTEN TO IN THIS ROUTINE BECAUSE IT IS CENTRAL
C     TO PROPER OPERATION OF MAIN PROGRAM
C   RHS=RIGHT HAND SIDE FROM MAIN PROGRAM (12 X 1 COLUMN VECTOR)
C   SRHS=RIGHT HAND SIDE WITH FINITE WAVE AMPLITUDE FACTORED IN (2 X 1)
C   DVISC=CONTRIBUTION TO ROLL DAMPING DUE TO VISCOUS EFFECTS
C   DVISCO= VALUE OF DVISC IN PREVIOUS ITERATION
C   RCALC=ROLL AMPLITUDE IN RADIANS CALCULATED BY ROUTINE
C   REST=ESTIMATED ROLL AMPLITUDE IN RADIANS
C   WSINV=1/WAVE STEEPNESS = WAVE LENGTH/WAVE AMPLITUDE
C   DINTG=VALUE OF INTEGRAL ON PAGE 5 EQ. 63 OF SCHMITKE
C   CB=BLOCK COEFFICIENT OF BREAKWATER SECTION
C   BEAM=BREAKWATER BEAM
C   DRAFT=BREAKWATER DRAFT
C   ZCG=CENTER OF GRAVITY OF BREAKWATER
C   KG=KEEL TO ZCG (CENTER OF GRAVITY) DISTANCE
C   VISKIN=KINEMATIC VISCOSITY OF SEAWATER
C   REYN=REYNOLDS #
C   CDF=SKIN FRICTION DRAG COEFFICIENT (SEE SCHMITKE, P 5)
C   SWET=WETTED SURFACE AREA OF HULL
C   CON=SEE APPENDIX 3 OF SCHMITKE (HE CALLS IT C)
C   RED=AVERAGE RADIUS FROM ORIGIN TO EDDYMAKING LOCUS (ASSUMED TO BE
C         CORNER OF BREAKWATER)
```

```
C   RBAR=AVERAGE DISTANCE FROM COORDINATE ORIGIN TO OUTSIDE SURFACE
C   RE = BILGE RADIUS
C   COEFF=FULL 12 X 12 MATRIX FOR 6 DOF EQUATION OF MOTION (SEE EQN. 4.12
C        AND 4.13 OF THIS THESIS
C   WAMP=WAVE AMPLITUDE
C   UD=EDDY MAKING PARAMETER (CALLED U IN APPENDIX 3 OF SCHMITKE)
C   FR=ANGULAR FREQUENCY
C   NITER = NUMBER OF ITERATIONS
C   RO = DENSITY OF SEAWATER
C   BEAM = BREAKWATER BEAM
C   VISKIN=KINEMATIC VISCOSITY OF SEAWATER
C   REST=ESTIMATED ROLL MOTION AMPLITUDE
C
C   ORDER, SCFAC,SOL ARE USED BY MATRIX INVERSION ROUTINE (NOT LISTED)
C      WHICH HAPPENS TO BE LU DECOMPOSITION, BUT ANY WILL DO
C      SOLUTION VECTOR RETRUNED IN SOL
C
C   COMMON VISCAL PASSES VALUES FROM CALLING PROGRAM WHICH DOES ALL INPUT
C
       SUBROUTINE RDAMP
       COMMON / VISCAL / WSINV,PI,FR,ZCG,RO,DRAFT,BEAM,VISKIN,CB,SWET,
      2COEFF(12,12),RHS(12),RE
       DIMENSION DUM(4,4),SRHS(4),SCFAC(4),SOL(4)
       INTEGER ORDER(4)
       REAL KG
C   THIS IS THE VALUE OF INTEGRAL IN EQUATION 4.22 OF THIS REPORT
       DATA DINTG /808481./
       DATA RED / 8.65/
       N=4
       NITER=0
C   INITIAL ROLL AMPLITUDE ESTIMATE IN RADIANS
       REST=0.2
C   FIRST CALCULATE WAVE AMPLITUDE BASED ON WAVESLOPE INPUT
       WAMP=(5.12*((2.*PI)/FR)**2)/WSINV
C   LAST CHANCE FOR NON-REPETITVE CALCULATIONS BEFORE MAIN LOOP
       KG=DRAFT+ZCG
C   THIS EQUATION FROM SCHMITKE:  ALSO USED BY PROGRAM NSRDC
       RBAR=(1./PI)*((0.887+.145*CB)*(1.7*DRAFT+BEAM*CB)+2*(ZCG))
C   START OF MAIN LOOP
C
C   FIRST SCALE FORCING FUNCTIONS BY WAVE AMPLITUDE
C   AND LOAD REDUCED COEFFICIENT MATRIX
   10  CONTINUE
       DO 15 I=1,2
       SRHS(I)=RHS(2*I)*WAMP
       SRHS(I+2)=RHS(2*I+6)*WAMP
       DO 15 J=1,2
       DUM(I,J)=COEFF(2*I,2*J)
       DUM(I+2,J+2)=DUM(I,J)
       DUM(I+2,J)=COEFF(2*I+6,2*J)
       DUM(I,J+2)=COEFF(2*I,2*J+6)
   15  CONTINUE
C   SEE APPENDIX 3 OF SCHMITKE FOR CALCULATION OF CON (C IN SCH.)
       UD=14.1-46.7*REST+61.7*REST**2
C   THE FOLLOWING EQUATION IS NUMBERED 112 IN SCHMITKE:   .24 COMES FROM
C        SOME EMPIRICAL TABLES
       CON=.24*(BEAM/KG)*DEXP(-UD*RE/DRAFT)
       REYN=(3.22*(REST*RBAR)**2)/(DRAFT*VISKIN)
       CDF=1.328*REYN**(-.5)+0.014*REYN**(-.114)
       DVISC=(4./(3.*PI))*RO*FR*REST*(CDF*DINTG+RED**3*SWET*CON)
C  NOTE: CDF*DINTG= CONTRIBUTION DUE TO HULL FRICTION
C        RED**3*SWET*CON=CONTRIBUTION DUE TO EDDYMAKING
C
C    LOAD ESTIMATED VISCOUS CONTRIBUTION(DVISC) INTO 2 DOF EQUATION OF MOT.
      DUM(4,2)=DUM(4,2)-FR*DVISC
      DUM(2,4)=-DUM(4,2)
```

```
C
C     CALL ROUTINES TO SOLVE SYSTEM
C*****************************************************************************
      CALL SCALES(DUM,N,(4),SCFAC)
      CALL LUDCMP(DUM,N,(4),ORDER)
      DO 17 J=1,4
   17 SRHS(J)=SRHS(J)*SCFAC(J)
      CALL SOLVLU(DUM,SRHS,SOL,N,(4),ORDER)
C*****************************************************************************
C
C  THE PORTION THAT HAS BEEN STARRED OUT MAY BE REPLACED BY ANY EQUATION
C     SOLVER    PLUG IN DUM AS MATRIX TO BE SOLVED
C               SRHS IS RIGHT HAND SIDE
C               SOL IS SOLUTION VECTOR
C            THE REST OF THE VARIABLES ARE IDIOSYNCRATIC TO THIS PARTICULAR
C            TECHNIQUE OF SOLUTION
C
C            DO NOT BE DISTURBED BY THE PARENTHESIS AROUND THE 4
C            THE FOUR JUST SPECIFIES THE ORDER OF THE MATRIX
C            THE PARENTHESES ARE REQUIRED BY THIS STUPID DIALECT OF FORTRAN
C            AVAILABLE ON THIS MICRO
C
C  FIND MAGNITUDE OF ROLL RESPONSE
      RCALC=DSQRT(SOL(2)**2+SOL(4)**2)
      NITER=NITER+1
      WRITE(12,900) NITER,REST,RCALC
C  ECHO RESULTS (FILE OPENED IN MAIN PROGRAM)
  900 FORMAT(" # iterations= ",I3,"EST. ROLL ANG =",E13.6,"CALC  ROLL AN
     2G = ",E13.6)
C  IF CALCULATED ROLL AMP. CLOSE ENOUGH TO ESTIMATED, FINISH UP AND GET OUT
      IF (DABS(REST-RCALC) .LT. .017450) GO TO 30
C  ELSE GET NEW ESTIMATE
      CALL ROLLES(REST,RCALC)
C  AND GO BACK TO BEGINNING OF LOOP
      IF (NITER .LT. 15) GO TO 10
C  UNLESS 15 ITERATIONS HAVE OCCURRED IN WHICH CASE PRINT MESSAGE,
C    LOAD WHAT HAS BEEN OBTAINED SO FAR AND WRITE MESSAGE TO SCREEN
      GO TO 40
   30 CONTINUE
C  LOAD VISCOUS DAMPING CONTRIBUTION INTO FULL 12 X 12 MAIN MATRIX
C  DON'T BE DISTURBED BY MINUS SIGN, ITS JUST PART OF THE SIGN CONVENTION
C  USED IN THIS PACKAGE
      COEFF(10,4)=COEFF(10,4)-FR*DVISC
      COEFF(4,10)=-COEFF(10,4)
      RETURN
   40 CONTINUE
C  WRITE ERROR MESSAGE (I'VE NEVER HAD THIS HAPPEN)
      WRITE(1) " NUMBER OF ITERATIONS EXCEEDED 15: CONTINUING",13,10
      GO TO 30
      END
C  SUBROUTINE TO ESTIMATE ROLL ANGLE BASED ON PREVIOUS ESTIMATIONS AND
C  THEIR CALCULATED VALUES
       SUBROUTINE ROLLES(REST,RCALC)
       DOUBLE PRECISION REST,RCALC
       TDIFF=REST-RCALC
       REST=REST-.75*TDIFF
       RETURN
       END
```

APPENDIX D

ROUGH ESTIMATION OF FORCES CONTRIBUTING TO HORIZONTAL SHEAR

Assumed: 4 foot significant sway displacement

5 ft/sec^2 significant sway acceleration

all forces lumped at two frequencies: 0.3 hertz = peak acceleration, 0.033 hertz = peak displacement.

High Frequency:

Inertia: mass of breakwater = 0.112 kslug/ft

added mass = 0.055 kslug/ft

inertial force 5. x (0.112 + 0.055)

= 0.82 k/ft

Damping: hydrodynamic damping = 1.68 kslug/sec-ft

velocity amplitude = $\frac{5 \text{ ft/sec**2}}{2\pi \times 0.3}$

damping force amplitude = 2.65 x 1.68

= 0.45 k/ft

Restoration: displacement amplitude = $\frac{5 \text{ ft/sec**2}}{(2\pi \times 0.3)\text{**2}}$

= 1.4 ft

restoring constant (from program BRKMOOR)

= 5 k/ft (for entire breakwater)

restoring force amplitude = 0.047 k/ft

Excitation: Since displacement and inertia are 180 degrees out of phase and both are 90 degrees out with respect to damping, wave force amplitude must be for equilibrium:

$\sqrt{\{0.82-0.047)^2 + 0.45^2\}} = 0.92$ k/ft

This is about right for a two foot significant wave.

The phase with respect to the displacement would be $\tan^{-1}$ (0.77/0.45) = 30 degrees as pictured on Figure 5.48.

Low Frequency:

Inertia: Added mass = 0.085 kslugs/ft

displacement amplitude = 4.0-1.4 = 2.6 feet

Acceleration = $(2 \times \pi \times 0.033)^2 \times 2.6$ ft

= 0.114 ft/sec^2

inertial force = (0.085 + 0.113) x 0.114

= 0.022 k/ft

Damping may be neglected at this low frequency.

Restoration: 2.6 ft x 5 k/ft /150 feet = 0.09 k/ft

By the same logic as above, these forces require approximately 0.068 k/ft wave excitation force for equilibriation. Figure 5.30 shows a phasor diagram of the resulting force configuration.